

POLITECNICO DI TORINO

MASTER DEGREE IN ENERGY AND NUCLEAR ENGINEERING

SMALL SCALE CO₂ CAPTURE



Supervisors:

Prof. Marco Carlo Masoero

Prof. Grégoire Léonard

Candidate:

Riccardo Bonanno

Luglio2020

Summary

As a consequence of anthropological processes, the environment needs more concerns and regulations. One of the challenges is the capture of carbon dioxide (CO_2) which has been elaborated to reduce the greenhouse effect. At this moment the use of CO_2 capture systems is mainly envisaged in large scale plants. In this thesis, some of the most diffused technologies have been studied and compared to each other for application to small-scale CO_2 emitters. In fact, there are many small or medium-sized plants that do not pay sufficient attention to the emission of carbon dioxide but which, on the whole, have a significant impact on the greenhouse effect. Usually, the installation of big amine plant, for example, is not interesting for this kind of industries, then small-scale CO_2 capture could be an alternative, also if they do not achieve the same performances of larger plants.

The present study has taken as example a cogeneration unit installed in Liegi University, which gave the possibility to have real data, used as input for computations. It is powered by a biomass boiler of 12 MW and produces 257 kg of CO_2 per MWh_{th} and 457 kg of CO_2 per MWh_{el} for a total of 16000 kg CO_2 per year. The technologies analysed are Post-Combustion Carbon Capture (PCCC) and are amine solvents and membrane separation. The global work wants to point out which one of them is the most profitable from energy and cost point of view for small-scale use.

After a general introduction about carbon capture technologies, the first part regards the description of membrane technology and physical phenomena that govern it. Membranes used for CO_2 capture are less widespread than others method and many researchers are still working on it. The biggest drawback of this technology is the brief lifetime of membranes (around 3-4 years) and the relatively low purity in the permeate stream (i.e. the captured CO_2) which makes it impossible to use only one-stage configuration. Despite their drawbacks, the membrane is still interesting because they imply a minor consumption of energy and their modularity allows to save much space.

The base module of membrane has been modelled with the help of Aspen Custom Modeler (ACM) software, which permitted to insert the physical laws which governs the phenomena. The base module was then implemented in Aspen Plus software which gave the possibility to build different process configurations. The study of configuration regarded both the use of compression or vacuum conditions. At the end of the analysis only two configurations demonstrated to achieve almost 99% of CO_2 purity with almost 87% of CO_2 separated. The most convenient configuration uses 400 m^2 of polymeric membrane (Polaris type) and the related process needs 0.99 MWh per tonne of CO_2 separated. These results have been compared with amine technology.

The second part instead interests the use of CO_2 absorption with amine solvents, one of the most common and mature technologies. This one achieves a higher separation rate, but also induces a higher consumption of energy. A pre-existing model in Aspen Plus software has been studied and adapted to our case study. The used model allows the evaluation of the process energy requirement and studies the oxidative degradation in the absorber which is the cause of most of the solvent loss. Also, the operating conditions are analysed in amine plant to check when the efficiency of separation is maximum and when energy consumption is minimum. The results bring to a product with almost 99% of purity and 99% of CO_2 removed. The need of thermal power is equal to 4.5 MW used in the stripper which represents the major part of the energy consumption.

At the end, an economic analysis has been done for the two technologies and it resulted that amines are characterized by a higher capital and total operational cost respect membrane one which results cheaper. Although the good economics results, many interrogatives remain about robustness and reliability of membrane. In fact, membrane plant results to be not enough mature yet, mostly regarding what impact the impurity can have on it. The research on more performing membranes is going on and many solutions are already available but still in experimental phase. The biggest obstacle for membranes is the development of an economical and sustainable way of producing them at large-scale. In conclusion, the amine separation plant is the best choice in case of maturity in the technology and robustness. However, membranes are a competitive

investment that can be more advantageous once some aspects such as the effect of impurities in separation performance and large scale production have been studied in more detail.

Index

SUMMARY	2
CHAPTER 1: INTRODUCTION.....	7
1.1 Background.....	7
1.2 Global warming.....	11
1.3 Greenhouse effect	13
1.4 Consequences of global warming	15
1.5 Future forecasts	17
1.6 Objectives	18
CHAPTER 2: CO₂ CAPTURE SYSTEMS	21
2.1 Pre-Combustion Capture	22
2.2 Post-Combustion Capture	23
2.3 "Oxyfuel" capture in combustion	25
2.4 General Comparison of technologies.....	26
CHAPTER 3: MEMBRANE LITERATURE REVIEW.....	28
3.1 Membrane gas separation history	28
3.2 Principal features of membrane gas separation.....	28
3.3 Types of gas separation membranes	28
3.3.1 Classification according to the selective process.....	29
3.3.2 Classifications according to the technology used.....	30
3.3.2.1 Through non-dispersive contact.....	30
3.3.2.2 Supported-liquid membranes	31
3.3.2.3 Permeation method	31
3.3.3 Classification according to material	35
3.3.3.1 Polymeric membrane	35
3.3.3.2 Inorganic membranes: zeolite and carbon membranes	37
3.3.3.3 Hybrid membrane	38
3.3.4 Membrane geometry module configurations.....	40
CHAPTER 4: EFFECT OF IMPURITIES ON MEMBRANES.....	43
4.1 NO _x formation.....	43
4.1.1 Thermal NO _x	43
4.1.2 Fuel NO _x	45

4.3 SO _x formation	45
4.4 Humidity	46
4.5 Experimental test on impurity effect.....	48
4.5.1 Pilot scale testing of polymeric membranes for CO ₂ capture from coal fired power plants	48
4.5.2 The impact of impurities on the performance of CTA membranes for CO ₂ separation	50
CHAPTER 5: CASE STUDY	58
5.1 Cogeneration.....	58
5.2 Case study	59
CHAPTER 6: MEMBRANE MODEL DEVELOPMENT.....	62
6.1 Simulation parameters and assumptions	62
6.2 Design specifications	63
6.3 Aspen Custom Modeler	64
6.3.1 Writing code of ACM model.....	66
6.4 Aspen plus.....	69
6.4.1 Exporting model from ACM to Aspen Plus	69
6.4.2 Module construction in Aspen Plus.....	70
6.5 Other configurations	74
CHAPTER 7: AMINE ABSORPTION.....	79
7.1 Plant design	81
7.2 Possible solvents.....	83
7.3 Model construction	85
7.3.1 Pilot model	85
7.3.2 Case study	86
CHAPTER 8: ECONOMIC ANALYSIS	89
8.1 Membrane cost evaluation	89
8.2 Amine plant cost evaluation	91
8.3 Summarizing results.....	93
CHAPTER 9: CONCLUSION AND PERSPECTIVES	94
Conclusion	94
Perspective.....	95

Chapter 1: Introduction

1.1 Background

The continuous increase in anthropogenic carbon emissions since the industrial revolution has led to CO₂ concentrations above 400 ppm in the atmosphere, far from a concentration of 280 ppm in the preindustrial period. The effects of this increase have been evidenced in the last decades. In particular, the sea level has increased, the ocean and atmosphere have warmed, and the amounts of ice diminished.

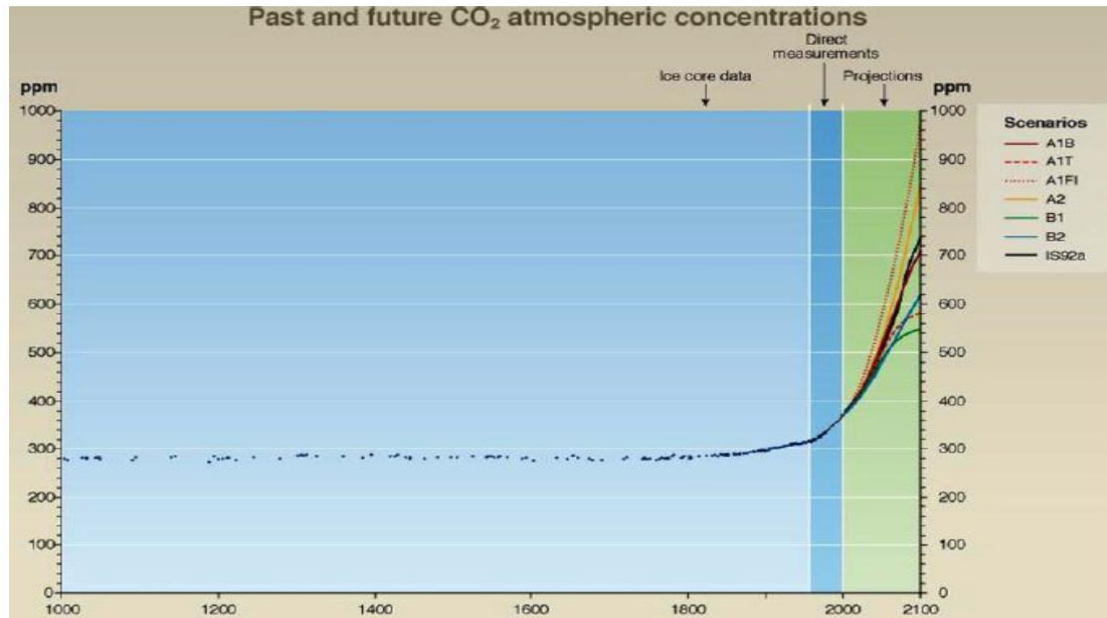


Figure 1.1 CO₂ concentration 1000-2100. Source [Hiroshi Otha, 2006].

In view of a reduction in carbon emissions to the atmosphere that can limit the temperature rise in the earth to below 1,5°C by 2030, different scenarios have been suggested.[IPCC Side Event ,2018] Among possible strategies, the complete substitution of the currently installed fossil-fuel-based technologies by renewable and clean sources is the preferred one. However, the emission reduction needed to achieve the target is still too far from the reality of industry and today's lifestyle, which leads to emissions decreasing still too slowly. In the "Emission Gas Report of IPCC" [IPCC Side Event, 2018] authors reported that the current policies are sufficient to stay below 2°C and pursue 1,5°C. In particular global greenhouse gas (GHG) emissions do not show sign of peaking, global CO₂ emissions from energy and industry increased in 2017, following a three years period of stabilization. Furthermore, total emissions reached a record high of 53,3 Gt CO₂e (CO₂ equivalent) in 2017, an increase of 0,7 Gt CO₂e compared with 2016. In contrast, global GHG emissions in 2030 need to be approximately 25% and 55% lower than in 2017 to put the world on a least-cost pathway to limiting global warming to 2°C and 1,5°C respectively, as evidence in (Figure 1.2) [IPCC Side Event ,2018].

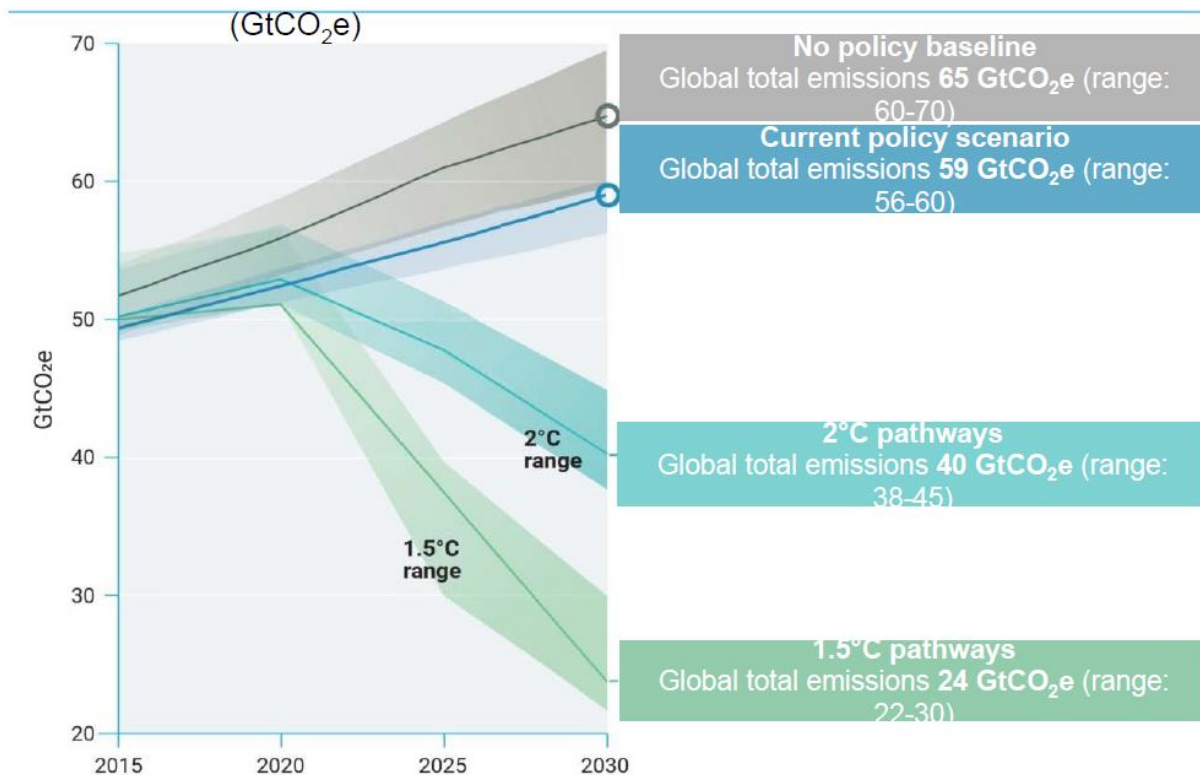


Figure 1.2 Annual global total greenhouse gas emissions. Source [IPCC Side Event ,2018]

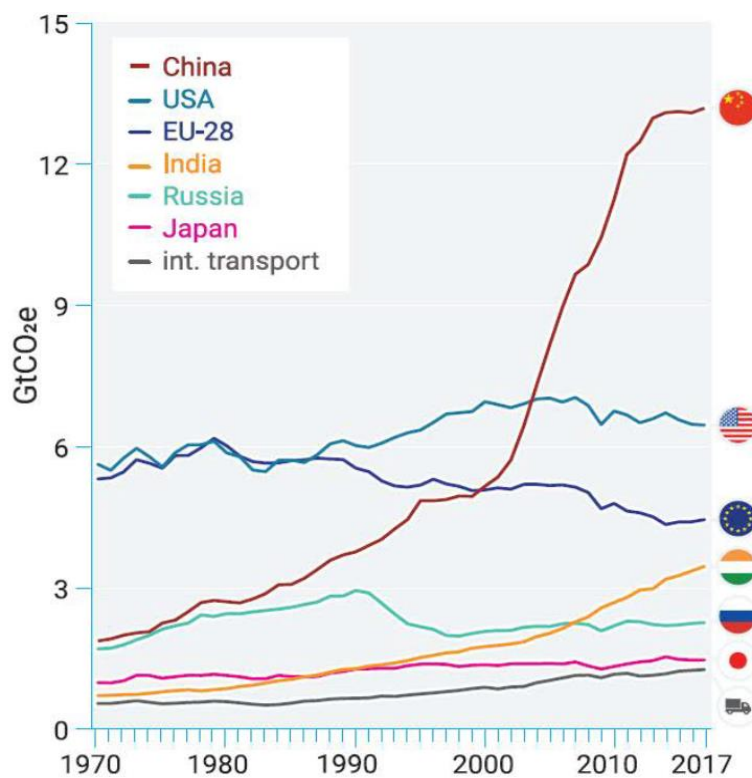


Figure 1.3 Global greenhouse gas emission levels for majors' emitters. Source [IPCC Side Event ,2018]

Nowadays, the whole society is still mostly based on fossil fuels, and the trend of their use varies depending on the country and policies (Figure 1.3). Coal, natural gas, and oil are extensively used in the transportation sector, heat, and electricity generation, and in the petrochemical industry. In view of a revamping of existing installations, the use of renewable energy sources is foreseen as the preferred strategy to overcome the different impacts of all these sectors on the environment. The emission reduction would affect six key sectors principally in a possible scenario (Figure 1.4).

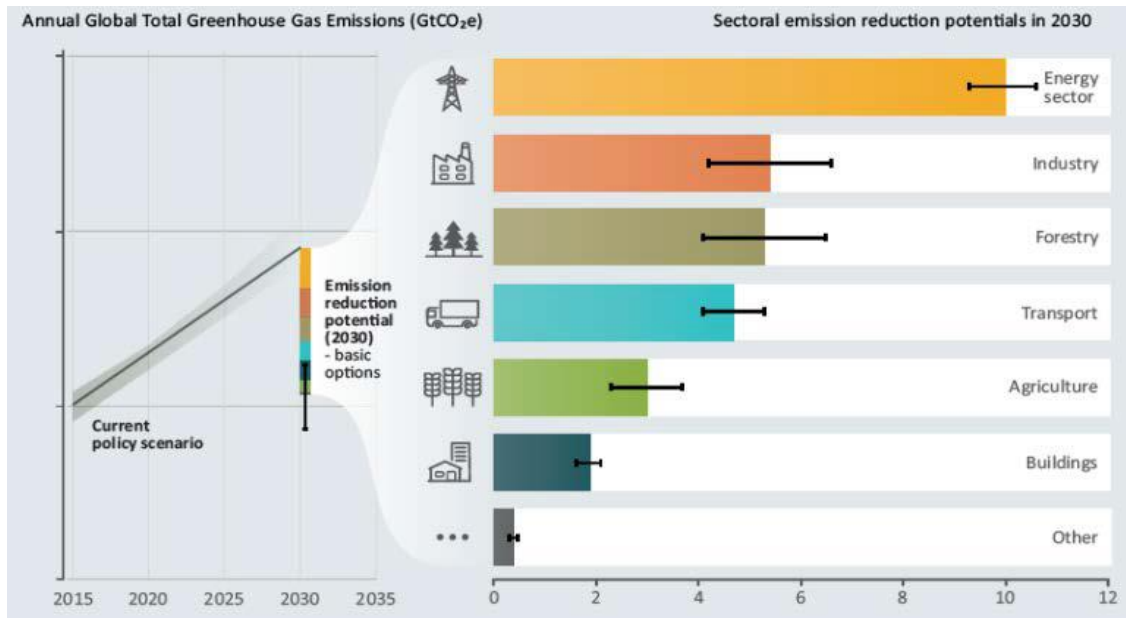


Figure 1.4 Potential emission reduction in 2030. Source [IPCC Side Event ,2018].

Based on this ideal strategy, already many sectors are shifting their fossil fuel consumption towards greener fuels. Typical coal gasification plants for power generation are nowadays being powered with biomass, hydrogen can be produced from water electrolysis making use of electricity coming from renewable technologies (only 1-2% is produced in this way, the rest of it needs fossil fuel sources), bioethanol is used more and more as fuel for the transportation sector, and in many countries a high percentage of electricity consumed on a daily basis comes from renewable sources such as wind and solar power. However, although the right path has been mapped out, the use of fossil fuels remains strong and predominant in the global scenario both in transport (Figure 1.5) and in total consumption (Figure 1.6).

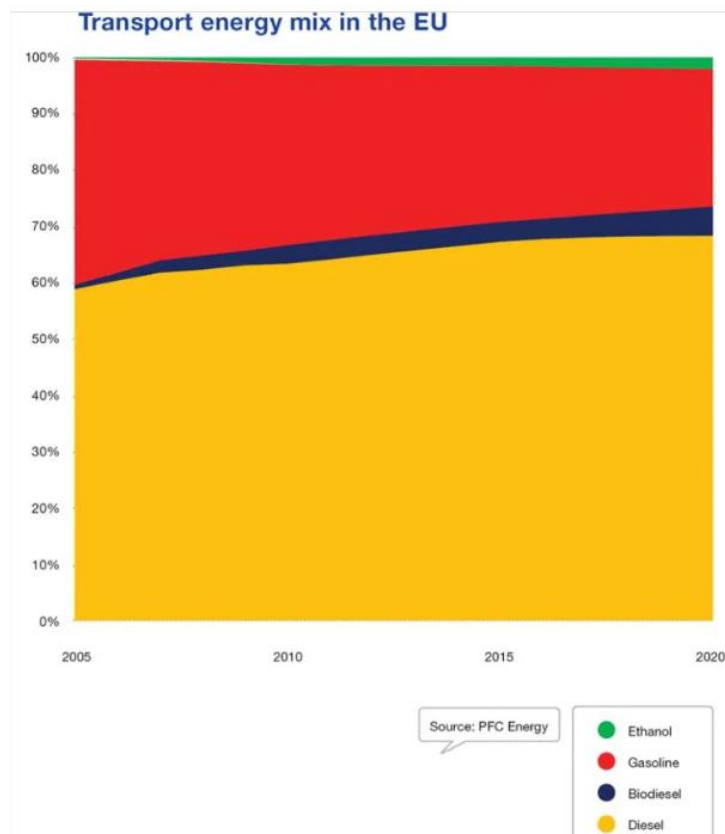
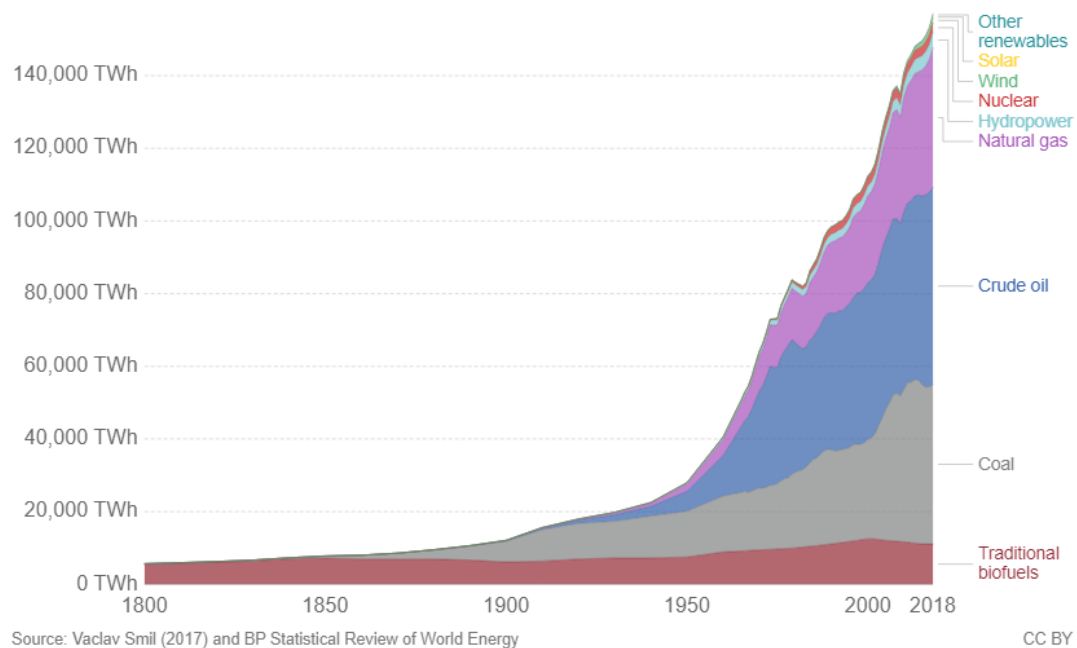


Figure 1.5 Energy transport mix in Europe. [FuelsEurope, 2020].

Global primary energy consumption

Global primary energy consumption, measured in terawatt-hours (TWh) per year. Here 'other renewables' are renewable technologies not including solar, wind, hydropower and traditional biofuels.

Our World
in Data



Source: Vaclav Smil (2017) and BP Statistical Review of World Energy

CC BY

Figure 1.6 Global primary energy consumption. Source [Vaclav Smil, 2017].

1.2 Global warming

Although political debate and public opinion have been interested in the phenomenon of "Global warming" only for fifty years now, its study within the scientific community has lasted much longer. In fact, in 1827, Jean Baptiste Fourier showed how the temperature of the Earth was linked to the atmosphere that surrounds it, which can reduce heat loss like a greenhouse [James Rodger Fleming, 2005]. A few years later, in 1865 John Tyndall studied the interaction between some polyatomic molecules in the gaseous state and infrared radiation managing to demonstrate how the Earth's climate has closely linked the concentration of water vapor and carbon dioxide in the atmosphere [John Tyndall's, 1859]. The first hypothesis of global warming for anthropogenic causes is due, instead, to Svante Arrhenius, in 1896. He was firmly convinced of man's influence on changes due to the release of CO₂ following the combustion of coal. This theory was not immediately accepted with great success and the scientific community was divided among those who tried to confirm Arrhenius' thesis and those who wanted to prove otherwise.

At first, it seemed impossible that human activity could somehow influence even minimally something of such a great extent as the Earth's climate. In the years fifty of the last century, a new hypothesis made its way: people could affect climate change, but if on the one hand, it released carbon dioxide into the atmosphere, on the other hand, it also produced powders and aerosols that had the effect of lowering the terrestrial temperature, reducing the greenhouse effect. During the Cold War, Charles Keeling managed to accurately quantify the concentration of CO₂ in the atmosphere, checking its continuous increase and considered this fact as the cause of the effective temperature rise of the Planet. In 1975, an article was published by Broecker "Climatic Change: Are We on the Brink of a Pronounced Global Warming?" [W. S. Broecker, 1975]. This article affected public opinion so much as to bring the debate from the scientific community to the great diffusion and the problem of global warming became in all respects "global". This initiated the awareness of the masses and governments of many countries until the first world conference on the climate meet in 1979. Nine years later a "Commission was founded by the United Nations, the "UN Intergovernmental Panel on Climate Change" (IPCC), to analyse the phenomenon of global warming starting from its causes and, through future forecasts, trying to limit it as far as possible.

The scientific study is carried out through two distinct procedures, relying on methodologies specific to statistics and complexity theory: on the one hand, the scientific data that can be measured and are significant for the so-called detection, i.e. the reference parameters of the possible causes (air temperature, ocean temperature (SST), solar activity, greenhouse gas concentrations) are analysed in order to verify the long-term trend that attests the warming or not (analysis of the historical series); on the other hand, climate simulation models are used that take into account more or less all the factors involved in the regulation of the climate system or built from the knowledge of the state of the art of the functioning of the climate taking into account the physical laws and the various feedback processes. These models, once constructed, are validated on the basis of past climate data or by applying the model to past times and verifying the goodness or badness of the simulated climate with the actual past climate.

These simulations make it possible to highlight both the causes of climate change and to make future prognoses; the attributions of the causes are typically carried out by inserting or removing energy forcings and verifying the output of the model on the basis of past data or by weighing the contributions of each anthropic and natural factor. (In this way many simulations have shown that CO₂ forcing would be indispensable to recreate the climate data of the recent past by triggering many other positive feedback, thus resulting, according to scientists, as the primary cause of the phenomenon).

Temperature anomaly represents the difference between annual and long-term average atmosphere temperature (Figure 1.7), while (Figure 1.8) shows the relation between CO₂ and global warming.

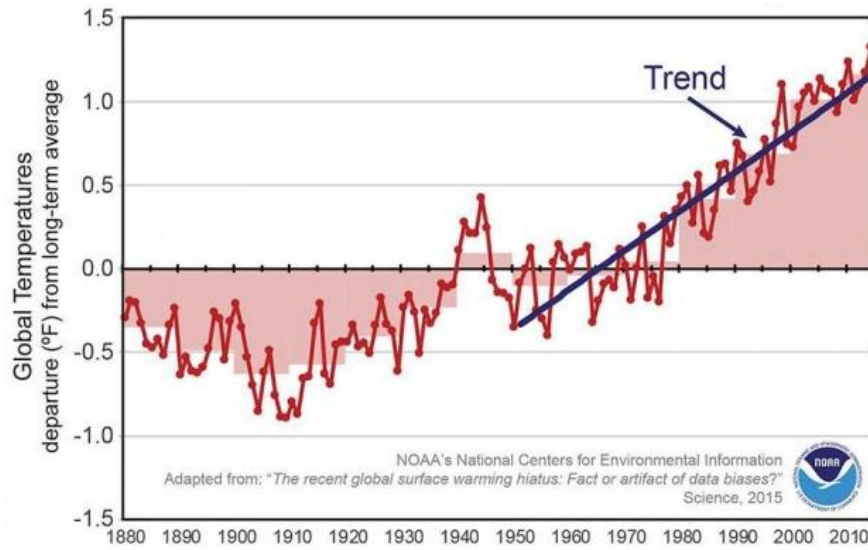


Figure 1.7 Temperature -variation from 1880 to 2010. Source[NOAA's, 2015].

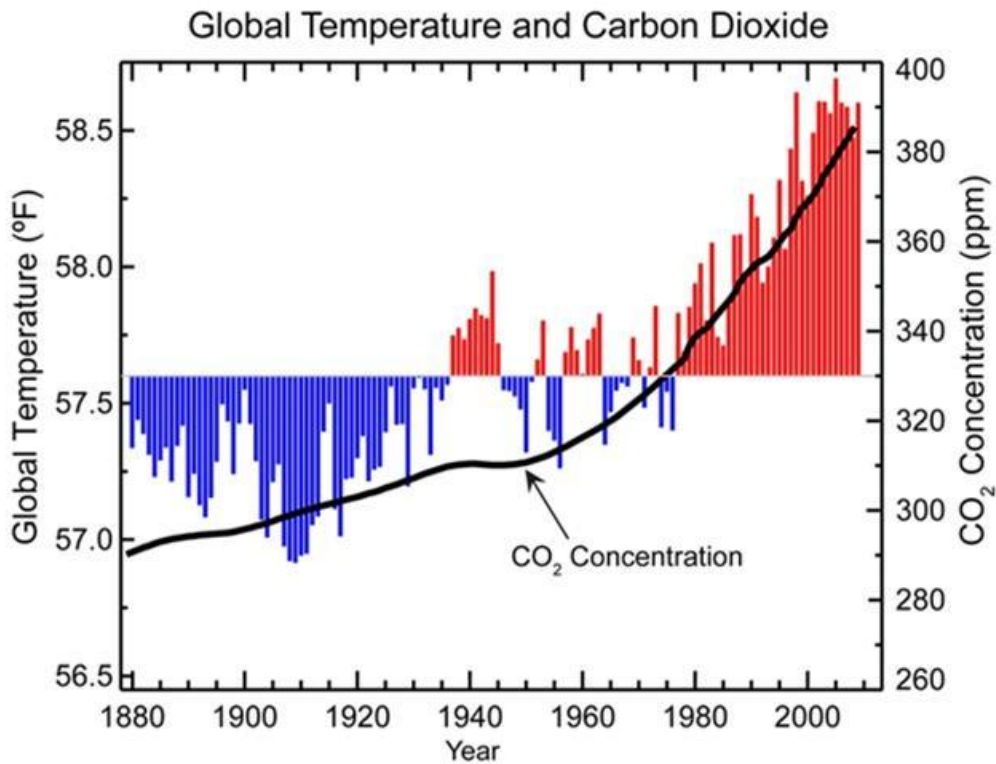


Figure 1.8 Global temperature respect time and CO₂ concentration. Source [NASA, 2010]

The positive trend of the increase in temperature is undeniable, but the causes can be manifold. The Earth has a history of significant climate change in the past attributable to factors such as changes in the rotation axis or the intensity of the sun's rays or related to volcanic activity. However, global warming characterizing the current historical period is not due to these elements, but to the anthropic effect of the change of the composition of the Earth's atmosphere concerning greenhouse gases.

1.3 Greenhouse effect

One of the natural factors that have allowed the development of life on Earth is this effect without which the average temperature of our planet would be around -18°C and this would result in the complete glaciation of the oceans. The thermal energy that the Earth receives from the sun would not be enough to reach the ideal temperature without green house effect. The sun's rays that hit the earth's surface are only a part of those that meet the most exterior layers of the atmosphere. The figure shows the scheme that represents how the solar energy that reaches Earth is divided. About 30% is reflected by clouds, from the surface the Earth itself and the air molecules by back-scattering effect, while 20% comes absorbed by molecules such as ozone and water vapor. In this way, the Planet absorbs only the 50% of the sun's rays and then re-emits them but with different wavelengths compared to the initial ones. The difference between the two spectra is linked to the great temperature diversity of the emissive surfaces which causes a shift in the Earth's spectrum towards higher wavelengths. The maximum emission for the Sun is fully visible ($0.48\text{ }\mu\text{m}$), while for the Earth it stands in the infrared ($10\text{ }\mu\text{m}$).

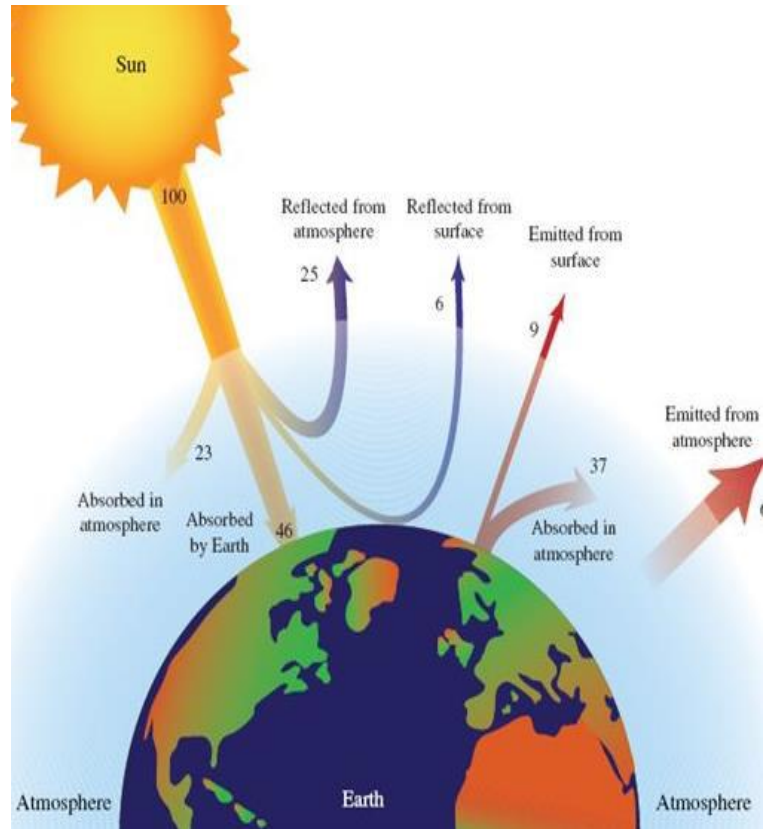


Figure 1.9 Emission spectrum for the Sun and for the Planet Earth

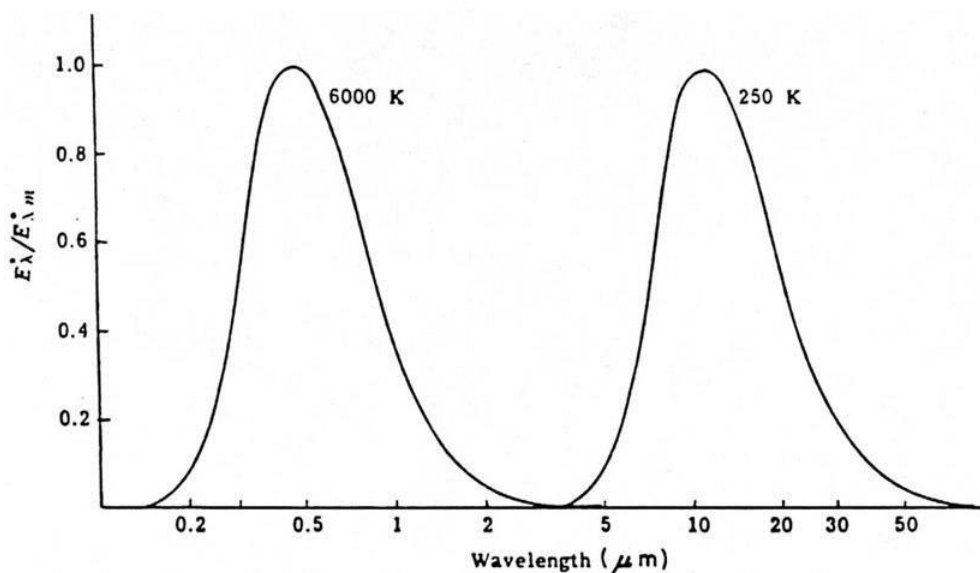


Figure 1.10 Wavelength characteristic of sun (left) and earth (right). Source [Yang Chen ,2006].

Infrared wavelength rays are more easily absorbed by the molecules present in the atmosphere, which in turn reissue them in part towards the earth's surface causing a significant return of heat flow and the so-called greenhouse effect. The gases that contribute to the greenhouse effect are numerous and, in most cases, they are naturally present in the Earth's atmosphere. Among these is water vapor (which causes approx. 65% of the effect), carbon dioxide (25%), methane (5%), ozone (3%), etc ...

Water vapor represents a large percentage since it has a very large spectrum of absorption in the IR and a concentration in the Earth's atmosphere that is significant, ranging between 10 and 50000 ppm. Its effect on global warming however is minimum since increasing its concentration in the atmosphere increases considerably the percentage of reflected solar radiation. To understand, however, the importance of carbon dioxide it is necessary to compare the absorption spectrum of CO₂ and H₂O vapor (Figure 1.11).

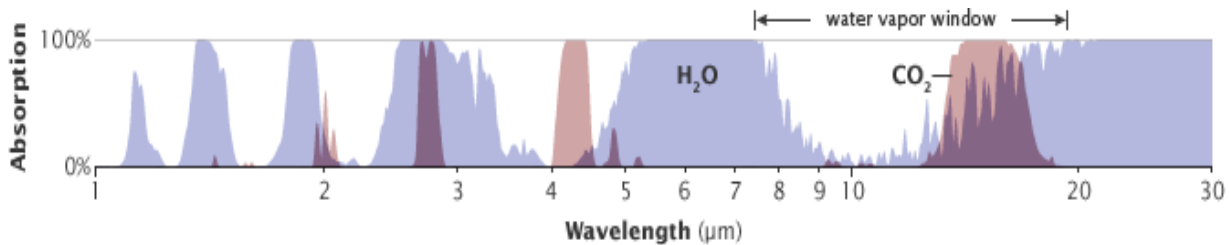


Figure 1.11 Absorption spectra of CO₂ and H₂O vapor. Source [Robert Rohde]

Around a wavelength of 15 μm as well as 4 μm, the water has transparency windows in which however, carbon dioxide absorbs. It must be considered that most of the other greenhouse gases, in addition to being present in the atmosphere in reduced concentrations have an absorption spectrum completely or partially superimposed on that of water and therefore their effect is strongly mitigated. For this reason, although impossible to demonstrate accurately, the main cause of global warming is attributed to the additional greenhouse effect generated by anthropogenic carbon dioxide, responsible for around 64% of this warming (rest being due to other greenhouse gases mentioned above) [IPCC's report, 2014]. The release into the atmosphere of tons of carbon dioxide by humans has caused a surge in its concentration in the atmosphere as shown in the figure below. It can be observed that the CO₂ level never exceeded 300 ppm until the 1950s, while at present it is around 400 ppm and rising

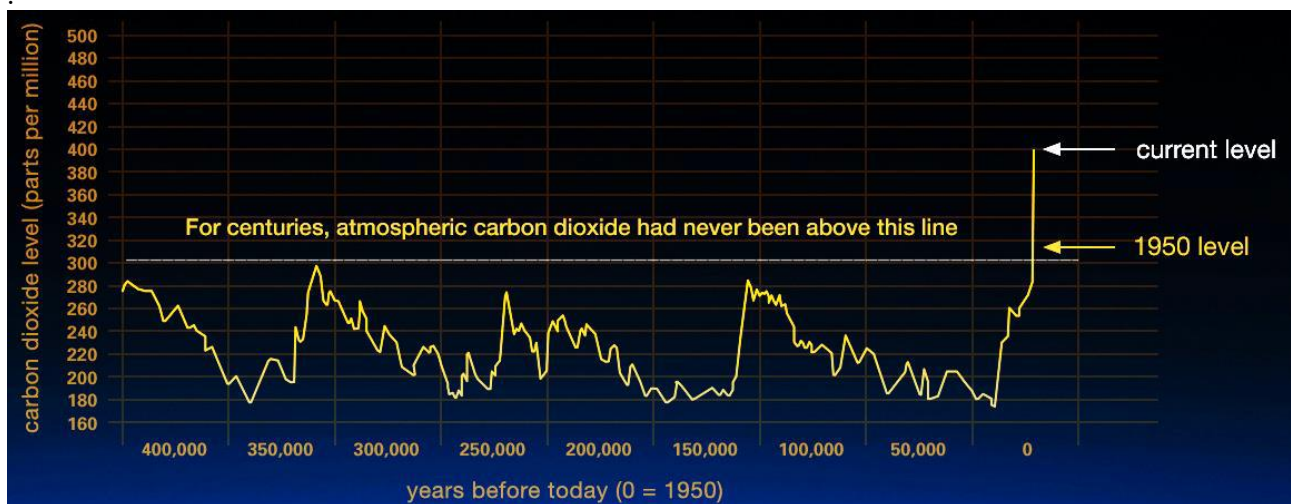


Figure 1.12 Carbon dioxide concentration with time. Source [NASA, 2008].

The carbon dioxide released by natural phenomena is far higher than that generated from man, but we must consider the global system to understand why this gas is the main cause of the problem. Considering the carbon cycle every year tons of carbon dioxide are released into the atmosphere naturally, for example from the biosphere and volcanic eruptions, but the oceans and biological activity tend to maintain concentration in the atmosphere approximately constant. The anthropic effect, however, broke this balance by making sure that the CO₂ concentration has increased dramatically.

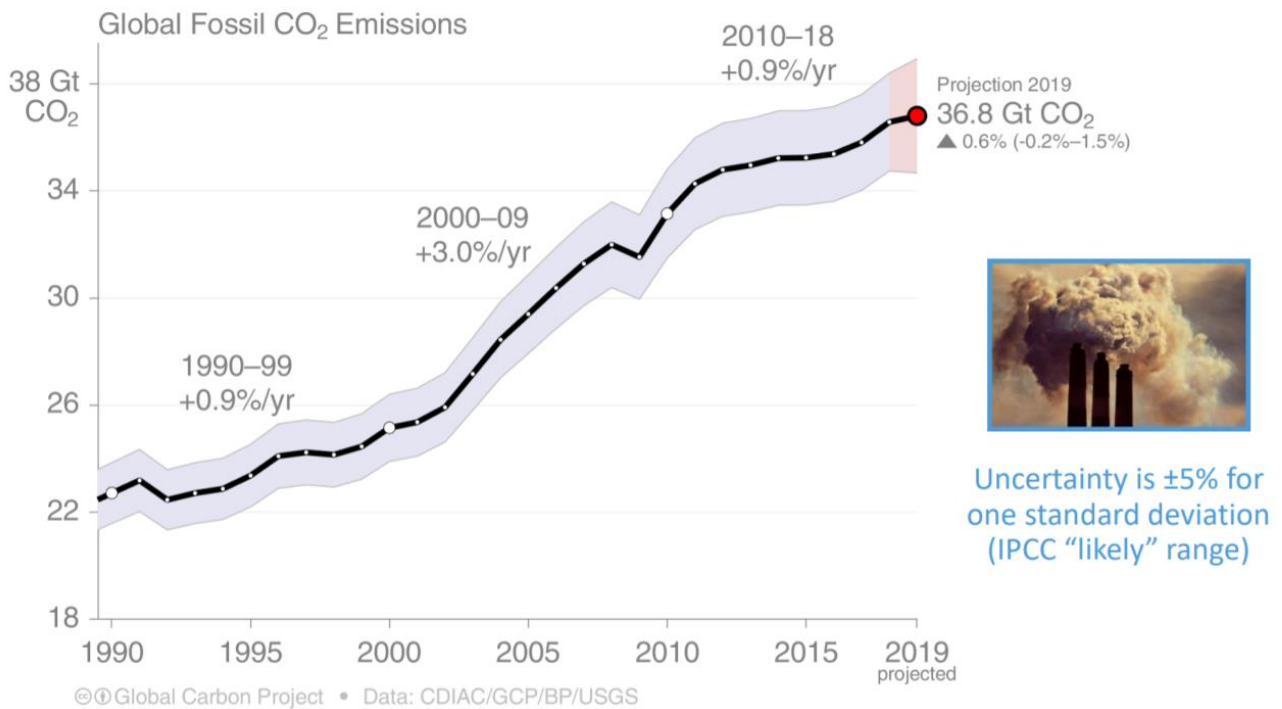


Figure 1.13 Carbon emission per year in Gigatons. Source [Global Carbon project ,2019].

The amount of carbon dioxide emitted by anthropic effect is reported and it is clear that growth has continued due to the increase of the following industrialization, passing from 23 Gt/year in 1990 to about 36.8 Gt/year in 2019.

1.4 Consequences of global warming

The changes associated with global warming are manifold and now undeniable. The average temperature of the earth's surface rise with the latest NASA data is around 1.1 ° C compared to the end of the 19th century and 2016 holds the record as the hottest year for 150 years now.

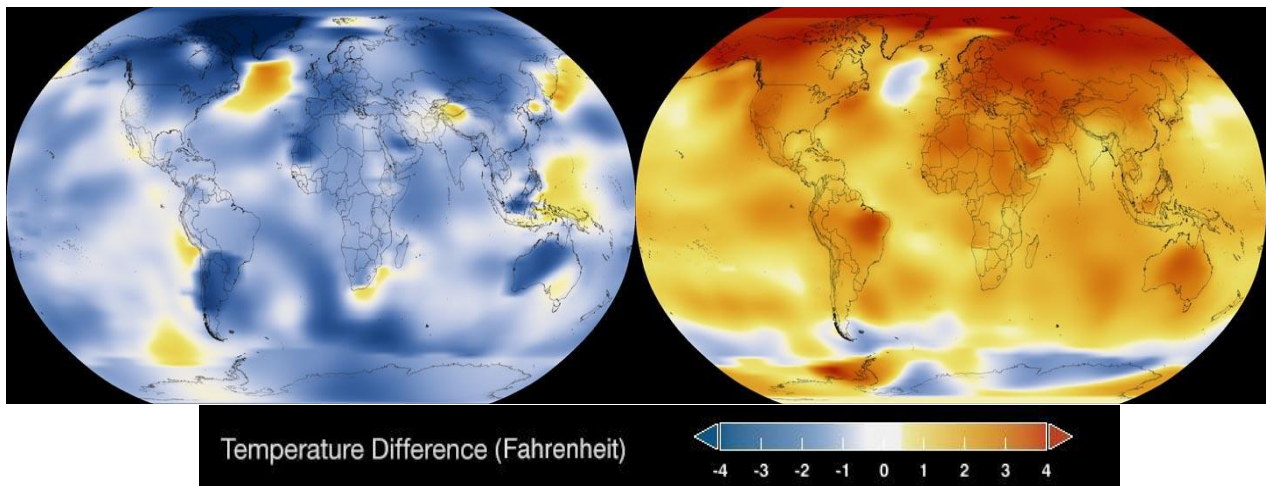


Figure 1.14 Graphical benchmark of temperature difference between 1890(left) and 2019(right). Source [NASA, 2010].

Rising ocean temperatures have caused the average temperature of the oceans down to 700 m depth to increase by about 0,17°C since 1969, resulting in a strong environmental imbalance. It must also be considered that an increase in ocean temperatures corresponds to greater evaporation and growth in the greenhouse effect caused

by water vapor. Furthermore, ocean acidification was recorded due to the atmospheric CO₂ absorbed by the oceans.

The graph in Figure 1.15 shows the rise in sea level from 1995 and how easy it is to witness the rapid growth. The factors that influence this aspect are mainly two: one, local, linked to the melting of both polar and mountain glaciers, while the other, global, due to the thermal expansion caused by the increase of sea temperature. Currently, the average rise level is considered to be around 10 cm in total since 1995, which alarms some communities that live along the coasts or on the islands especially in the warmer areas of the planet.

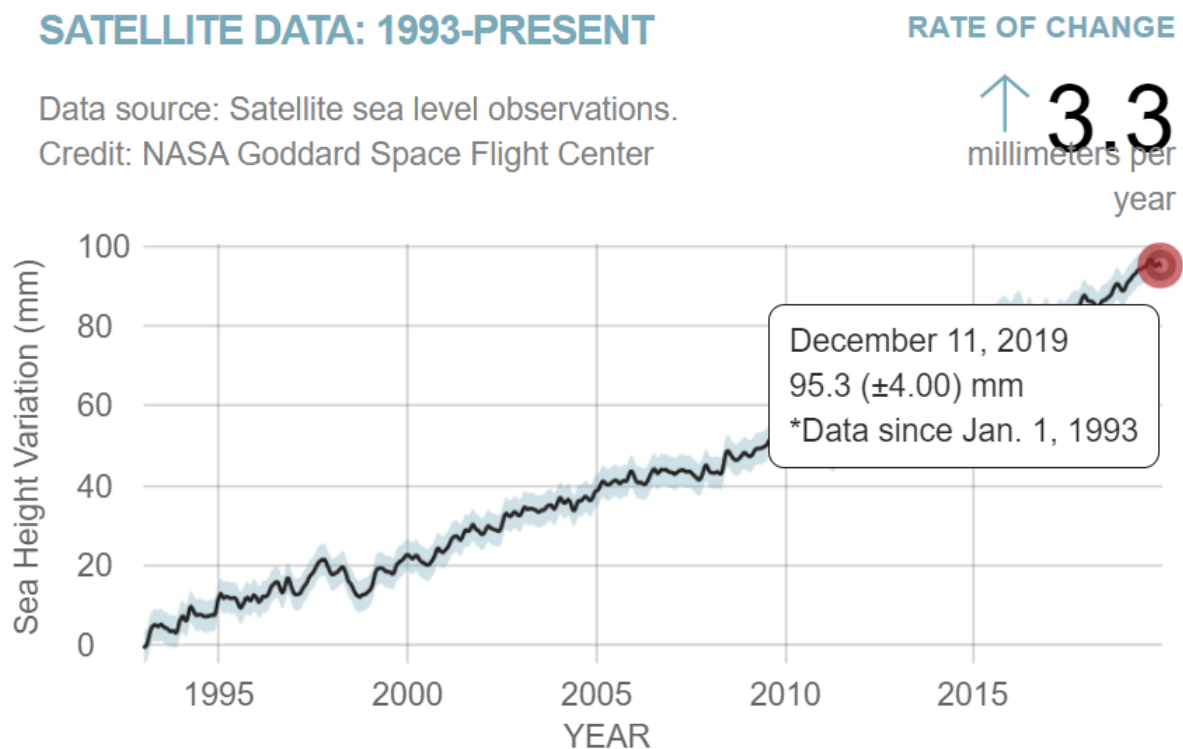


Figure 1.15 Sea level increase during years. Source [NASA, 2019].

The melting and regeneration of ice at the poles is a natural phenomenon, but which is distributed due to global warming. Satellite images are shown Figure 1.16. An estimate of the mass loss rate of ice at the poles is 127 Gt/year for Antarctica and 286 Gt/year for the Arctic.

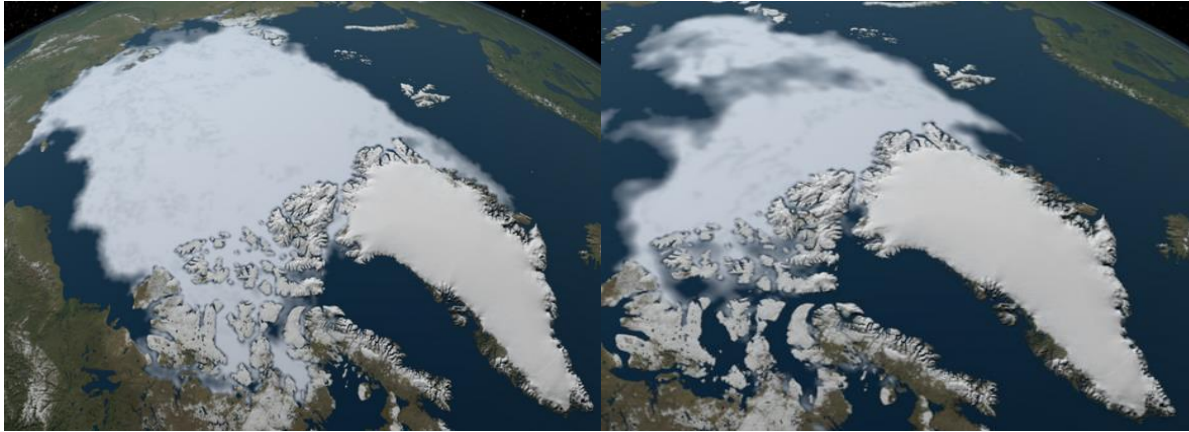


Figure 1.16 Comparison Arctic region 1984(left) 2016(right)

Melting of glaciers and polar ice caps, reduction of snowfall, together with the polar ice caps, the melting of perennial ice on mountains is an alarming phenomenon. Moreover, glaciers are also guaranteeing a continuous freshwater reserve during the year. In this way, the availability of water is decreasing, possibly contributing to long periods of drought, and associated socio-economic problems.

1.5 Future forecasts

There is no alternative to reducing the emission of carbon dioxide in the atmosphere to avoid disastrous consequences on a global level. Before choosing the best mitigation solution, though, the way to go is to look at what the future emissions may look like. Taking into account the distribution of the population, energy consumption, lifestyle and of many other factors, the "Representative Concentration Pathways", (RCPs), have been proposed, plausible scenarios whose difference lies in the achieved concentration of greenhouse gases into the atmosphere. These different RCPs permit to sign the right path about greenhouse effect. It would indeed be impossible to accurately predict volcanic eruptions or variations in the solar heat flux that would have a significant impact on the climate changes. Two different forecasts are given below: the first analyses the temperature variation, the second the rise in sea levels. In both cases, two possible scenarios are reported that represent the two extremes: the blue RCP is representative of a system in which the greenhouse gas emissions are very limited, while the red one to one where emissions are not limited effectively. In the case of uncontrolled emissions, a significant increase in temperature is expected, even up to 6°C by 2100. By managing instead to strongly control the release of greenhouse gases and particularly of CO₂, the temperature could remain constant or increase slightly, without departing excessively from the current one (2°C difference). In reference to the rise in sea level, we have a catastrophic prediction with a one-meter rise (red RCP) and a more calming one with a value of around 40 cm (blue RCP).

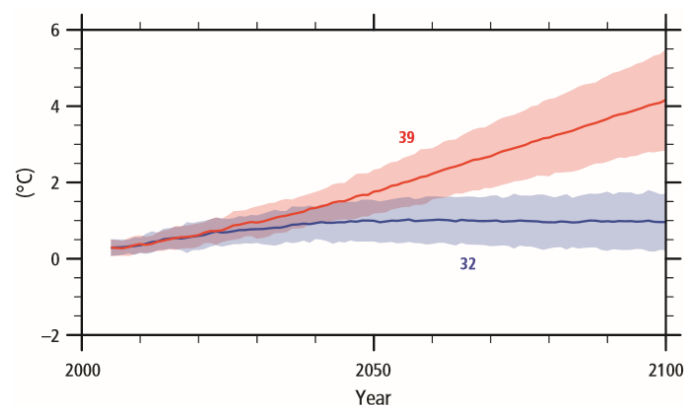


Figure 1.17 Projections of temperature difference. Source[IPCC Side Event ,2018].

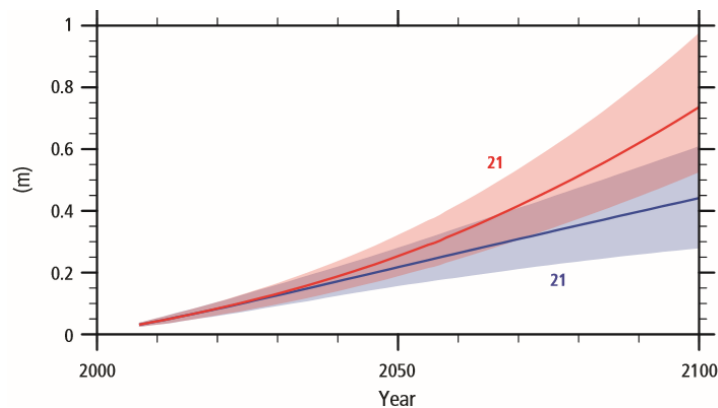


Figure 1.18 Projections of sea level increase difference. Source [IPCC Side Event ,2018].

After taking note of the problems related to global warming and the anthropogenic causes to its, basically, some governments have decided to try to stem it by establishing international agreements. Surely the best known is the Kyoto protocol initialled in 1997 which obliges its signatories to commit to the maintain greenhouse gas emissions below a certain threshold. Over time, other agreements were made and in 2015 the 21st annual session of the UNFCCC ("United Nations Framework Convention on Climate Change") Conference of the Parties took place, during which 196 countries unanimously decided to take a common road to limit gas emissions greenhouse and stem global warming. The political choices follow the guidelines proposed by the IPCC which are based on two parallel paths: the mitigation and adaptation. As far as mitigation is concerned, the will is to reduce overall the emissions of greenhouse gases and in particular CO₂. To reach this objective, the methods are manifold:

- Energy saving: with a reduction in consumption, for example, by encouraging energy efficiency measures (increase in the efficiency of the plants that produce electricity or in the devices that use it);
- Use of strong renewable or nuclear energy, reducing dependence on fossil sources;
- Use of clean and less impacting fuels;
- Reforestation and other measures to imprison carbon dioxide in a natural way;
- Separation and storage of CO₂ artificially.

The thesis work focuses precisely on this last point and for this reason, the next chapter is dedicated to an in-depth study of this theme through a description of the different techniques used.

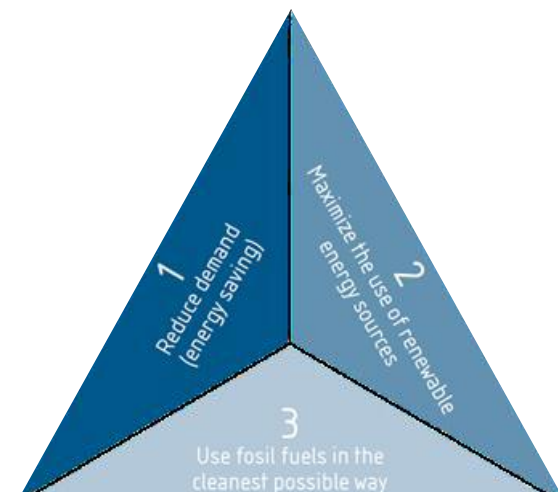


Figure 1.19 TRIAS energetica. Source [Freiburg,1996]

1.6 Objectives

As has already said, it is not possible to change immediately the entire energy park, which is mostly based on fossil fuels, to renewable sources. It is a long path and in the meantime, one intermediate solution that could be rapidly applied at large-scale is to capture CO₂, which consists in separating and capturing CO₂ from combustion and process gases instead of releasing it to the environment. The main processes configurations are pre-combustion capture, post-combustion capture and oxyfuel-combustion.

- Post-combustion: CO₂ is captured from exhaust fumes after the combustion of fossil fuels. For instance, this could be done by absorption in a suitable chemical solvent. In this case, the CO₂ is then separated from the solvent and compressed to be transported and stored. Other methods of post-combustion separation are high-pressure membrane filtration, cryogenic separation, adsorption. This process is suitable for implementation in existing plants since working on the flue gas does not require any modification of the upstream components.
- Pre-combustion: The fuel is converted before combustion into a mixture of hydrogen and carbon dioxide using a process called gasification. The carbon dioxide can then be separated, transported and stored, while hydrogen, can be used as a fuel for electricity generation and, potentially, to power hydrogen cars. A typical example of this process is an Integrated Gasification Combined Cycles (IGCC) plant in which coal is transformed into syngas before combustion of the CO₂-free hydrogen.
- Oxyfuel or oxygen combustion: This process involves the use of pure oxygen, or highly enriched air, in the combustion chamber. This type of combustion mainly produces steam and concentrated carbon dioxide, which is easier to separate (only needs to condensate water out). CO₂ is then sent to storage.

The CO₂ captured can be then re-used or stored (CCS-“Carbon Capture and Storage”, CCU- “Carbon Capture and Utilization”). CO₂ captured in one of the above ways can be transported, usually in a liquid or supercritical state, by various carriers such as ships with special tankers or pipelines. During the transportation in pipeline, it is important that the CO₂ is maintained in liquid or supercritical conditions. For this reason the pressure maintained is around 100 bar, in addition water and oxygen must be removed to prevent corrosion. Instead, in ship transportation the CO₂ is cooled down to -30°C at 20 bar in a liquefaction unit (IPCC,2016).

In this work two technologies will be compared from an economic and energy point of view. In the collective industrial panorama, there are many realities that present small or medium sized plants that participate to the emissions of CO₂. The technologies for the capture of these are not yet available in the market and the purpose of this study is precisely to study the economic and design feasibility of them. There are not many researches or projects on CO₂ capture systems from flue gas in at small or medium scale. For this reason, in the present work will make an in-depth study of two technologies, membrane separation and amine absorption (adsorption being analysed in a different work). The comparison of both will be made through the construction of the respective plant models applied to a cogeneration plant installed at the University of Liège. The goal for each technology is the capture of most of the incoming CO₂ and the achievement of a high degree of purity of CO₂ in the product stream. The exact capture rate does not need to be 100%, as decreasing the capture rate may be relevant to achieve high performance at low costs. Once these conditions are reached, the technologies will be compared from an economic and energy point of view. With two economic models the capital costs (CAPEX) of technologies have been assessed. The methods applied for their calculation are similar in the results for equivalent components, it was necessary to apply both for the same analysis as some components in one were not in the other and vice versa. From the capital cost then the operating cost (OPEX) was derived and to this was added the cost purely due to energy consumption. The latter differs considerably between the two technologies because amines need thermal energy while membranes need mostly electrical energy. The energy analysis focused precisely on the different type of energy consumed and the different end-use. Finally, again regarding the energy analysis, the heat and cold requirements for the respective technologies were calculated. While membranes only need to remove heat, amines need to supply it and remove a little amount in some parts of the plant.

The introduction of Chapter 1 discussed the problem of global warming, the greenhouse effect and all the natural phenomena arising from it.

Chapter 2 reports the different technologies concerning CO₂ capture and the different cases in which they are used are reported. In addition, an objective comparison is made between them, highlighting the advantages and disadvantages of each of them.

Chapter 3 is a literature review on membrane technology. In this chapter, key facts about membranes are reported such as the history of membranes, the advantages and disadvantages of this technology and the physics that govern the phenomenon of separation. In addition, the different types of membranes are presented both according to the type of module technology and the type of materials.

Chapter 4 Impurity effect due to NO_x, SO_x and humidity is treated. Two experimental test are reported to valorise the further assumption on membrane life reduction.

Chapter 5 presents then the case study concerning the co-generation plant installed at the University of Liège, which provides both electricity and hot water to the campus. The purpose of this work is to find an economical solution for capturing its CO₂ emissions.

Chapter 6 It explains what the guidelines are to proceed with the construction of a model and the phases of its construction are presented. So, speaks about the development of the membrane model and explains how the basic membrane model was built on Aspen Custom Modeler and then how this was implemented on Aspen Plus. Subsequently, the different configurations with both counter-pressure and vacuum operation were studied and then led to the final configuration capable of achieving a purity level of 99% and stage-cut over 80%.

In Chapter 7 the technology of amine absorption and the operation of the main components is presented. The chapter studies the separation by amines and explains how modifying some parameters of a pre-existing model on Aspen Plus can achieve our separation goals.

In Chapter 8 an economic analysis of the two technologies is made, which shows the capital and operating costs of each technology and also shows the greater or lesser energy consumption.

Finally, the conclusion highlights the main findings of this work and suggests some perspectives for future developments within this research project.

Chapter 2: CO₂ capture systems

One of the possibilities to slow down global warming is to reduce emissions of greenhouse gases and carbon dioxide, which is the main cause of this phenomenon. To do this, as already stated in the previous chapter the roads are numerous. This chapter starts with an analysis of the different options for CO₂ capture that are usually part of larger technological systems such as Carbon Capture and Storage (CCS) or Carbon Capture and Utilization (CCU). The first distinction that is usually done is depending on the source of the CO₂ that can be atmospheric air, or industrial gas. Then, different configurations of CO₂ capture systems already mentioned in Chapter 1 (pre-combustion, post-combustion, and oxyfuel capture) will be described with more details.

Direct capture of CO₂ from the air:

considering the low concentration of carbon dioxide in the Earth's atmosphere, about 415,22 ppm [NOAA/NCEI, 2020], its separation from the air would seem to be far from a sustainable process. However, we must take into account the enormous amount of volume available. The separation is usually carried out using solid adsorbents. The efficiency of these systems, however, is very low and these technologies should rather be seen as long-term techniques. The research on this technology is still growing but with good results. The big questions are the practicality in large scale plants and the lack of accurate cost estimates which need more studies. Despite this, capture is feasible and many aspects of it point out the interest for this technology.

In the work “The urgency of the development of CO₂ capture from ambient air” [Klaus S. Lackner, 2012], long term considerations are made. Large scale plants could create net negative emission. In the model of Cao and Caldeira's, the authors indicate that the major part of the excess CO₂ currently being stored in the oceans and on land (vegetation) will rapidly be returned to the atmosphere. It is important to quantify the role that air capture could play in atmospheric CO₂ reduction and also the right time to apply the measures. It is possible to consider two scenarios.

For the first one, average emissions between today and 2050 will have raised atmospheric level by 1,5 ppmv/year, leading to 450 ppmv. Probably by 2050 the energy consumption will be doubled but at the same time generation efficiency and a shift in energy mix will have reduced fossil fuel consumption by one third leaving 20 Gt CO₂/y to be dealt with by CCS and air capture which, in this scenario, will remove 10 Gt CO₂/y from the atmosphere. By assumption, the price of captured CO₂ from air has become affordable, i.e., less than \$50/t CO₂. Worldwide, annual air capture costs would add up to as much as \$500 billion. For comparison, at \$100/bbl, the annual cost of US oil consumption (19.5 million bbls/d) amounts to \$712 billion. If stabilization at 450 ppmv is sufficient, further ramping up of air capture would not be necessary. Thus, a reduction rate of CO₂ in the air comparable to today's emission rate is feasible within a decade provided there is the perception of urgency and the political will to solve the problem. If it is decided that 350 ppmv is the safe target, it would take about five decades to return to those levels.

In the second scenario, it is supposed that the world ignores CO₂ emissions issues, leading to an increase of 3 ppmv/y through 2050. So the concentration will be 510 ppmv and an annual rate of increase in atmospheric CO₂ concentration of 4 ppmv in 2050. For 2100 with the same rate the level would exceed 700 ppmv. Stabilizing at 350 ppmv by 2150 would require an annual reduction of 7 ppmv. This scale is enormous, and it would be much more difficult for air capture to help solve this problem than the problem in the first scenario.

Hence, it is understandable that a reduction by 100 ppmv may be plausible while a reduction by many hundreds of ppmv is likely to be prohibitively expensive, even if one assumes cost-effective implementations of air capture technology. This example demonstrates that the possibility of affordable air capture technology does not provide any justification for a delay and overshoot global strategy. [Klaus S. Lackner, 2012]

Capture from CO₂-rich gases:

the power plants related to the production of thermal or electrical energy represent the largest emissions. As far as transport is concerned, carbon dioxide capture is rather difficult because of various factors (among other the compacity required for transport applications) and therefore the best solution is linked to the use of increasingly "cleaner" fuels, coming from renewable sources or carbon-free, as in the case of hydrogen or electro fuels that are based on CO₂ and renewable hydrogen. With reference to power plants, the capture and

storage of CO₂ can be pursued through different options depending on the configuration of the systems themselves.

Below are represented in a schematic way different processes for CO₂ capture. These processes are described in the following section, except for industrial processes, which depend on the specific industrial configuration of the plant (such as cement plant or steel mills for instance):

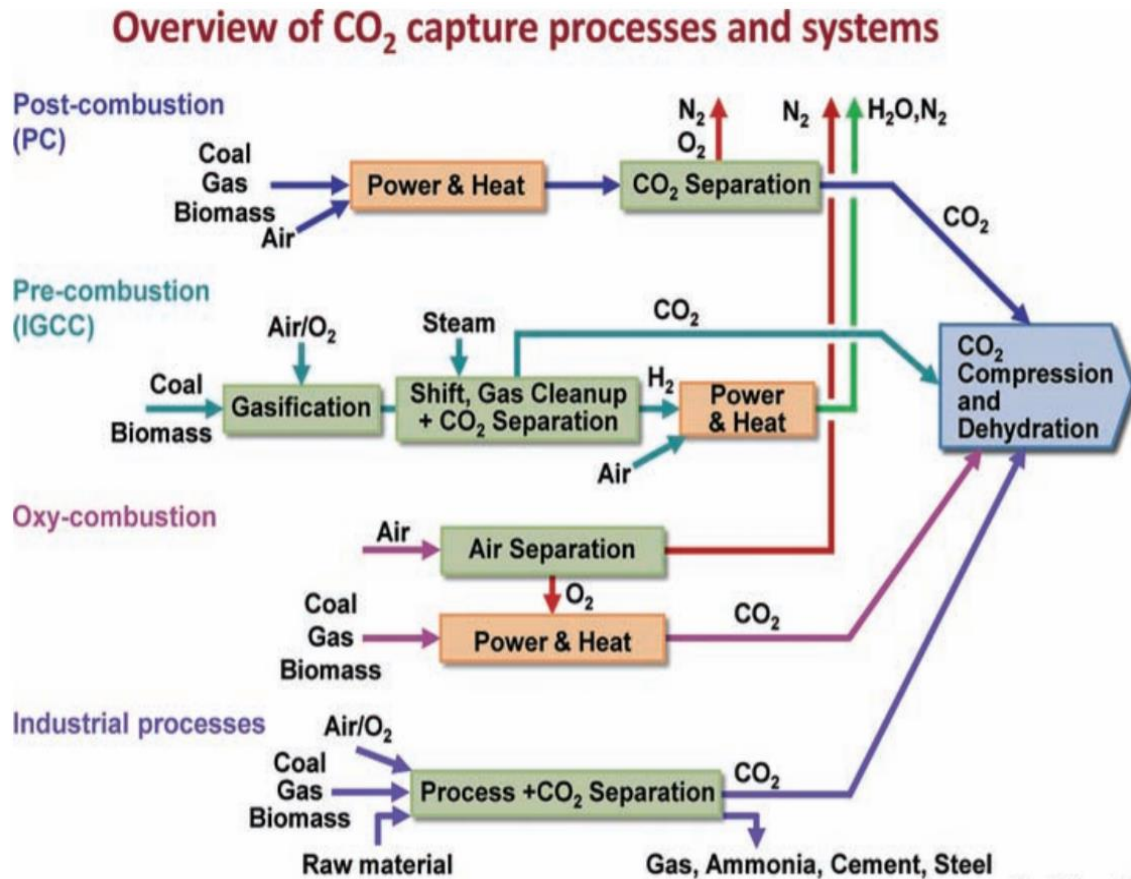


Figure 2.1 Flow sheet representation of CO₂ capture process. Source [EASAC, 2013].

2.1 Pre-Combustion Capture

This configuration consists in the separation of CO₂ before the fuel combustion, be it fossil fuel or biomass. Using steam reforming or gasification processes, the carbonated fuel is converted into CO₂ and H₂. If the gasification and the electricity generation from H₂ take place in the same process using gas and steam turbines, then the process is called integrated gasification combined cycle (IGCC). Alternatively, hydrogen may be used for other purposes (ammonia production, steelmaking...).

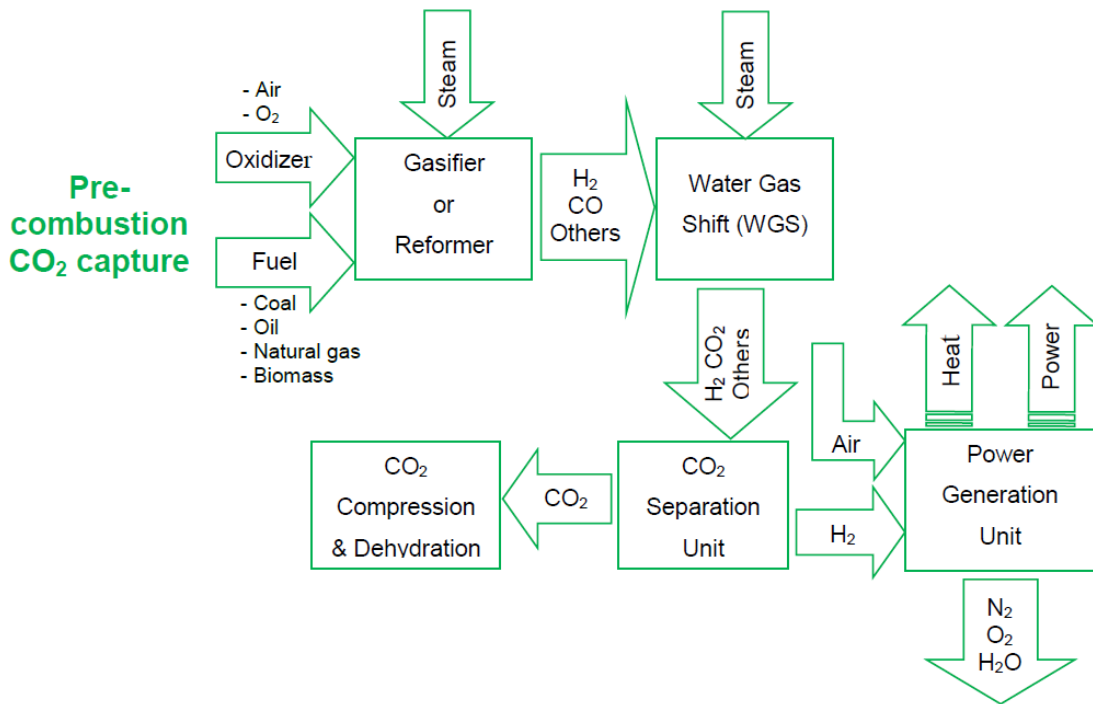


Figure 2.2 Pre-Combustion Capture scheme process. Source [José D. Figueroa, 2008].

The first step is characterized by the formation of Syngas (Synthesis gas), which is a gaseous mixture composed mainly of carbon monoxide and hydrogen. Rather than directly exploiting the syngas to produce energy or chemicals, it is first pre-treated with steam in a Water Gas Shift (WGS) reactor to shift all the carbon into CO₂ molecules and to produce more hydrogen, which are then separated from each other. Since syngas is rich in CO content, the reaction that will occur most is:



Where H₂O is added in large amounts under the form of steam, to push equilibrium towards the products. The pre-combustion process is already used in some industrial applications like the H₂ production for ammonia synthesis.

However, some drawbacks characterize this technology:

- To drive WGS reaction, large amounts of steam have to be produced; of course, this has a non-negligible cost.
- Separation of CO₂ from H₂ is usually done with physical solvents due to the large CO₂ partial pressure. This makes it easier than in post-combustion capture, but nevertheless also implies an energy penalty.
- Since in pre-combustion capture process the fuel is decarbonized, the molecule that will release energy is H₂. If this occurs by combustion, there is a need for turbine design to accommodate H₂-firing power plants (H₂ combustion will involve very high temperature, which may damage turbine blades material).
- Pre-combustion capture exists only in combination with the gasification system, therefore their feasibility is strictly related to the feasibility of the gasification system.

2.2 Post-Combustion Capture

In the post-combustion CO₂ capture, CO₂ is separated from the flue gas resulting from the fuel combustion. Typical CO₂ concentrations in the flue gas vary from 3% to 15% depending on the fuel type, the main flue gas

component will be N_2 being brought with the combustion air. This method is also our case of study in which we want to evaluate the most profitable technology for post-combustion capture in small scale plants.

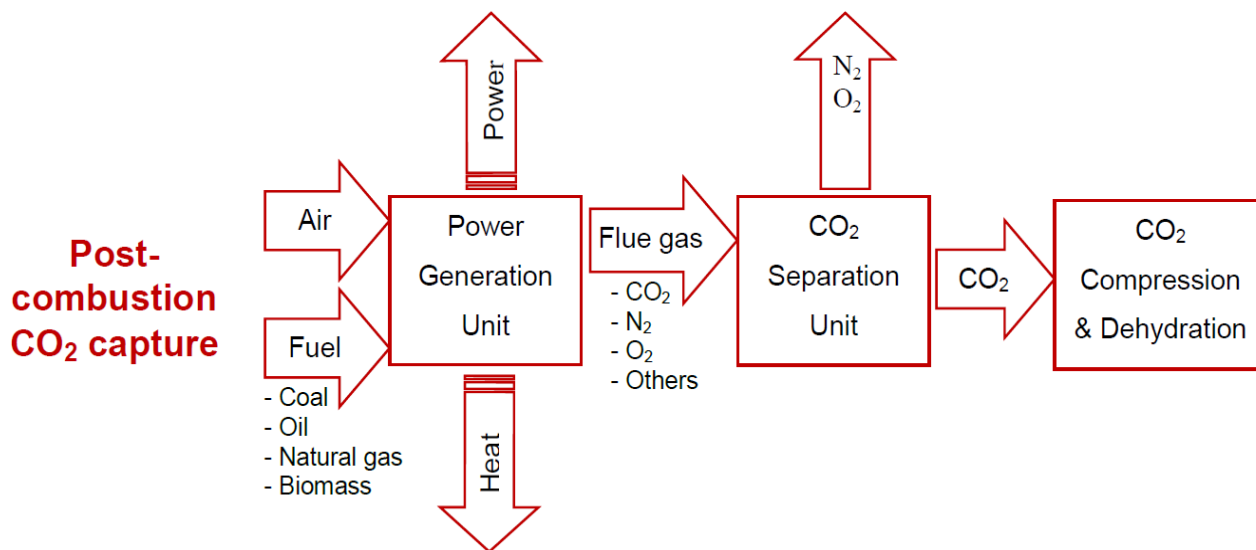


Figure 2.3 Pre-Combustion Capture scheme process. Source [José D. Figueroa, 2008].

The most used capture technique is the solvent loop with chemical absorption and regeneration. Typical post-combustion units can capture 85%-95% of the CO_2 present in the fuel gas. The process is named chemical wash: the gas flow is set in contact with a solvent in an absorption column. The solvent is very often a mixture of water and amine. Amines are organic groups like ammonia, in which hydrogen atoms have been replaced by hydrocarbon groups. For instance, here is the chemical structure of the benchmark solvent for CO_2 capture, monoethanolamine (usually a 30 wt% solution in water).

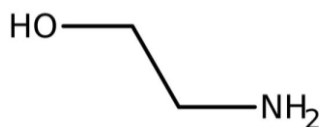


Figure 2.4 Monoethanolamine structure.

Other technologies exist to separate CO_2 from combustion gases, such as cryogenic separation, use of biotechnologies (algae for instance), ... In the present work, we will focus on two other technologies. The first one is the use of a membrane for the separation of CO_2 from flue gas. Using the chemical potential gradient due to the difference of concentration, the permeability of the gas through the membrane and the pressure gradient, it is possible to separate CO_2 . This technology is less mature than the previous one but its use in small case plants can be determining as it allows a compact design of the CO_2 capture unit.

The last technology also relevant is the PSA (Pressure swing adsorption). In adsorption processes, one or more components of a gas or liquid stream are adsorbed on the surface of a solid adsorbent and separation is obtained [Lopes FVS, 2011]. This process differs from absorption, in which a fluid (the absorbate) permeates or is dissolved in a liquid (the absorbent). Note that adsorption is a surface-based process while absorption involves the whole volume of the material. After the adsorption step, when the adsorbent bed is almost saturated, the flue gas flow is stopped and the bed is regenerated through a pressure decrease (Pressure Swing), a temperature increase (Temperature Swing, TSA) or a combination of the two (Pressure and Temperature Swing, PTSA). The adsorbed components (adsorbate) are thus desorbed and recovered, and the solid adsorbent is ready for

another cycle of adsorption. However, in this work we will not go into further detail on the PSA but we will limit ourselves to its presentation.

2.3 “Oxyfuel” capture in combustion

The oxy-combustion CO₂ capture process (OxyCCC) eliminates nitrogen from the flue gas by combusting a hydrocarbon or carbonaceous fuel in either pure oxygen or rather a mixture of pure oxygen and a CO₂ rich recycled flue gas [IPCC, Climate change, 2014]. Indeed, combustion of fuel with pure oxygen has a combustion temperature of about 3500°C, which is far too high for typical power plant materials. The combustion temperature should be limited to about 1300-1400°C in a typical gas turbine cycle and to about 1900°C in an oxy-fuel coal-fired boiler, using current technology. The methodology commonly implemented to moderate the temperature is thus to recirculate a fraction of the flue gas to the combustor. The flue gas resulting from an oxy-combustion has a high concentration of CO₂ and water vapor. CO₂ can be separated from water by condensing the water out and further low-temperature purification processes can be used if a deep water removal is required. Nevertheless, other impurities may be present depending on the fuel used (e.g. SO_x, NO_x, HCl, Hg), on the diluents in the oxygen stream supplied (e.g. N₂, Ar, excess O₂) and on possible air leakage into the system.

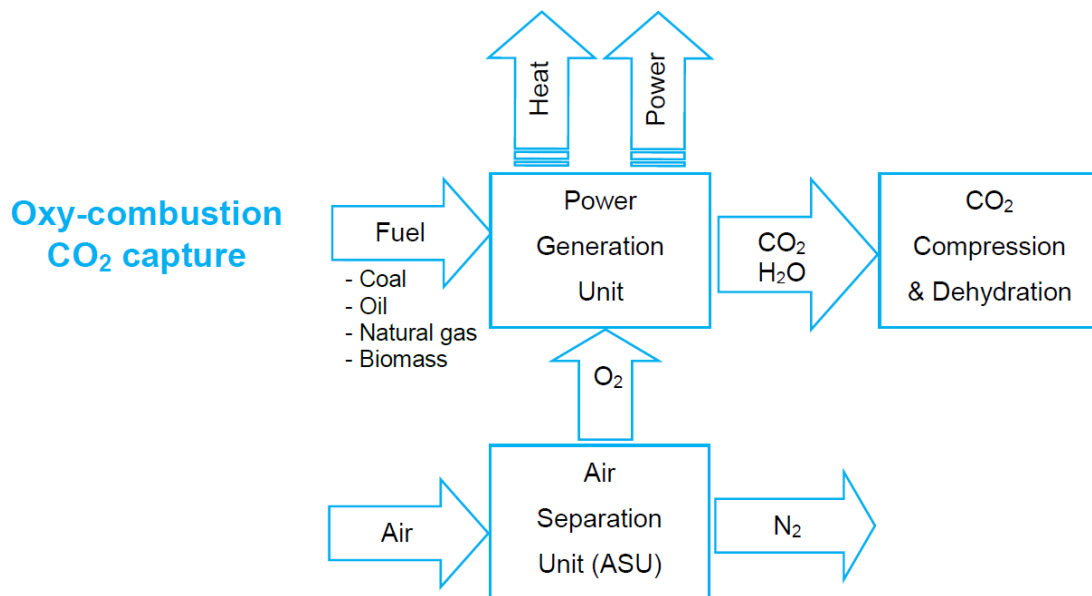


Figure 2.5 Oxy-combustion CO₂ capture process. Source [José D. Figueroa, 2008].

The concentrated CO₂ stream is then compressed and transported by pipeline. The degree of separation obtained in this way is very high, with mixtures of 96% CO₂. Although elements of oxy-combustion technology are already in use in the aluminium, iron and steel and glass melting industries, oxy-combustion technology for CO₂ capture has yet to be deployed on a commercial scale. Medium-scale testing combined with targeted laboratory studies have provided fundamental scientific knowledge and have generated experience with the large individual and integrated unit operations [Ahn S., 2012]. However, large-scale demonstration of the technology is still required.

2.4 General Comparison of technologies

A wide comparison can be made between these three major processes, in particular in the table below (Table 1) are reported all advantages and disadvantages of each one:

Table 1 Advantages and disadvantages of different CO₂ capture approaches. Source [José D. Figueroa, 2008].

	Advantages	Barriers to implementation
Post-combustion	<ul style="list-style-type: none"> • Applicable to the majority of existing coal-fired power plants • Retrofit technology option 	<p>Flue gas is ...</p> <ul style="list-style-type: none"> • Dilute in CO₂ • At ambient pressure <p>... resulting in ...</p> <ul style="list-style-type: none"> • Low CO₂ partial pressure • Significantly higher performance or circulation volume required for high capture levels • CO₂ produced at low pressure compared to sequestration requirements
Pre-combustion	<p>Synthesis gas is ...</p> <ul style="list-style-type: none"> • Concentrated in CO₂ • High pressure <p>... resulting in ...</p> <ul style="list-style-type: none"> • High CO₂ partial pressure • Increased driving force for separation • More technologies available for separation • Potential for reduction in compression costs/loads 	<ul style="list-style-type: none"> • Applicable mainly to new plants, as few gasification plants are currently in operation • Barriers to commercial application of gasification are common to pre-combustion capture • Availability • Cost of equipment • Extensive supporting systems requirements
Oxy-combustion	<ul style="list-style-type: none"> • Very high CO₂ concentration in flue gas • Retrofit and repowering technology option 	<ul style="list-style-type: none"> • Large cryogenic O₂ production requirement may be cost prohibitive • Cooled CO₂ recycle required to maintain temperatures within limits of combustor materials • Decreased process efficiency • Added auxiliary load

Table 2 Overview of development of post-combustion capture and high-temperature solids-looping processes. Source [2019 IEAGHG report].

TECHNOLOGY		TRL AT PREVIOUS REVIEW	CURRENT TRL	CURRENT DEVELOPMENT TRAJECTORY	PREDICTED LCOE DECREASE C.F. STANDARD TECHNOLOGY
Liquid absorbents	Aqueous amine	6–9	6–9	→	Low
	Amino acid and other mixed salts	–	6	↑	Low
	Ionic liquids	1	4	↓	–
	Encapsulated absorbents	1	2–3	→	–
	Water-lean absorbents	–	5	↑	Medium
	Precipitating	4–5	4–6	→	Medium
	Liquid–liquid separating	4	4–5	↑	Low
	Catalysts	1	6	↑	Medium
Membranes	Polymeric membranes	6	6	↑	Low
	Membrane contactors	–	5–6	→	Medium
	Hybrid processes	6	6	↑	Medium
Solid sorbents	Pressure-swing adsorption (PSA) and temperature-PSA	3	6	→	Medium
	Temperature swing adsorption	1	6	↑	Medium
	Ca looping	6	6	→	Medium
Cooling and liquefaction		3	5	→	Medium
Electrochemical separation		1	4	↑	High
Algae-based capture		1	4	↓	–
Direct air capture		–	5	→	–

↑ = the technology has commercial backing, and/or large scale evaluation/ demonstration of the technology is either currently underway or planned

→ = while there may be ongoing pilot-scale demonstrations, there are no plans at present for larger-scale demonstration, or the technology is not being progressed by a commercial partner

↓ = while some pilot or laboratory-scale evaluation has occurred, current research is at a less advanced scale than previous levels

So each capture process has different characteristics and particularities which are more or less feasible especially in function of the type of plant. In this case of study, the cogeneration plant of Liegi University already exists, so it is more reasonable to use post-combustion process.

Several technologies are present in the literature for each process. For post combustion, three technologies have been selected among the possible choices, namely amine absorption, membranes and adsorption. Amine technology has been selected as a benchmark for comparison, being the most mature available technology. Then, membranes and adsorption have been selected as they are compatible with post-combustion capture (for a retrofit of existing plant), their level of maturity is reasonable (better than amino-acid or ionic liquid absorption for instance) and they are per nature modular technologies (based on surface rather than volume), so they would be well suited for compact plants and small-scale units.. In Figure 2.5 the most important technologies are reported, and the figure points out the cost reduction benefit in function of the time necessary for the commercialisation.

Chapter 3: Membrane literature review

3.1 Membrane gas separation history

Research on membrane gas separation mainly expanded in the last three decades. Smith (2020) studied the history of membrane technology starting from the initial idea of Graham (1866). In the early 1970s, the basis for modern membrane gas separation was created through the development of high-flux asymmetric membranes and large-surface-area membrane modules for reverse osmosis applications. In 1980, Monsanto launched its hydrogen-separating Prism membrane [Henis and Tripodi, 1980]. Cynara, Separex, and Grace Membrane Systems started producing membrane plants to remove carbon dioxide from methane in natural gas in the mid-1980s. Dow also launched its first commercial membrane system for nitrogen separation from the air around at the same time. Also, the applications of gas separation membranes are expanding from dehydration of air and natural gas to organic vapor removal from air and nitrogen streams [Baker, 2002]. Strong research is done for introducing energy-saving technologies by focusing on the creation of advanced membrane materials, development of high-efficiency modules with a large amount of area per unit volume, controlling capability of microscopic transport phenomena inside the membrane, and high-speed manufacturing method [Kookos, 2004].

3.2 Principal features of membrane gas separation

The properties of membranes make them ideal for industrial operation. Below are reported the most attractive characteristics compared with other separation methods also used in industrial sector [Mulder, 1996] :

- Low maintenance costs, due to absence of moving parts.
- Absence of phase and temperature change phenomena, leading to lower energy requirement.
- Easy plant operation due to steady continuous process.
- Ideal for use in offshore platforms, where space and portability are very important factors.
- Easy to scale up based on laboratory or pilot-scale data to modular design of membrane.
- Can easily be combined with other separation processes (hybrid processing)
- Low environmental impact due to absence of chemical additives.

Despite these characteristics there are some disadvantages:

- Their lifetime is short with respect to other technologies.
- The probable presence of impurities in flue gas leads to low efficiency and life decrease.
- Expensive fabrication method.
- Incapability to handle corrosive substances.
- For polymeric membranes, high flue gas temperatures are not sustainable.

These last aspects of membrane are the most studied in the moment, and good results have been achieved regarding the operating performance at high temperature and impurity. However, the industrial production of these membranes is still not efficient so they are not yet produced in large scale. [R. W. Baker, 2012]

3.3 Types of gas separation membranes

The use of membrane is the simplest technology for gas separation. Industries use the membrane for different tasks, in this chapter we will see how they differ from each other for the different uses and a focus will be done regarding their use in CO₂ capture process. For example, in industrial scale they are often installed in low-capacity plants for CO₂ removal in natural gas streams. Membranes with high permeability and selectivity is the most wanted one for specific gas separation processes along with other properties such as stable, thin, low-cost and package-able into high-surface-area modules. Typical membranes installed are polymeric hollow fibres permeable to CO₂, water, ammonia, and to a minor extent to methane and nitrogen. Research is nowadays focused on the development of new membrane materials with increased performance such as metal organic frameworks (MOFs), mixed matrix membranes (MMMs), or composite carbon molecular sieve

membranes (CMSMs). However, the experience with these membranes is limited and still more research on the preparation methods, precursor materials, and long-term measurements are required, and economics evaluations are missing. All these different materials applied to membrane construction will be addressed in the following paragraphs. Membranes can be sorted according to different criteria. In the following, we first study the membranes based on the type of selective process they are used for. Then, membranes will be described in light of the technology used and main membranes materials will be presented. Finally, main way to make membrane modules will be described.

3.3.1 Classification according to the selective process.

The size-separation membranes exploit the difference in size between the molecules of the gas mixture. In particular, only small molecules are able to cross the barrier and a rich atmosphere is generated in low-pressure permeant gas. Reverse separation membranes, instead, are based on the interaction between the barrier and the permeant gas [C.Lau and P.Li , 2013]. The solubility and selectivity ensure that specific molecules, although possibly larger than others, they can get through the membrane [D. Havas and H. Lin, 2017]. A diagram of the operation of these two types of separation is shown in the figure below. Regarding CO₂ capture reverse separation appears to be more efficient and has a greater margin of improvement. [D. Havas and H. Lin, 2017]

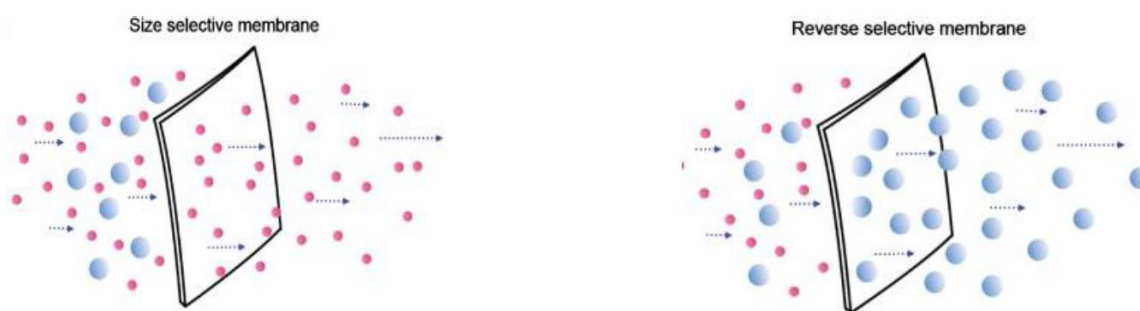


Figure 3.1 Separation mechanism through size on the left and indirect selectivity on the right. Source [D. Havas and H. Lin, 2017].

In Table 3, are reported the kinetic diameter¹ and critical temperature of different gases, as they influence the permeability of these gases through the membrane. The CO₂ molecule is a little smaller than the N₂ molecule, thanks to a more compact shape, therefore it is characterized by greater diffusivity; in addition to this, it has a high solubility in most polymers for example. It is known that the solubility of a gas in a polymeric membrane solid is very favoured by its ability to go into condensed phase. One measurement of condensability is the critical temperature T_c, in particular high critical temperatures indicate a strong condensability. Then this favours CO₂, which has a T_c of 305.4 K against a value of nitrogen equal to 126.2 K.

¹ **Kinetic diameter** is a measure applied to atoms and molecules that expresses the likelihood that a molecule in a gas will collide with another molecule. It is an indication of the size of the molecule as a target.

Table 3 The kinetic diameter and critical temperature of some common gases in gas separation process.

Gas	Kinetic diameter (Å)	Critical Temperature (K)
CO ₂	3.30	304.2
N ₂	3.64	126.2
CO	3.76	132.9
SO ₂	3.60	430.8
H ₂ S	3.60	373.2
NO	3.20	180
H ₂ O	2.65	647.3

3.3.2 Classifications according to the technology used

There are three technologies mainly applied [P. Luis and T. Gerven, 2012]: nondispersive contact, supported liquid and permeation.

3.3.2.1 Through non-dispersive contact

As shown in Figure 4.2 membranes based on the principle of non-dispersive contact separate the gas mixture from a liquid absorbent. In this case the membrane is porous and has no reverse selectivity, but its main task is to increase the contact area between the surface of the gaseous and liquid phase. The liquid used behaves exactly like an absorber, chemical or physical, which is therefore capable of capturing CO₂ quickly. Two aspects play a fundamental role in these systems: the porosity of the membrane that indicates the extent of the area of interaction between the two phases and the affinity of the absorber to CO₂.

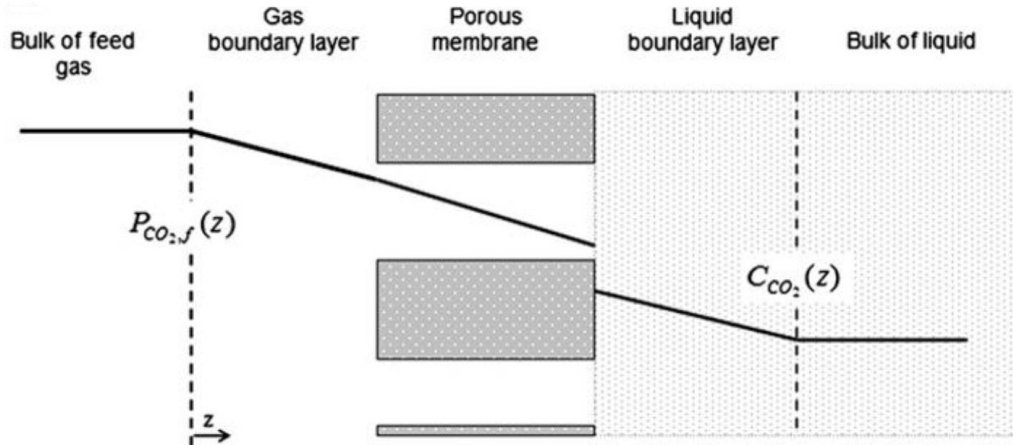


Figure 3.2 Separation process through non-dispersive contact. Source [P. Luis and T. Gerven, 2012].

By effectively studying the size of the pores, the morphology of the membrane, the characteristics of the liquid absorbent and the interaction between these two elements it is possible to modify these parameters and consequently the mass transferred. In relation to the simple absorption process, more flexibility is achieved regarding the characteristics that the gaseous mixture must possess. In addition, increasing the contact area increases absorption efficiency. It is possible to achieve a reduction in regeneration energy consumption and the membrane ensures that the liquid absorbent is not consumed.

With respect to other techniques that exploit the membranes, the process seems to be more effective because the porosity guarantees excellent kinetics of absorption and the choice of the correct liquid guarantees an excellent degree of selectivity. The critical aspects are the wettability of the membrane, which slows down the

gas flow, and the low stability of the system over time due to absorbent volatility and possible membrane-liquid interactions.

3.3.2.2 Supported-liquid membranes

The correct term for these systems should be "imprisoned liquid membranes". Like visible in the Figure 4.3, a substance in the liquid state is blocked on the surface or inside the membrane. The growing interest in this possibility is linked to the use of ionic liquids in the capture of the CO_2 , which can be trapped by modifying the properties of the barrier. The liquid phase attracts selectively the carbon dioxide that permeates through the membrane driven by the pressure difference maintained between the two sides of the membrane to ensure gaseous flow.

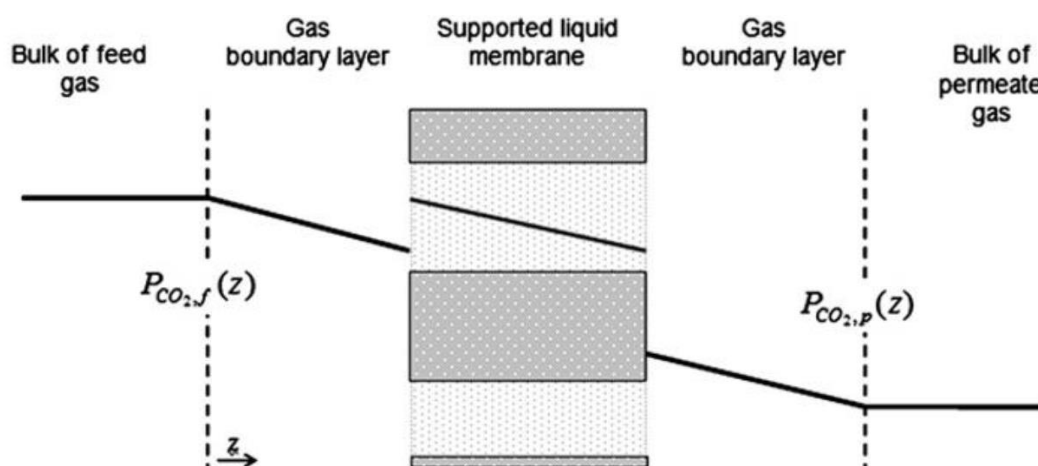


Figure 3.3 Separation process through liquid support. Source[P. Luis and T. Gerven, 2012].

Polymeric membranes allow great flexibility in such system, mostly considering the interactions with the present liquid phase, which must permeate and remain trapped. The use of inorganic membranes appears indeed difficult, especially with amines as an absorbent phase. These compounds, in fact, have high volatility and therefore they are not good for imprisonment. The solution seems to be the use of ionic liquids with zero volatility, ensuring the necessary stability. Another parameter that affects this aspect is the viscosity which must have the right balance: if it is excessively high it affects the gas permeability and thus separation efficiency, whereas if too low, the loss of the fluid component would be a problem.

3.3.2.3 Permeation method

The structure of a membrane can be macro-porous, micro-porous, or dense (non-porous). Only micro-porous or dense membranes are selective. However, macro-porous membranes are widely used to support thin micro-porous and dense membranes when significant pressure differences across the membrane exist. Although micro-porous membranes are topics of considerable research interest all current commercial gas separation processes are based on the dense polymer membrane, sometimes supported by a macro-porous layer (which is then called an asymmetric membrane). The membrane is not porous but dense and uses reverse separation to capture CO_2 , as the diagram in Figure 3.4.

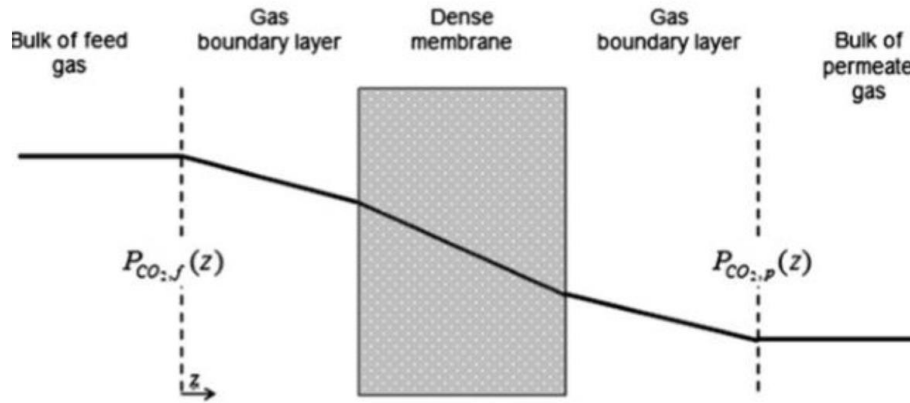


Figure 3.4 Separation process through permeation. Source[P. Luis and T. Gerven, 2012].

The transport through the membrane is one of the fundamental aspects to understand and to improve the process performance. Various models have been developed over the years to describe the transport rate. The choice of a transport model depends greatly on the separation under consideration, the membrane used and the purpose of the transport model. The various models, which do exist in literature to describe the transport of components through a membrane, are based on theoretical or phenomenological fundamentals. Theoretical models make use of molecular parameters, derived from thermodynamic and physical relations. Phenomenological models are based upon a theoretical background, but the values of their parameters have no fundamental meaning anymore. It is possible to divide the most relevant models to describe the transport of components through a dense membrane into; thermodynamics of irreversible processes, Maxwell-Stefan theory and solution-diffusion models.

- Thermodynamics of irreversible processes (TIP) is a phenomenological model for multi-component systems. The driving force is the chemical potential gradient (or for gas separation partial pressure gradient). A flux of a component can be caused by any other driving force in addition to its own conjugated force.
- Maxwell-Stefan theory is a theoretical model for system with up to three components. Theoretical models often require complex experiments to determine the fundamental parameters, such as the friction coefficients in the Maxwell-Stefan equation. As a result, the Maxwell-Stefan equations are only used for binary or ternary systems. The permeability of the gas is incorporated in the friction coefficient. Indeed, the driving force of a component is equal to the friction with other components and expressed as a linear function of the velocities. As a result, the fluxes are given implicitly. Therefore, also a correct solution model has to be used.

In this work the solution-diffusion model is assumed, so the gas at the high-pressure side of the membrane dissolves in the membrane and diffuses down a concentration gradient to the low-pressure side. It is further assumed that sorption and desorption at the interfaces are fast compared to the diffusion rate in the polymer. The gas phase on the high and low-pressure side is in equilibrium with the polymer interface. The permeants (component of permeate) are separated because of the differences in the solubility and mobility of the permeants in the membrane material. Diffusion is the process by which matter is transported from one part of a system to another by a concentration gradient. With polymeric materials it is possible to obtain barrier films with high selectivity and permeability ensuring in this way a very good process efficiency. Gas transport through most polymeric membrane follows in fact solution-diffusion mechanism which is based on the solubility and diffusivity of the gas in a material. Solution-diffusion mechanism relies on the solubility of species combined with chemical potential gradient to pass through the membrane as reported in the previous paragraph. The solubility of gas in the elastomeric polymer is very small and is described by equation 4.3. However, for steam or organic liquids which cannot be viewed as ideal, this law cannot apply. Instead, the diffusivity is the kinetic parameters that indicates how fast penetrants move through the membrane. Diffusivity depends on the geometry of the penetrant, so that when the size of the molecule increases the diffusion

coefficient decreases. However, the diffusion coefficient depends on the concentration and interactions so that even large organic molecules that can swell the polymer can have a large diffusion coefficient [R. W. Baker, 2012].

At steady state, gas diffusion through dense (nonporous) polymeric membrane can be described by Fick's first law:

$$j_i = -D_{if} \frac{dc_i}{dl} \quad (3.1)$$

where D_{if} is the gas diffusivity coefficient of component which is represented with the letter i . D_{if} is a function of temperature and the permeant concentration c_i for a given polymer-permeant system. For non-condensable gases, D_{if} is normally regarded as constant, independent of concentration. For condensable gases, it is generally considered concentration dependent due to the plasticizing effect of the permeant (swelling of the polymer membrane or interaction leading to morphological changes) [Paul, D.R. and Yu.P, 1994]. So D_{if} reflects the mobility of the individual molecules in the membrane material. The flux of permeate passing through the membrane is defined as the (j_i), which gives a measure of the amount of penetrant absorbed by the membrane under equilibrium conditions.

For a membrane thickness of l , integration of Eq. 4.1 over the membrane thickness gives:

$$j_i = -D_{if} \frac{(c_{i0(m)} - c_{il(m)})}{l} \quad (3.2)$$

The concentration of component i at the feed interface of the membrane can be written similar to Henry's law as:

$$c_{i0(m)} = K_i P_{i0} \quad (3.3)$$

where K_i (similar to Henry's constant of component i in a solvent) is the sorption coefficient of component i in the membrane. It reflects the number of molecules dissolved in the material, and P_{i0} is the feed side partial pressure in component i . Sorption coefficient is a function of temperature and may be function of pressure (or concentration). This law is valid when K_i is independent of ambient pressure and the penetrant concentration is directly proportional to ambient pressure.

The concentration of component i at the membrane-permeate interface can similarly be expressed as:

$$c_{il(m)} = K_i p_{i_l} \quad (3.4)$$

Combining Eqs. 4.3 and 4.4 with Fick's law, Eq. 4.2, gives:

$$j_i = \frac{D_{if} K_i (P_{i0} - p_{i_l})}{l} \quad (3.5)$$

The product ($D_{if} * K_i$) can be defined as P_i , which is called the *membrane permeability for component i* and is a measure of the ability of the membrane to permeate a specific gas i . The measure of the ability of a membrane to *separate* two gases i and j is the ratio of their permeabilities α_i , called the *membrane selectivity*:

$$\alpha_i = \frac{P_i}{P_j} \quad (3.6)$$

Eq. 4.5 can be written as:

$$j_i = \frac{P_i(P_{i0}-p_{il})}{l} \quad (3.7)$$

Eq. 3.7 is widely used to rationalize the properties of gas permeation membranes accurately and predictably. The solution-diffusion model described above can be utilized to elaborate relationship between polymer structure and membrane permeation. Baker (2000).

Another important parameter is the Fractional Free Volume (FFV). It is a nondimensional coefficient which represents the available void volume inside the membrane. It is calculated by the relative difference between total volume of polymer, V (macroscopic, measured), and the volume occupied by polymeric chains (V_{occ}), estimated with literature methods:

$$FFV = \frac{V-V_{occ}}{V} \quad (3.8)$$

For example, membrane separation performance for CO_2/N_2 separation from flue gas is mainly described using two parameters, namely CO_2 permeance and CO_2/N_2 selectivity. The CO_2 permeance is defined from (4.7) as:

$$J_i = \frac{P_{CO_2}}{l} = \frac{j_{CO_2}}{(P_{CO_2,0}-p_{CO_2,l})} \quad (3.9)$$

The permeance J_i indicates a material's attitude to the passage of matter or energy through the material itself. Is commonly expressed in gas permeation unit (GPU) or in barrer:

$$1 \text{ (GPU)} = \frac{10^{-6} \text{ cm}^3 \text{ (STP)}}{\text{cm}^2 \cdot \text{s} \cdot \text{cmHg}} = 7.501 * 10^{-(12)} * \frac{\text{m}^3 \text{ (STP)}}{\text{m}^2 \cdot \text{s} \cdot \text{Pa}} \quad (3.10)$$

$$1 \text{ barrer} = 3.35 * 10^{-16} \frac{\text{mol} \cdot \text{m}}{\text{m}^2 \cdot \text{s} \cdot \text{Pa}} = M * 3.35 * 10^{13} * \frac{\text{g} \cdot \text{cm}}{\text{s} \cdot \text{cm}^2 \cdot \text{bar}} = 10^{-10} \frac{\text{cm}^3 \text{ (STP)} \cdot \text{cm}}{\text{cm}^2 \cdot \text{s} \cdot \text{cmHg}} \quad (3.11)$$

The CO_2/N_2 selectivity is expressed as the ratio of CO_2 permeabilities over N_2 permeabilities as shown by equation (4.6). The main goal of membrane-based CO_2 separation is to achieve high CO_2 recovery (>90%) with high CO_2 purity (>95%) from flue gas. In order to do so, high CO_2 permeance and selectivity are required [Y. Chen , 2016]. So, from (4.6):

$$\alpha_{CO_2/N_2} = \frac{P_{CO_2}}{P_{N_2}} \quad (3.12)$$

3.3.3 Classification according to material

3.3.3.1 Polymeric membrane

The energy required for regeneration of the system is low compared to all the other technologies likewise amine absorption and PSA. When referring to polymeric membranes, the most common ones are based on cellulose acetate (CA), cellulose triacetate (CTA), polysulfone (PSf), polydimethylsiloxane (PDMS), polymethylpentene (PMPS), polycarbonate (PC), polyimides (PI), and polyamides (PA) (Nunes and Peinemann, 2001) [Nunes.S. and Peinemann, 2001]. Regarding commercial polymeric membranes, CA based membranes are the earliest and the most used glassy polymeric membranes, accounting for around 80% of the total commercial polymeric membranes installed. These membranes reach a working lifetime of 3.5 years, even when operated under harsh conditions of H_2S and increased CO_2 concentrations.

However, a common problem for all polymeric membranes is the plasticisation effect. Where an adsorbed gas (CO_2 or organic vapours) causes a swelling of the polymer matrix. This effect leads to a larger inter-chain spacing within the polymer, accelerating the diffusion of gases, and hence decreasing the selectivity [Mark, J.E., 1999]. So, for this reason the thickness of membrane is really important, since a thinner membrane is more susceptible to CO_2 exposure, experiencing rapid plasticization at any pressure [Horn, N., Paul, D., 2011]. Another strong limit of these materials, as we already said, is related to the stability and in particular the thermal and chemical resistance, which strongly limits the possibility of use. The use in harsh application is limited to amorphous polymers since the phases crystalline represent an obstacle to gas permeability.

Another fundamental aspect is related to glass transition temperature: very different behaviours are linked to glassy and rubbery structures. Indeed, the FFV is related to the glass transition temperatures. [Aaron, D. and Tsouris C, 2005] A rubbery polymer obtains rapid thermodynamic equilibrium and has high freedom polymer structure which results in high permeant diffusion. [John Wiley, 2004] On the other hand, a glassy polymer takes a long time to reach thermodynamic equilibrium due to steric hindrance² and this results in non-equilibrium micro-cavities within a rigid polymer structure. [Paul and Yampol'skii Y.P., 1993] It should be noted that the FFV can be influenced by several factors including the concentration of plasticisers, aging history as well as membrane thickness [Yampolskii, 2006].

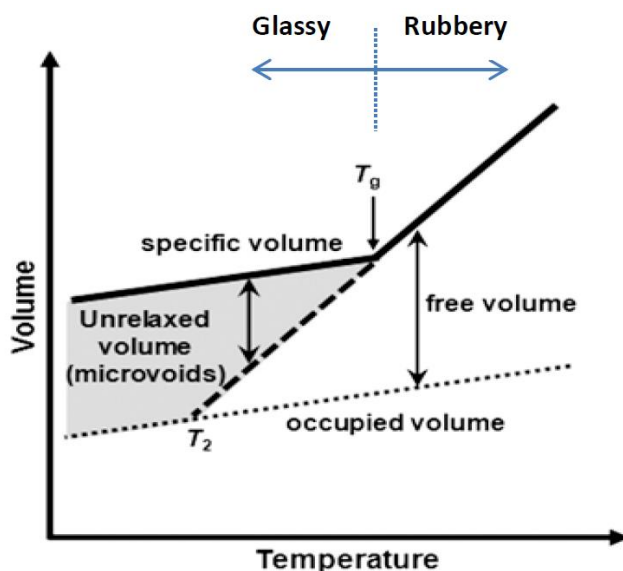


Figure 3.5 The correlations of polymer specific volume versus temperature. Source [Yoshimizu, 2012].

² **Steric hindrance** phenomenon produced by the reciprocal electrostatic repulsion between the electronic clouds of the atoms and the bonds that form a molecule due to their overlapping or excessive approach

So glassy polymers operate at temperature below T_g and have a rigid structure. They are used for the high selectivity and permeability of CO_2 . They are the polyacetylenes, functionalized polysulfides and intrinsic micro porosity polymers (PIMs). In this case the high performance is due to the large amount of free volume, the weak interactions between the chains and the presence of bulky substitutes. PIMs, for example, have very good properties, due to the solubility and exceptional diffusivity that the gas has in it, due to porosity and to the rigidity of the polymer chain. Looking at the structure of PIM-1 in the figure below, it is possible to see how the rotation is completely inhibited around any link in the main chain that is therefore very rigid. The resulting porosity allows easy gas permeation and for CO_2 . [I. Sreedhar and R. Vaidhiswaran, 2017] Over the years other polymers with intrinsic porosity have been developed, mainly to increase the mechanical properties of the membrane and the selectivity of carbon dioxide [Z. Yeo and T. Chew, 2012].

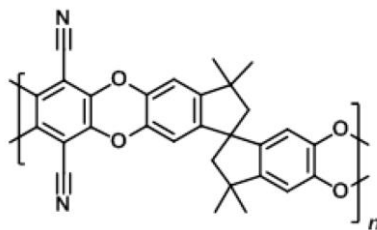


Figure 3.6 Molecular structure of PIM-1. Source [P. Luis and T. Gerven, 2012].

On the contrary, rubbery membranes operate above T_g and have a flexible structure. They have lower permeabilities than glassy polymer [Robeson, L.M. and Liu, 2015]. Literature uses the so-called Robeson diagram to present the upper bound of properties for this kind of membranes, which implies a necessary trade-off between selectivity and permeance. Looking at the results for CO_2/CH_4 separation, the membranes located close to this bound are mostly glassy. It is also possible to distinguish in the graph also the so called thermally rearranged polymers (TR polymers) indicated with blue dots, these, as pictured in the graph, have performances considerably higher than the classic polymers, so much so that Robeson's limit has been raised with a dotted line (the advent of TR polymers was subsequent to the construction of Robeson's diagram). These are particular polymers re-arranged thermally and will be addressed below.

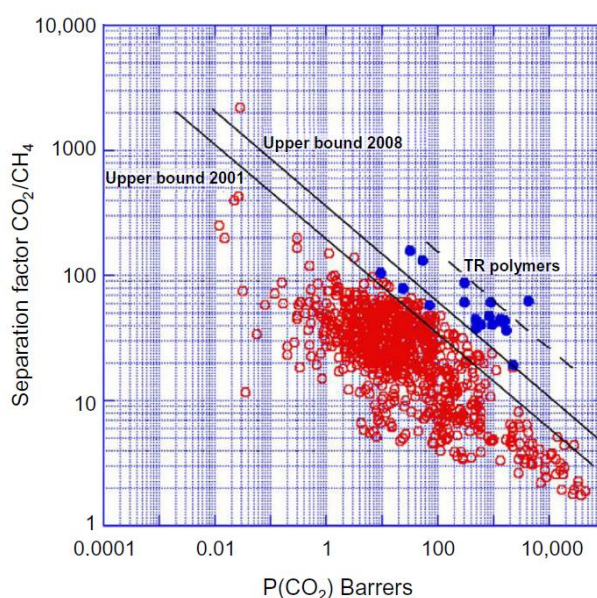


Figure 3.7 Robeson plot for polymeric membranes for the gas mixture CO_2/CH_4 . TR, thermally rearranged. Source [P. Luis and T. Gerven, 2012].

For example, typical values of polymeric membrane not TR likewise Polaris™ membrane from membrane Technology and Research, Inc. (USA) can achieve high CO₂ permeances (1000-2000 GPU) [W. Yave, 2009]. However, its selectivity is below 30, value signed by Robeson upper bound at 57°C (flue gas temperature) [Y. Chen, 2015]. To overcome the upper bound for CO₂/CH₄ separation using polymeric membranes, different strategies have been recently proposed in the open literature. The two initial strategies have been related to the identification of new potential polymeric materials [Cho, 2011] and chemical modifications of the currently existing polymeric membranes [Achoundong, 2013]. Blending polymers to limit the mobility of the polymer chains to reduce the plasticization effects [Hosseini, 2009], and the preparation of polymers with micro-porosities (PIM) [Robeson, 2008] are also strategies investigated in the literature in recent years. Recent work on CO₂ separation using polymeric membrane focused on copolymers which generally have a hard (glassy) polymer segments such as polyamide (PA) or polyester and a soft (rubbery) polymer segment such as polyethylene oxide (PEO) [Powell, 2006]. The hard segment supports the materials by giving enough mechanical strength while soft segment is the main CO₂ selective layer.

The last investigated strategy refers to thermally rearranged (TR) polymeric membranes. These TR polymers, which have polybenzoxazole (PBO) structures, are formed via the molecular thermal rearrangement of aromatic PI containing ortho-hydroxyl groups to the imide ring. These polymers have reached CO₂ permeabilities up to 2000 Barrer and selectivity of 40, well above the Robeson upper bound (also displayed in Robeson's diagram). The problem with this process is that after polymerization they are unsolvable in organic solvent and this does not permit to do film with them, so the large scale production is not profitable. [Robertson, 2011]

3.3.3.2 Inorganic membranes: zeolite and carbon membranes

Most drawbacks of polymeric membranes can be solved with inorganic membranes. They present higher permeabilities and selectivity, have higher thermal and chemical stabilities under harsh conditions, and plasticization is avoided [Winston, 2011].

The inorganic membranes are divided into two major groups: porous and dense membranes [Hsieh, 1996]. Dense inorganic membranes, such as those of palladium and its alloys, or perovskite ceramic membranes are mainly used for highly selective separation of hydrogen and oxygen at high temperatures, respectively [Spillman, 1995]. Instead, porous membranes show a molecular sieving or adsorption mechanism, and some examples are glass, zeolites, alumina, zirconia, and carbon membranes. Zeolites are microporous structures with pore diameters ranging from 0.3 to 1.3 nm, they are crystalline aluminosilicates with well-defined micro porosity [S. M. Auerbach, 2003]. Ideally, they have a perfect molecular sieving transport mechanism, and are composed of silicon, aluminium, and oxygen supplemented with charge-balancing cations.

Zeolites exist in nature and can be obtained synthetically. However, because of their nature, it has become challenging to prepare large zeolite membranes as they form defects in the inter-crystalline pores between two adjacent grains, and are affected by large openings (or cracks) when exposed to thermal treatments (500°C) for their synthesis. Although these membranes should present very high selectivity by kinetic diameter discretization, the formation of all these defects (especially for larger surface areas) has reduced the separation efficiency.

Differently from polymeric membranes, the zeolite ones act the gas permeation through adsorption-diffusion mechanism and not by solution-diffusion. In adsorption-diffusion mechanism, a molecule is first adsorbed on zeolite surface via physical adsorption then diffuses through along zeolite surface due to chemical potential gradient. [Okamoto, 2001] Among all physical adsorbents, zeolite shows an attractive trade-off between properties under the conditions of post-combustion flue gas CO₂ capture with relatively low CO₂ partial pressure (0.1-0.2 atm) and temperature (57°C). [S. Choi, 2009], [C. Chen, 2014] During operation, zeolite will be saturated by the adsorbed species that further block the pores of zeolite thus making it harder to permeate via simple diffusion and enhance separation performance towards adsorbed species. The parameters that influence the diffusion are also: pore diameter, molecule kinetic diameter, temperature, degree of coverage, and the presence of other components in the case for multicomponent diffusion [T.C. Bowen, 2004]. Generally, permeation via adsorption-diffusion zeolite is more effective compared with solution-diffusion polymers that

are limited by Robeson plot.[L. Robeson, 2009] Si/Al ratio and the number of neutralizing cations inside the pores are also factors that affect zeolite adsorptive properties [S. M. Auerbach, 2003], [R. Krishna and J. M. van Baten, 2010]. For the past few years, zeolite membranes have been used for a continuous separation process.

For CO₂/N₂ separation, inorganic membranes mainly employ molecular sieving and surface diffusion as transport mechanism. However, CO₂ and N₂ molecules have a similar kinetic diameter (3.33 and 3.64 nm for CO₂ and N₂, respectively) thus making it difficult for simple molecular sieving to separate them. Surface diffusion in combination with molecular sieving then becomes the main factor for separation. However, the polarizability of the CO₂ molecule is about twice that of N₂ molecules [R. Krishna and J. M. van Baten, 2010], [M. A. Morrison and P. J. Hay, 1979]. In addition, CO₂ is more condensable than N₂ (critical temperatures are 304.1 K and 126.2 K for CO₂ and N₂, respectively).[V. Bondar, B. Freeman and I. Pinnau, 2000] Zeolite surface can interact more strongly with CO₂ compared with N₂ resulting in high CO₂/N₂ selectivity. In order to have good selectivity, zeolite crystals need to be interconnected with each other to form a continuous polycrystalline structure [L. Shan, 2011]. For this purpose, a secondary growth method is widely used to prepare dense zeolite membranes.[R. Krishna and J. M. van Baten, 2010] This method involves the deposition of a zeolite seed (small pre-synthesized zeolite particle) layer on a solid support followed by densification via hydrothermal synthesis of the zeolite membrane or polymer cast on top of zeolite layer [M. C. Lovallo, 1998]. A popular framework for CO₂ capture is FAU : faujasite (FAU) type zeolites with relatively low Si/Al ratio show the highest adsorption selectivity towards CO₂ as shown by several experimental and simulation studies [S. Choi, 2009] , [C. Chen, 2014]. FAU type crystal structure has a pore size of 0.74 nm. FAU-type zeolite is divided by its Si/Al ratio into zeolite X (Si/Al < 1.5) and zeolite Y (Si/Al < or > 1.5-3.8).[S. M. Auerbach, 2003] Calculation of CO₂/N₂ separation previously done by Krishna [R. Krishna and J. M. van Baten, 2010] showed that FAU membrane can achieve 500 in selectivity and a permeability of 10000 barrer.

3.3.3.3 Hybrid membrane

The major hurdles in preparing zeolite membranes lie in the difficulties in reproducibly fabricate defect-free zeolite layer so that it can separate components via selective adsorption-diffusion. In addition, inorganic substrates are thick, brittle, expensive and not adaptable to continuous fabrication, so the scale-up of inorganic membranes is complicated and costly. On the other hand, polymeric membranes are easier to be fabricated continuously in large scale and easier to be scaled up in the form of spiral-wound and hollow-fibre modules. However, gas separation performance of polymeric membrane is still limited by Robeson's upper bound contrary to zeolite membranes which have higher separation performance.

It is possible to integrate zeolite particles and polymeric membranes using either composite membranes or mixed matrix membranes. Both mechanisms of diffusion are present in polymer/zeolite composite membranes. Nevertheless, solution-diffusion is the main mechanism in polymer/zeolite membrane because polymer fills inter crystalline pore and it is in direct contact with feed stream. In addition, many literatures works report that the zeolite layer only contributes to additional mass transfer resistance to overall separation process. [Y. Chen , 2015], [L. Zhao, 2016] Membrane scheme of composite membrane is depicted in Figure 3.8 below and the reported CO₂/N₂ separation using zeolite-based membrane is tabulated in Table 4.

Table 4 CO₂/N₂ separation performance using Zeolite-Based Membrane. Source [Y. Chen , 2015].

Zeolite	Polymer	Configuration	Support	Feed (CO ₂ :N ₂)	CO ₂ Permeance (GPU)	CO ₂ /N ₂ Selectivity
NaY	PVAm	Composite	PES	20:80, 57 °C	1100	>200
NaY	PDMS/Pebax	Composite	PES	20:80, 57 °C	940	30
NaY	PEG-200	Composite	PES	20:80, 57 °C	745	25.4
CHA	PDMS	Composite	PES	20:80, 50 °C	1269	17.34
NaY	-	Composite	PES	25 °C	789	72.3
13X	PEBAX	MMM	-	N/A	3.43	47
NaY	PES	MMM	-	20:80, 25 °C	1838	38
CHA	PTMSP	MMM	-	1:7, 60 °C	315	6.2
SAPO-34	PSf	MMM	-	25 °C	314.02	26.1
LTA	PEBAX	MMM	-	N/A	97	54
NaX	PEBAX/PES	MMM	-	25-45°C	3.026	42.03
NaY	-	-	Al ₂ O ₃	130°C	11.65	>550
NaY	-	-	Al ₂ O ₃	130°C	328.5	41
SAPO-34	-	-	Al ₂ O ₃	50:50, 22°C	3583.70	32

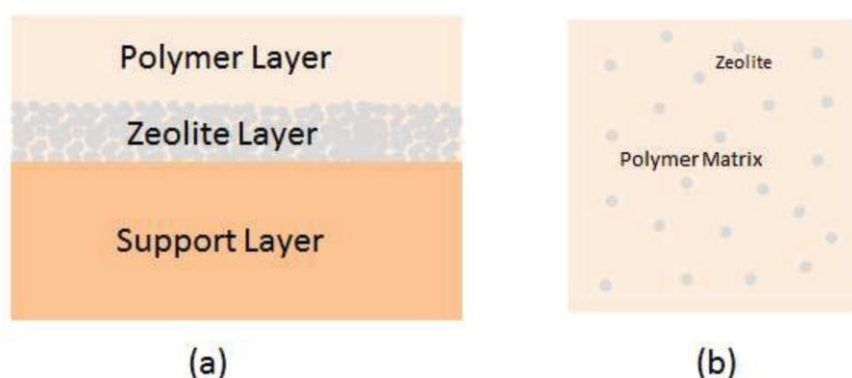


Figure 3.8 Integration of zeolite and polymeric membrane using (a) Composite membrane (b) Mixed Matrix Membrane. Source [Y. Chen , 2015].

Besides fabricating composite membrane, mixed-matrix membrane of polymer and zeolite have also been studied for post-combustion CO₂ capture. Mixed matrix membranes (MMMs) are membranes that are composed of polymers embedded with inorganic particles, see figure 4.8 on the right. [N. Bryan, 2014] By combining those two materials, combination in terms of high inorganic selectivity plus lower cost and better handling of polymer materials can be achieved. [C. M. Zimmerman, 1994] Nevertheless, material selection and polymer-inorganic poor interaction are the main hurdles in developing MMMs. Bryan, [L. Zhao, 2016] incorporated zeolite 13X in PEBAX to make MMM for post-combustion CO₂ capture. Nevertheless, exposure of prepared membrane to high temperature accelerated the polymer aging and the free volume was collapsed. As displayed in Table 4, current zeolite-based membrane performance is around 1000 GPU and 50 CO₂/N₂ selectivity.

In conclusion, polymer/zeolite membranes that use composite configuration have better separation than MMM and have similar separation to those that use inorganic support. It can be said that defect formation in used zeolite has the same effect to performance compared with poor zeolite-polymer interaction. Moreover, with the benefits of cost reduction from polymer incorporation, polymer/zeolite composite membrane could be the sought material for post combustion CO₂ capture. Correct combination mechanism and configuration should

be explored further so that the resulting composite membrane will gain benefits from materials that compose it.

3.3.4 Membrane geometry module configurations

The area necessary for industrial scale separation usually is large. The particularity of this technology is the possibility to package membrane area. The two main industrial membrane geometries are hollow fibre and spiral wound, shown in figure below, Figure 3.9.a and Figure 3.9.b respectively.

The hollow fibre geometry allows a larger membrane surface area at parity of the external volume of the module, compared to the spiral one. The latest developments has a ratio of 10000 m^2 of surface area per m^3 of module compared to $3000 \text{ m}^2/\text{m}^3$ of spiral wound modules. SEM micrographs evidenced this, showing the cylindrical structure of the fibre whose section consists of a porous layer and a dense layer, which constitutes the selective part. The gas to be purified flows inside the fibre: part of it permeates through the membrane along the length of the fibre, the remaining part comes out of the fibre at the end of the module. Each module contains a series of fibres arranged in parallel and has one outlet for the permeate and one for the retentate.

The spiral geometry module contains a long, flat rectangular membrane, adequately supported, spirally wound around a central collector tube that collects the permeate gas. It is in fact a plate-and-frame system wrapped around a central collection pipe. Membrane and permeate-side spacer material are then glued along three edges to build a membrane envelope. The feed side spacer separating the top layer of the two flat membranes also acts as a turbulence promoter.

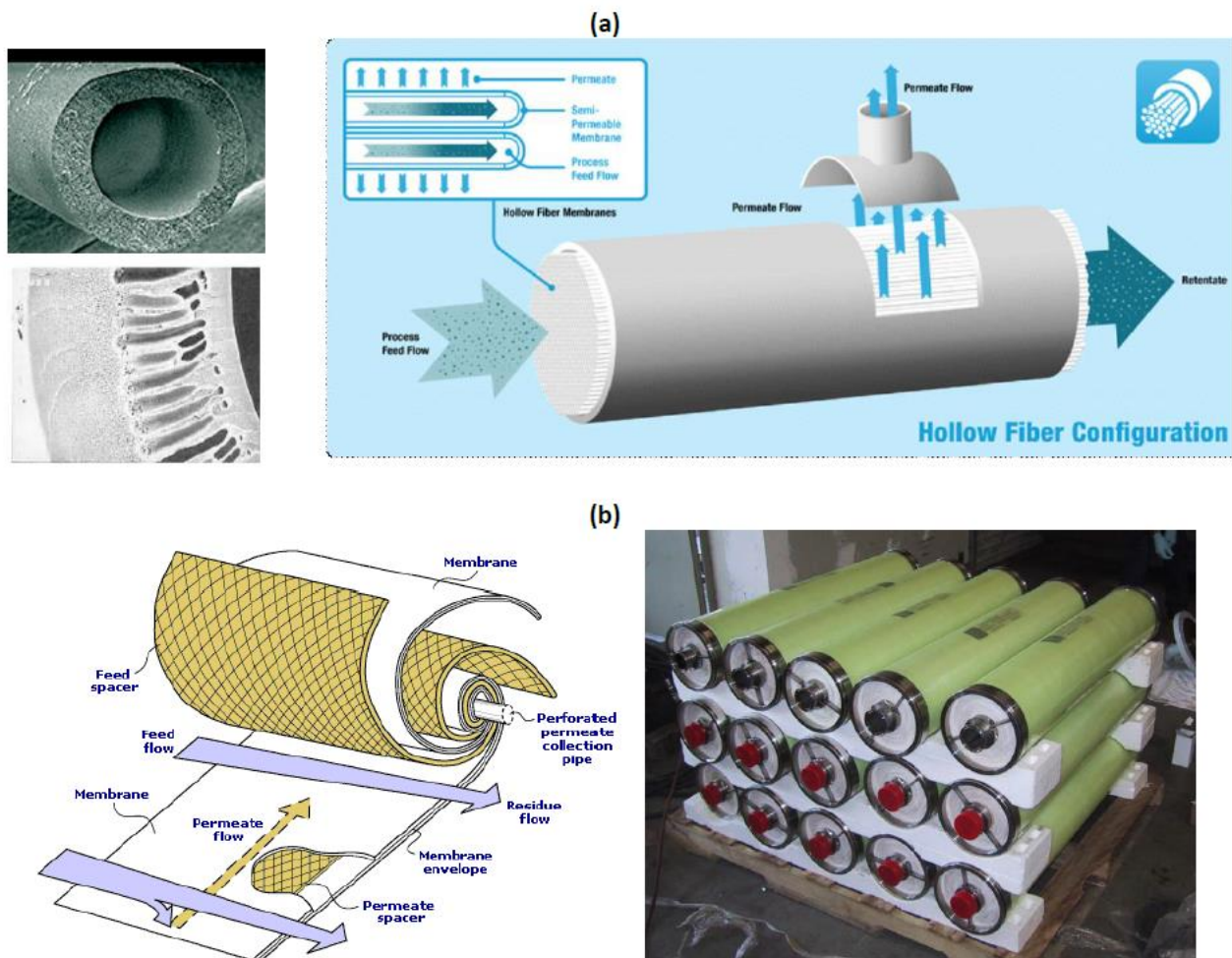


Figure 3.9 (a) SEM image of the cross-section of a hollow fiber membrane (left) and diagram of a hollow fiber membrane module (right). (b) Functional diagram of a flat spiral wound membrane (left) and picture of a spiral wound membrane module ready for in. Source [M. G. De Angelis, 2015].

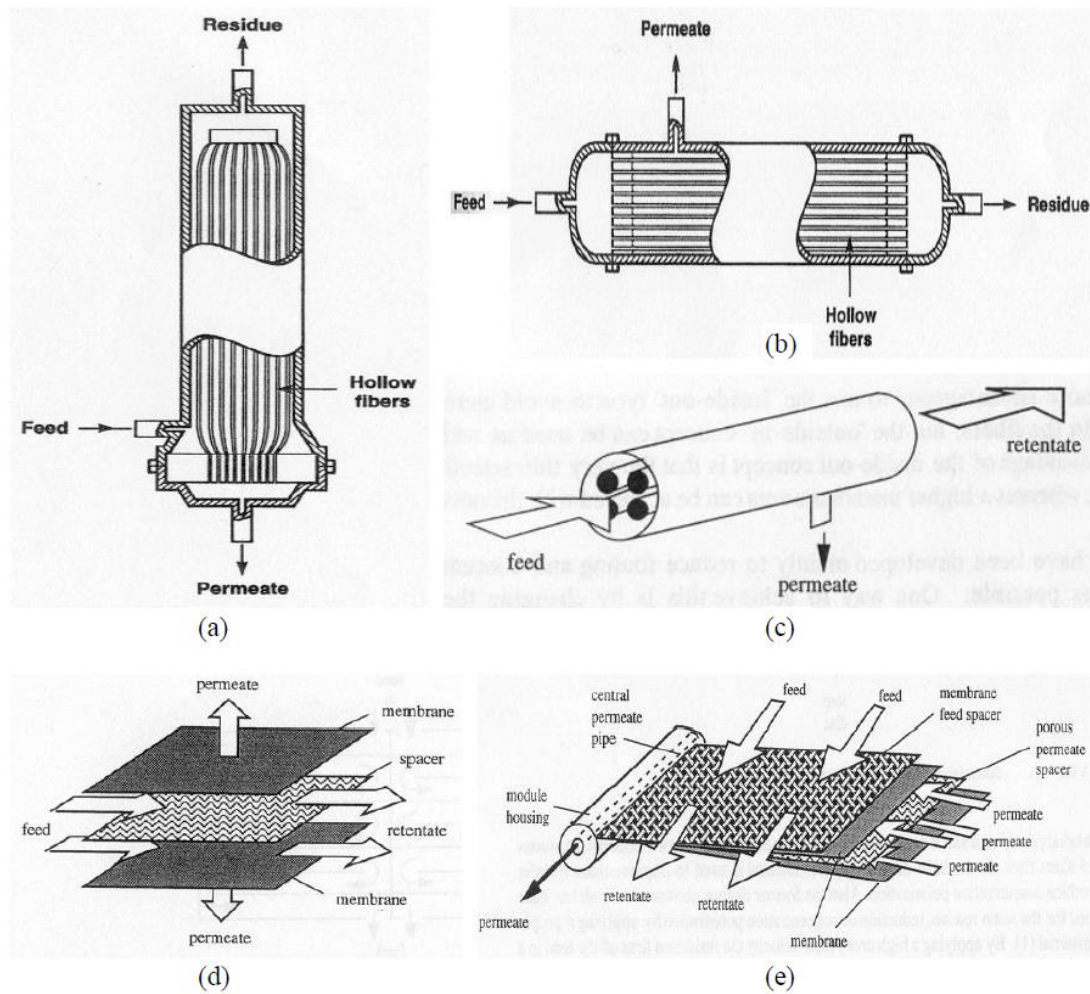


Figure 3.10 Schematic drawing of (a) Hollow fibre module for shell-side feed, (b) Hollow fibre module for bore-side feed, (c) Tubular module, (d) Plate-and-frame module, and (e) Spiral-wound module (Source: Baker, 2000; Mulder, 1996). Source [Baker, 2000].

The choice of the most suitable membrane module type for a particular membrane separation must balance a number of factors. The principal module design parameters that need to be considered for decision are summarized in the Table below.

Table 5 Parameters for membrane Module Design. Source [Baker, 2000].

Parameter	Hollow fibres	Capillary fibres	Spiral-wound	Plate & frame	Tubular
Manufacturing cost (\$/m ²)	2-10	5-50	5-50	50-200	50-200
Concentration polarization/fouling control	Poor	Good	Moderate	Good	Very good
Permeate-side pressure drop	High	Moderate	Moderate	Low	Low
Suitability for high-pressure operation	Yes	No	Yes	Marginal	Marginal
Limitation to specific types of membrane material	Yes	Yes	No	No	No

Usually, hollow-fibre modules are preferred. These modules have relatively poor control over gas flow across the membrane surface and are much more susceptible to concentration polarization effects. However, their cost per unit membrane area is significantly lower than that for equivalent spiral-wound modules. Due to its large membrane area per separator volume, along with ease of construction and self-supporting feature, the hollow fibre is the most desirable configuration. Most of today's gas separation membranes are formed into hollow fibre modules, with perhaps fewer than 20% being formed into spiral-wound modules [Baker, 2002]. But it is also true that, the ease of flat membrane preparation, low pressure build-up of the permeate stream, and low pressure loss of the feed stream promote the popularity of spiral wound membranes in current separator designs [Baker, 2002] , [Koros, 1987]

Table 6 Principal gas separation markets, producers, and membrane systems. Source [Baker, 2000].

Company	Principal markets/ estimated annual sales	Principal membrane material used	Module type
Permea (Air Products)	Large gas companies	Polysulfone	Hollow fibre
Medal (Air Liquide)	Nitrogen/Air (\$75 million/year)	Polyimide/polyaramide	
IMS (Praxair)	Hydrogen separation (\$25 million/year)	Polyimide	
Generon (MG)		Tetrabromo polycarbonate	
GMS (Kvaerner)	Mostly natural gas separations	Cellulose acetate	Spiral-wound
Separex (UOP)	Carbon dioxide/methane		Hollow fibre
Cynara (Natco)	(\$30 million/year)		
Aquilo	Vapor/gas separation, air dehydration, other (\$20 million/year)	Polyphenylene oxide	Hollow fibre
Parker-Hannifin		Polyimide	
Ube		Silicone rubber	Plate-and-frame Spiral-wound
GKSS Licensees			
MTR			

Chapter 4: Effect of impurities on membranes

The presence of impurities in flue gas can lead to a reduction of membrane lifetime and efficiency of the separation process, so it is preferable to reduce them. Then pollutants emissions control measures have to be put in place either by avoiding their creation (primary measures) or by removing them from the flue gases (secondary measures). One method could extract the impurities from flue-gas (secondary measures) but this procedure is typical for large-scale plant. Small and medium sizes biomass cogeneration plant (CHP), also if attractive for local biomass available at low cost, are more expensive per unit of rated power. This does not permit to have emissions control measures for secondary pollutants, because not economically sustainable.

So, primary emissions control must be favoured to avoid the formation of undesired compounds such as NO_x and SO_x. Primary control measures consist of the optimization of fuel quality and combustion process. As said about small biomass plants, secondary measures are most of the time not economically viable and only primary measures are used in such case. Primary measures comprise a wide range of techniques such as the modification of fuel composition or humidity, the fuel particle size and the type of combustion equipment, the excess air control, the flue gases recirculation, and the injection of catalytic converters. For an existing plant, the combustion equipment is fixed, but the operator can modify the fuel composition and humidity, the amount of excess air as well as the amount of flue gases recirculated in the furnace. In the article by Sartor et al. (2014,), the authors present a model to predict the emissions of Liege University CHP plant. In particular, this simulation model can estimate the effect of excess air and flue gases recirculation on the boiler efficiency and therefore on the whole plant conversion efficiency but is limited to a complete combustion process from a generic biomass fuel of the type C_mH_nO_xN_yS_z. As a result, only the CO₂ and SO₂ emissions are simulated. Like many of the small and medium biomass CHP plants, the plant installed at the University of Liege does not have any secondary measures as already said and, as a result, operates close to the limit in terms of NO_x emissions.[K. Sartor, 2014] The model developed in this article is simple enough to be easily integrated into the complete simulation model of the biomass plant and district heating network but is robust enough to give good indications of emissions levels for a wide range of fuel composition and combustion configurations (excess air, humidity and flue gases recirculation).

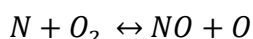
In this study, only the production of NO_x, SO_x and humidity have been taken into consideration. In the successive paragraphs, the formation of these substances will be explained. Their impact on the membrane will however be detailed in the case of humidity only, as humidity is systematically present in flue gas, whatever the fuel type. Nevertheless, two experimental works are briefly reported which quantitatively analyse the impact of impurities on membranes.

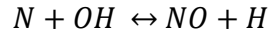
4.1 NO_x formation

The word NO_x refers to both nitric oxide (NO) and nitrogen dioxide (NO₂), in combustion processes, NO emissions are generally much larger than NO₂ emissions. NO_x occurs in the flue gases through three main formation processes respectively referred to as thermal NO_x, fuel NO_x and prompt NO_x (NO formatted at the beginning of the combustion process in the condition of the poor, pre-mixed mixture). In the present contribution, prompt NO_x are neglected as their formation occurs in fuel-rich and high-temperature conditions whereas, in a boiler furnace, the conditions of air/fuel mix are generally lean to promote complete combustion and limit the CO emissions. The two remaining mechanisms are developed below [Sunil Kumar, 2002]. It results that thermal NO_x appear at about 1400 °C and then increase rapidly with temperature (beyond 1600 °C) while fuel NO_x formation is independent from the flame temperature level. As the flame temperature is much lower in biomass combustion chambers (typically about 1000 °C), thermal NO_x is usually neglected.

4.1.1 Thermal NO_x

Thermal NO_x can be represented by three reactions “extended Zeldovich mechanism”:





The quantity of NOx increases with temperature but also with oxygen concentration and residence time in the combustion chamber. The residence time of the flue gases in the furnace is assessed by the following equation:

$$t_{res} = \frac{V_{cc}}{\dot{V}_{fg}}$$

where V_{cc} is the combustion chamber volume (m^3) and \dot{V}_{fg} is the volume flow rate of the flue gases (m^3/s). The residence time in a typical boiler is approximately a few seconds. A detailed kinetic analysis can be used in the model to determine the real NO formation rate. This kinetic analysis considers the kinetic reaction rate of the three Zeldovich mechanisms leading to the real NO formation in function of the residence time of the flue gas.[Sunil Kumar, 2002] This can be assessed by the following equation:

$$y_{NO_r} = \theta * y_{NO_{eq}}$$

where y is the molar fraction, which is determined by the chemical kinetic analysis of the NO formation mechanisms. The subscript equation (eq) stands for the equilibrium state assessed by the equilibrium model whereas the subscript r stands for the real molar fraction of NO (non-equilibrium concentrations). θ is the reaction extent.

Practically, thermal NO formation takes place mainly when the flame temperature exceeds 1600 °C as the residence time required to achieve the equilibrium state of NO is reached in several hundredths of seconds (the exact time depending on the flame temperature and fuel composition). The flame temperature is also coherent as it increases when air excess tends to 0 and when the weight water mass fraction in fuel (especially biomass) decreases. This effect is depicted in Figure 4.1. The trends given by the developed model for NOx formation and emissions (Figure 4.2) are similar to those found in the literature [Van Loo S, 2008] for biomass combustion.

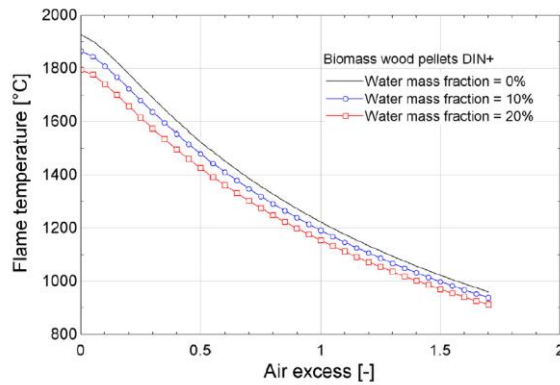


Figure 4.1 Influence of air excess and humidity on maximal flame temperature. Source [Sunil Kumar, 2002].

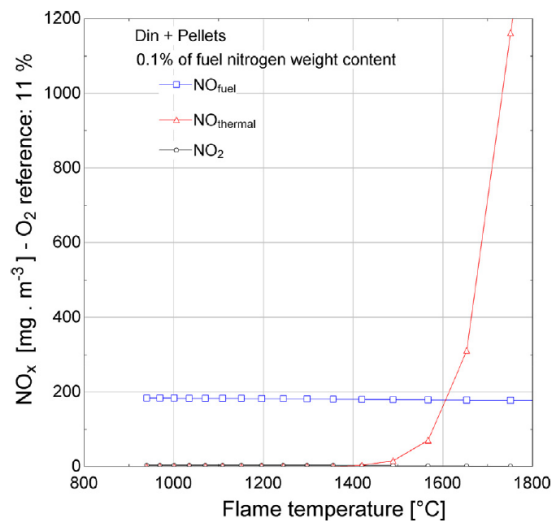


Figure 4.2 Simulation results of NOx emissions versus temperature. Source[Sunil Kumar, 2002].

4.1.2 Fuel NOx

As a result of combustion, the nitrogen contained in the fuel oxidises to form NO. Through a series of intermediate reactions, the nitrogen is released from the fuel in the form of a free radical which then forms N₂ and NO. The formation of NOx is very similar in coal combustion. Two main patterns generally lead to the formation of NOx. In the first one, N converts to HCN (or NH₃) which then partially becomes NO. In the work of [K. Sartor, 2014] the results of [Bartok W, 1991], [Miettinen H, 2013] are quoted and analysed (reported here for completeness). Both noted that for small concentrations of nitrogen in the fuel, N is almost completely transformed (70%-100%) into NO.

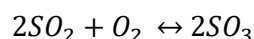
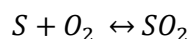
Also in [K. Sartor, 2014] work, there is a reference to [Vermeulen I, 2012] work, in which the authors studied how the ratios H/N and O/N in the biomass influence NO fuel formation. The most important trends point out that: for weight ratio H/N above 25 and ratio O/N above 140, all fuel N converts to NO, which is consistent with the point mentioned previously for low N-containing fuels.

Then as biomass wood pellets are approximatively made of 50% C, 6% H and 44% O (weight fraction) with a maximal nitrogen weight fraction of 0.3%, the maximal ratio H/N and O/N is respectively equal to about 25 and 145. Consequently, the composition is close to the threshold ratios mentioned above and one could consider that almost all fuel N contained in the wood pellets is converted to NO.

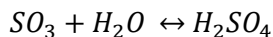
4.3 SOx formation

The most important sulphur polluting compounds are SOx and H₂S, this latest being however not favoured in oxidative environments such as a combustion chamber. The term SOx refers to six different gaseous sulphur compounds: among these oxides, the most important and the most widespread ones due to their high concentration are SO₃ and SO₂. The latter is a colourless, non-flammable and non-explosive gas with a suffocating odour, extremely soluble in water and is about twice as heavy as air. It reacts with O₂ to form SO₃ and by subsequent humidification H₂SO₄. Condensation of sulfuric acid at low temperatures is often an important issue in biomass boilers, and the reason why flue gases cannot always be cooled down to temperatures below 100°C, as sulfuric acid is very corrosive and would damage equipment.

The formation of SOx is mainly represented by the following balances:



The quantity of SO_3 produced is generally very modest, since in the presence of water this is easily transformed into sulphuric acid (H_2SO_4).



For this reason it is easier to find H_2SO_4 than SO_3 in the atmosphere. Also SO_2 released into the air can react catalytically or photochemically with other pollutants giving rise first to SO_3 and then to sulphuric acid (H_2SO_4) sulphates (SO_4) and sulphurous acid (H_2SO_3). [K. Sartor, 2014]

SO_2 and its derivatives can be removed from the air by 'dry deposition' (in the absence of rain) on surfaces such as soil, water and vegetation or by 'wet deposition' thanks the rain. Atmospheric precipitation limits the accumulation of sulphur compounds in the air, this has advantages and disadvantages because acid rain can be a serious problem.

Since sulphur oxides are present in the fuel, they can be avoided in three ways: they are eliminated before combustion of the fuel, immobilized during combustion by transforming them into non-volatile products which are then separated, or finally they can be eliminated before their released into the atmosphere.

Another possibility is to use fuels without sulphur or that contain it to a lesser degree, such as methane or low-sulphur fuel oil. Finally, special combustion techniques (e.g. fluidised bed combustion) exist that can also be an alternative to secondary measures and abatement systems such as flue gas desulphurisation [K. Sartor, 2014].

4.4 Humidity

It has been demonstrated that humidity in the inlet of gas separation module can negatively affect the membrane efficiency [M. G. De Angelis , 2015]. The process considered was the pre-combustion one and regards the separation in syngas of CO_2 from CH_4 , but the results are still valid for our case. The authors report about a humid gas permeation plant that is a prototype developed within the University of Bologna and is unique in the world. Among the advantages of this pilot plant, following points are mentioned:

- possibility to operate with any gas
- possibility to vary the temperature and pressure of the gas supplied (20-60°C, and 1-15 bar)
- possibility to adjust the humidity from 0 to 95%
- measurement of gas permeability in a membrane with a uniform water concentration

The last point differentiates it from most experimental apparatus. Usually, a wet gas stream is fed to the membrane, maintaining vacuum or dry inert gas at atmospheric pressure on the downstream side. Under these conditions there is a simultaneous transport of gas and water molecules in the membrane, which can give rise to multi-component diffusion phenomena, and makes it difficult to interpret the effect of the presence of moisture on the membrane's separation performance. Instead, in the Bologna plant, the membrane is exposed to the same humidity on both sides, so that the water molecules are globally immobile since there is no gradient of concentration between mountain and valley. This type of technique allows to highlight only the effect of humidity on the morphology of the membrane, which has consequences on the transport of gases. The permeation test proceeds first by conditioning the membrane to the desired partial pressure of water and, once the system is balanced, the wet gas stream is flushed into the upstream side of the membrane. [M. G. De Angelis, 2015]

Experimental tests have been done on polymeric membranes. The permeability of mPI and rearranged mTR-PBO membranes has been analysed with respect to CO_2 and CH_4 , at 35°C and various relative humidity. First of all, at each humidity level, the effect of thermal rearrangement on the permeability corresponds to an increase of 2 orders of magnitude, so that thermal rearrangement appears to be very beneficial for the membrane permeability. As stated above, a drop in permeability to all gases is expected as humidity increases. The tests were conducted on the two membranes at a temperature of 35°C and humidity rising to 75% in the plant. In both types of materials and for both gases a drop in permeability is registered as humidity increases

(Figure 4.3). When comparing the effect of moisture on permeability in relative terms to dry permeability, it can be seen that, with the same relative humidity and for both gases, the mTR membrane is less and less influenced by the presence of moisture compared to the original polyimide membrane (Figure 4.3.b). In fact, at 75% humidity, the CO_2 permeability in the mPI membrane drops by 70%, while in the membrane TR falls less, by 58%.

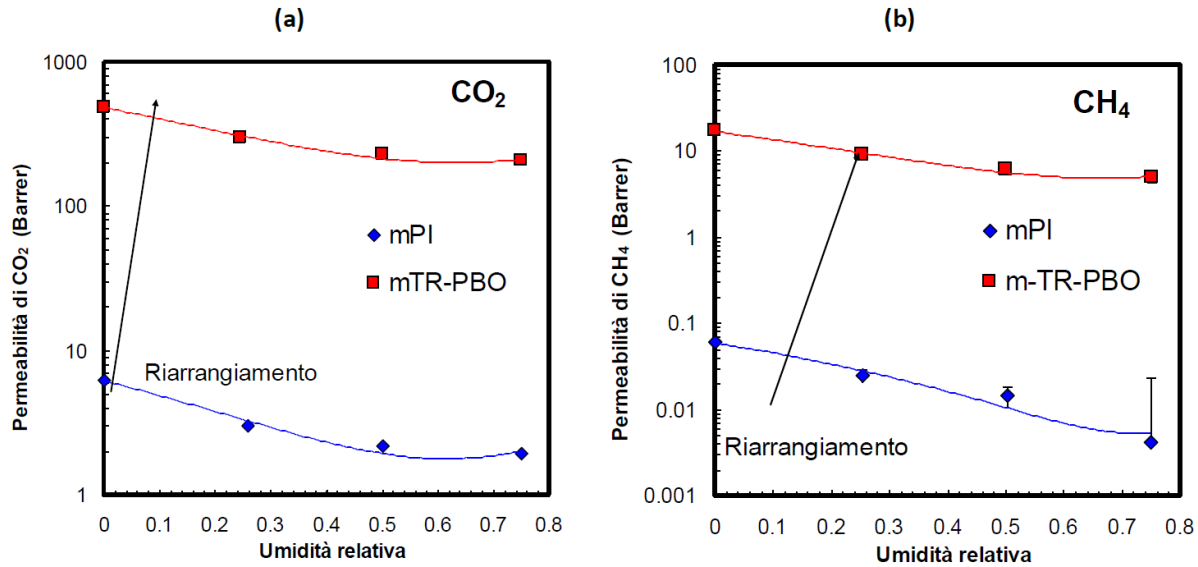


Figure 4.3 CO_2 permeability (a) and CH_4 (b) at different relative humidity in mPI and mTR-PBO polymer. Source [M. G. De Angelis, 2015].

Regarding the ideal CO_2/CH_4 selectivity data, estimated based on the data of permeability of pure gases in the mPI and mTR-PBO membrane at various relative humidity levels. The data are reported in (Figure 4.4.a). Selectivity is by a factor of about 3 in the mTR-PBO membrane compared to mPI. This phenomenon is associated with the increase in free volume (FVV), the increase in free volume promotes the permeability of all gases but favours that of components with lower permeability, CH_4 in this case. In fact, as the free volume increases, the permeability increases, but the membrane's selectivity decreases. The effect of moisture on selectivity is evident in (Figure 4.4.b), which shows the relative variation of selectivity, compared to the dry value: in particular, the ideal selectivity increases with humidity. This phenomenon can again be explained by the decrease in free volume associated with the absorption of moisture, which saturates part of free volume no longer available at the diffusion of gas. It can be seen that the phenomenon is more accentuated in the mPI membrane, characterized by a lower free starting volume and higher water absorption at the same humidity. [M. G. De Angelis, 2015]

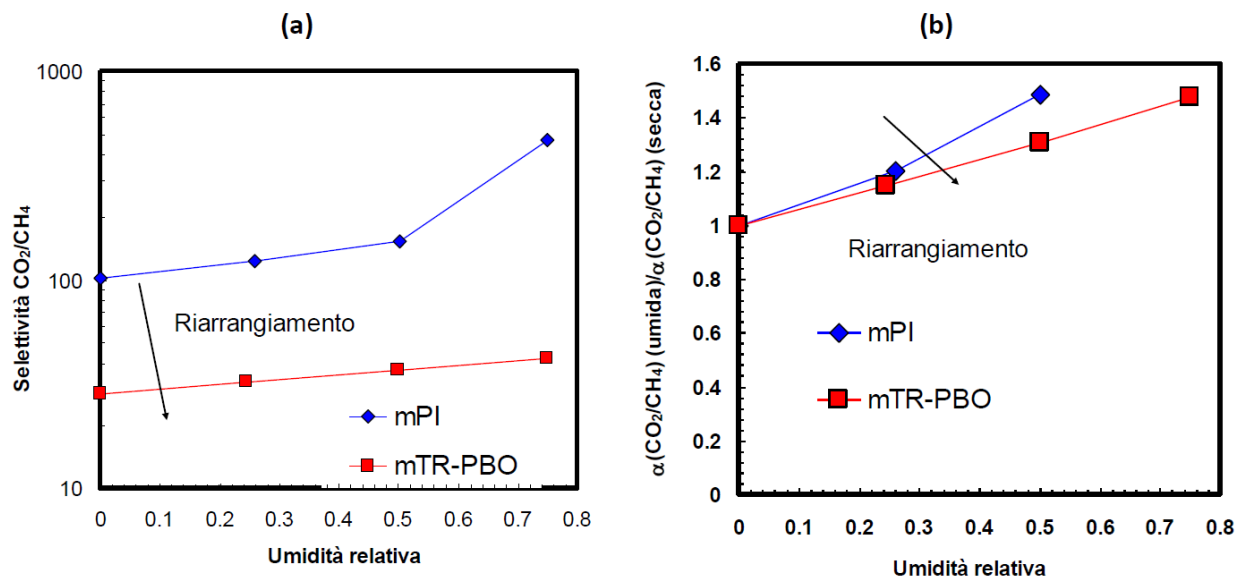


Figure 4.4 (a) Ideal selectivity at 35°C, at different relative humidity, in mPI and mTR-PBO membranes. (b) Relative variation of ideal selectivity respect dry value, at different relative humidity, in mPI and mTR-PBO membranes. Source [M. G. De Angelis, 2015].

In conclusion, thermally rearranged polymers, even though they have shown a more marked decrease in selectivity, are several orders of magnitude higher than permeability, which makes them more interesting for different technologies.

4.5 Experimental test on impurity effect

The presences of impurities in gas streams are well-known to alter the separation performance of the membrane materials by either competitive sorption, plasticisation, “pore blocking” and anti-plasticisation or by chemical degradation. There are not so many studies on this topic, however below are reported two works which explain how impurities can affect the membrane performance. The analysis of the following paragraph can help to understand how polymeric membrane can react and how their performances change in not perfect condition but in presence of impurity, humidity, and ageing.

4.5.1 Pilot scale testing of polymeric membranes for CO₂ capture from coal fired power plants

The aim of the project described by [Marius Sandrua, 2013] was CO₂ separation from flue gas of coal fired power plants using membrane technology. This involved several aspects: membrane up-scaling, materials durability and pilot testing in a power plant. Gas permeation experiments and material analyses pointed out that the membrane material and separation performances were not strongly affected by exposure to real flue gas contaminants. A pilot scale module with 1.5 m² of NTNU membrane was tested continuously for 6,5 months. The membranes showed constant separation performances with a maximum content of 75% CO₂ in permeate and a permeate flow of 525 l/day. The performances were kept constant despite several challenges related to power plant operation such as high levels of NO_x (600 mg/Nm³) and 200 mg/Nm³ SO₂, and frequent power plant outages.

For the membrane selective layer, polyvinylamine (PVAm) and polysulfone (PSf) were used. The module was built in a “plate frame” configuration consisting of 24 membrane sheets (25cm*25cm). The module contained 12 sandwich membrane elements, with two membranes per element.



Figure 4.5 Pilot membrane module. Source [Marius Sandrva, 2013].

The test parameters and flue gas composition are presented in Table 7. It indicates the unusually large amounts of SO₂, NO_x present in flue gas in the first part of the test.

Table 7 Test parameters and flue gas composition (MCR is maximum continuum rating, SCR selective catalytic reduction). Source [Marius Sandrva, 2013].

	From 23 rd May until mid July	From 17 th August to 2 Dec. 2011
Type of membranes (from NTNU)	FSC (Fixed-Site Carrier) flat sheet	
Membrane area in use	~ 0,25 m ²	~ 1,5 m ²
Membranes module (from Yodfat)	With 2 out of 12 elements (4 membranes)	With 12 elements (24 membranes)
Sines Power plant Unit 4	314 MWe, pulverised bituminous coal, flue gas cleaning (ESP, Wet FGD limestone-gypsum, SCR from mid August)	
Flue gas main composition:	Saturated gases at ~ 50 °C (~ 13% H ₂ O) Feed flow: 6-24 m ³ /h, vacuum 100-200 mbar	
• SO ₂	< 200 mg/Nm ³ , 6% O ₂ , dry gas	
• NO _x	500-600 mg/Nm ³ , dry gas (SCR out of service)	< 200 mg/Nm ³ , dry gas (SCR in service)
• Dust (fly ashes)	< 20 mg/Nm ³ , 6% O ₂ , dry gas	
• CO ₂	~ 12% vol. at MCR (lower at boiler low loads)	
• O ₂	~ 6% vol. at MCR (higher at boiler low loads)	

The operating conditions are shown in (Table 7): feed gas flow was 6-24 Nm³/h, feed pressure was atmospheric pressure, temperature was 450 °C, vacuum pressure in permeate was 100-200 mbar (average 130 mbar).

The membranes had constant separation performances for the entire period of testing. Variations of permeate flow rate and permeate content were observed and were attributed to fluctuating vacuum pump operation and fluctuating loading capacity of the power plant (Figure 4.6). The periods with low power plant electrical output decreased considerably the CO₂ content and the relative humidity of the flue gas and this influenced the flow rate and CO₂ content of permeate [Marius Sandrua, 2013]. There is a clear relation between flue gas low humidity and low CO₂ content and the decreases of permeate flow and CO₂ content. Remarkably, the permeate flow rate and CO₂ concentration recovered to initial values when the power plant was operated back to normal loading capacity and under constant conditions.

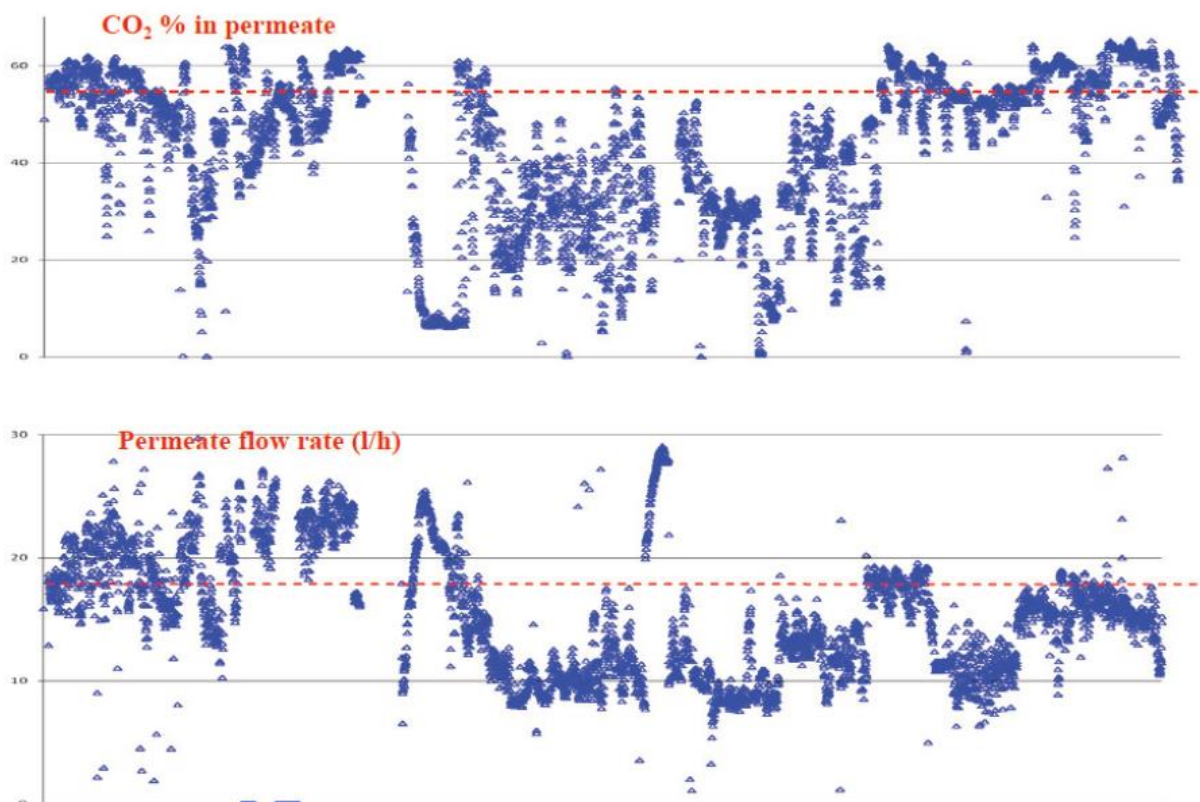


Figure 4.6 Raw data for permeate flow rate and CO₂ content measured from 17 August to 6 October 2011. Source [Marius Sandrua, 2013]

The membranes showed constant separation performances with a maximum of 75% CO₂ content in permeate and a permeate flow of 525 l/day. During periods of constant power plant operation, the values of CO₂ permeance and CO₂/N₂ selectivity were similar to values obtained in the laboratory at NTNU. Both CO₂ permeance and CO₂/N₂ selectivity were constant for the entire testing period. CO₂ permeances between 0.2 and 0.6 m³(STP)/(m² bar h) and CO₂/N₂ selectivity between 80 and 300 were obtained during periods of constant operation of power plant.

In conclusion, the membranes did not lose the separation performances during more than six months of continuous operation in very harsh and challenging conditions: frequent plant outages, high concentration of NO_x and SO₂ and various technical problems.

4.5.2 The impact of impurities on the performance of CTA membranes for CO₂ separation

In this work the composition of raw natural gas, syngas and flue gas depending upon the sources, the production and purification technologies has been studied. Even though Cellulose Triacetate membranes

“CTA” have been widely applied in industry for decades, there are very limited fundamental studies about the impact of impurities on the CTA membrane. In particular, the impact of water, sulphur oxides and nitrogen oxides, as well as aging experiments will be described [Marius Sandrua, 2013].

As is discussed also before, one of the most significant challenges in membrane separation is the presence of water in the processing gas streams. The water content in natural gas is roughly 20–1200 ppm and for flue gas from coal-fired power station, 9–20 %. The presence of water commonly accelerates the corrosion power of CO_2 present. In membrane separation processes, water vapour can alter the separation performance of the membrane unit by competitive sorption, plasticisation, and anti-plasticisation effects. The diffusivity and solubility of water in cellulose triacetate membrane has been well-studied (because widely applied in reverse-osmosis). [Marius Sandrua, 2013]

Generally, water is more permeable than other gases such as CO_2 , CH_4 and N_2 due to its relatively small kinetic diameter and high critical temperature. Water vapour can hinder the permeation of other penetrants. The condensation of the water can also form obstructions. Chen’s work [Chen, 2014] demonstrated the accumulation of water molecules in CTA. So, when the humidity increases, the micro-void diameters increase, indicative of plasticisation by water and the performance of membrane change. Interestingly, although the permeation of CO_2 and CH_4 were enhanced by the water (induced plasticisation effect), the CO_2/CH_4 selectivity was not significantly affected.

Looking at Sandrua’s results, it is possible to see that increasing the relative humidity of water over 10% led to lower the flux of permeate very rapidly (Figure 4.7). [Marius Sandrua, 2013]

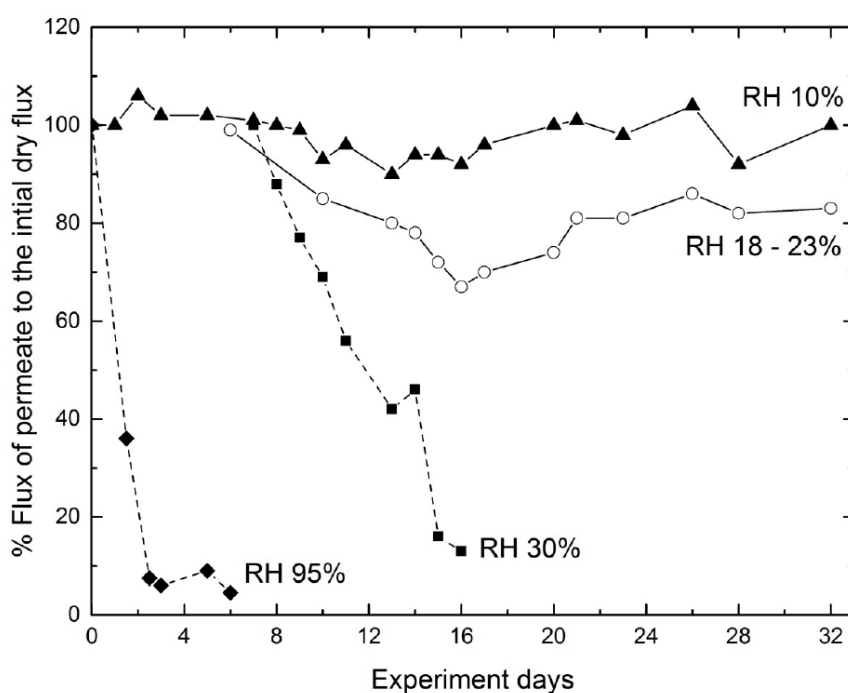


Figure 4.7 The change of permeate flux at different relative humidity of water in CO_2/N_2 separation by cellulose acetate membrane. Source [Marius Sandrua, 2013].

Then is showed how an higher percentage of water in inlet leads to a deep decrease of CTA membrane which not permits to use them in such conditions.

In addition, the permeability of the CTA membrane for both CO_2 and N_2 was enhanced after exposure to pH 3 and pH 7 solutions due to water-induced plasticisation, while the CO_2/N_2 selectivity hardly changed during the time (Figure 4.8 a, b and c). The changes were roughly 6% greater at pH 3 than at pH 7, which could be due to the stronger plasticisation impact of the hydronium ions in the acidic solution (When the pH of a

substance is above 7, it is a basic substance, if it is below 7, it is an acidic substance. The more the pH deviates from 7, the more basic or acidic it is a solution, and this affects her interaction with other substances being more aggressive (acid) or not. Results in mixed gas conditions were comparable.

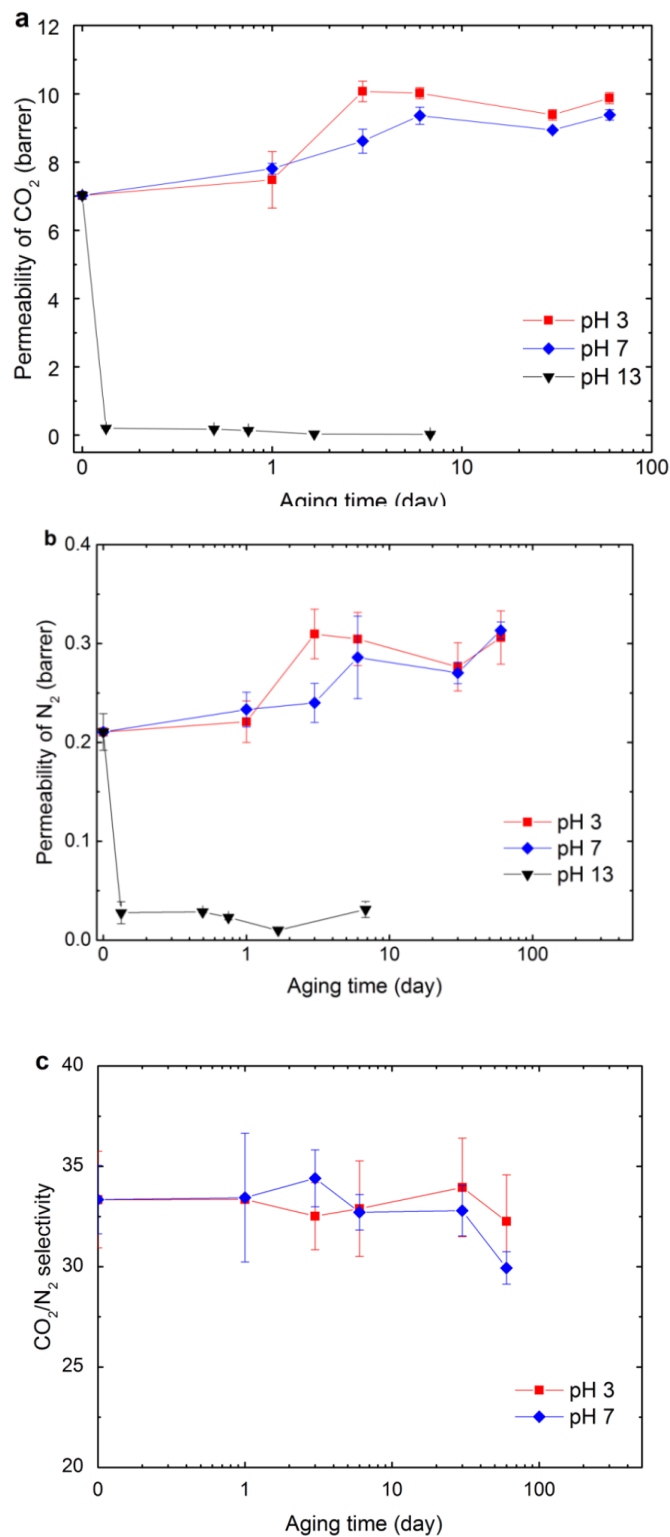


Figure 4.8 Gas separation performance of CTA membranes at 10 bar, 35°C after immersion in pH (3, 7 and 13) solutions (a) permeability of CO₂; (b) permeability of N₂; (c) selectivity of CO₂/N₂. Source [Marius Sandrua, 2013].

Also, the impact of Sulphur Oxides (SO_x) has been studied. The typical concentration of SO_x in post-combustion flue gas is 200–5000 ppmv and it can be reduced to 10–50 ppmv when desulphurisation treatment processes are applied. SO₂ is more permeable than other gases such as CO₂, N₂ and O₂ due to its strong condensability. In particular, the SO₂ permeability through a CTA membrane was reported by Kuehne. [Kuehne, 2018]. These authors observed increasing SO₂ permeability with SO₂ partial pressure, which could correspond to an SO₂ induced plasticisation effect. However, the partial pressure of SO₂ in common flue gas streams is much lower than the conditions in the Kuehne study so the plasticisation effect of SO₂ in a post-combustion capture membrane unit is expected to be minor.

Sulphur trioxide (SO₃) is the other component in the flue gas with concentration after desulphurisation around 20–30 mg/m³. Due to its low concentration in the flue gas, extremely high corrosive properties and the fact that it is a liquid at ambient condition, there are very few studies on SO₃. It was found that the presence of SO₃ significantly altered the membrane performance in both selectivity and gas transport and the combination of SO₃ with water vapour likely decomposed the polymer.

The concentration of nitrogen oxides in a power coal-fired station flue gas is in the range of 150 – 300 ppmv nitric oxide (NO) and < 10 ppmv of nitrogen dioxide (NO₂). Was found that the permeability of NO was less than CO₂ and higher than N₂. However, to the best knowledge of the author, there is no study on the impact of NO on CTA membranes. Also, the impact of NO₂ on the gas separation performance of the CTA membrane is not currently known.[Marius Sandrua, 2013]

Then the permeability of CO₂, N₂ and SO₂ through thin-film composite CTA membranes was studied at different feed pressures (Figure 4.9). All membranes were tested 2 weeks after fabrication to reduce the effects of physical ageing. The use of asymmetric membranes (dense membranes with macro-porous support) here was necessary to ensure the permeability of SO₂ could be detected, given the low partial pressure supplied. For the temperature range, 22–50°C, the permeabilities of N₂, CO₂ and SO₂ were independent of the feed gas pressure. It should be noted that while Figure 4.9.b provides the N₂ permeability in the CO₂-N₂ mixture, the data for the N₂-SO₂ mixture is highly comparable (Figure 4.10). At 80°C, the permeability of CO₂ and SO₂ both initially decrease with pressure, which is typical of glassy polymers becoming saturated. However, plasticization is not clearly observed. Conversely, there is a slight increase in N₂ permeability in both CO₂-N₂ (Figure 4.9.b) and N₂-SO₂ (Figure 4.10) mixtures across the entire partial pressure range, which might be indicative of plasticisation (swelling of the membrane) favouring the N₂ diffusivity.

For CO₂, the plasticisation occurs at 1200 kPa at 24°C for dense films and 500 – 800 kPa for thin films at 50 – 53°C. So, the plasticisation pressure should increase with temperature for a glassy membrane. A significantly higher CO₂ partial pressure than tested in Marius Sandrua's study should be required to observe CO₂ plasticisation.

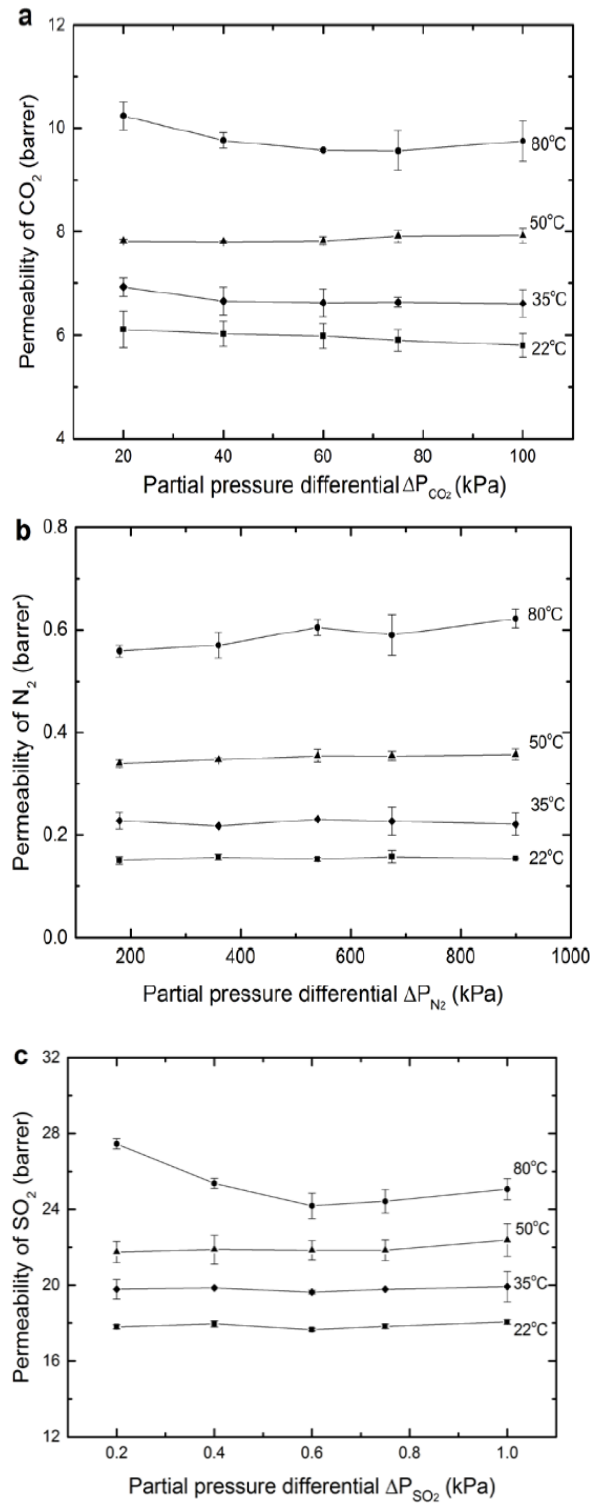


Figure 4.9 Gas permeability in CTA thin film composite membranes. (a) permeability of CO₂ in 10 v/v% CO₂ in N₂; (b) permeability of N₂ in 10 v/v% CO₂ in N₂; (c) permeability of SO₂ 1000 ppm SO₂ in N₂. Source [Marius Sandrua, 2013].

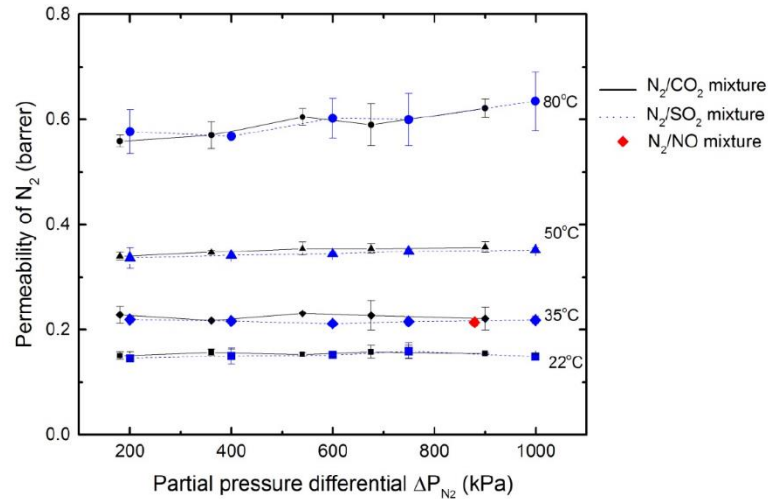
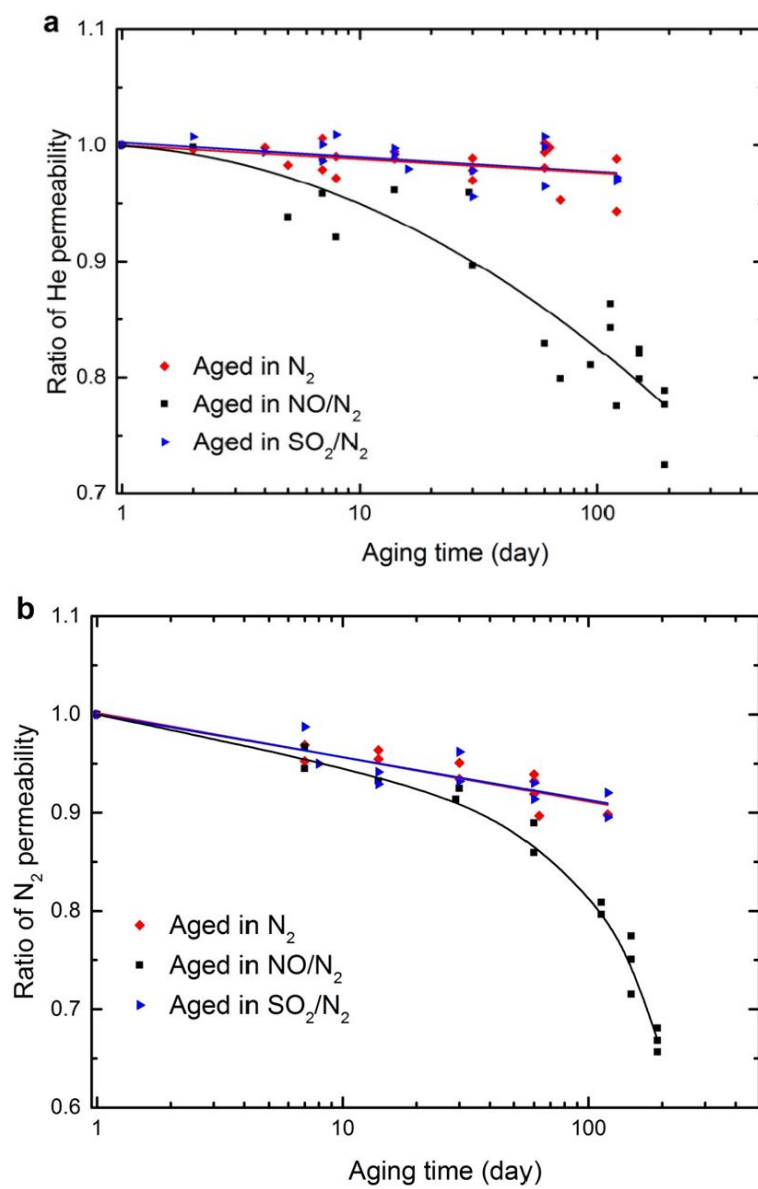


Figure 4.10 N_2 permeability in CTA thin film composite membranes with 10 v/v% CO_2 in N_2 gas feeding and 1000 ppm SO_2 in N_2 gas feeding. Source [Marius Sandrua, 2013].

Then the CTA membranes were aged separately in pure N_2 , and in N_2 containing 1000 ppm SO_2 and 979 ppm NO (988 ppm NO_x) to study the long-term impact of these impurities on membrane performance. After a specified ageing period (up to 120 days), the single gas permeation of He and N_2 was determined. The permeability of helium through the fresh CTA membranes at 7,5 bar and 35°C was recorded as $21,8 \pm 0,8$ Barrer, which is comparable with the literature. The permeability and selectivity of the aged membranes were expressed as the ratio to the permeability and selectivity of the original fresh membrane to eliminate the variability between membrane samples (Figure 4.11). Generally, the polymer chains of a glassy polymer are in a non-equilibrium state when a membrane is formed, and so membrane densification or ageing will occur over time. As the excess free volume of the membrane is reduced, gas permeability declines, as observed in this study (Figure 4.11). The decline in permeability is less for helium than in nitrogen, which is due to its smaller kinetic diameter. This results in an increasing (He/ N_2) selectivity as reported in (Figure 4.11.c). This ageing process was not affected by the partial pressure of 0,75 kPa SO_2 with 1000 ppm (Figure 4.11). Although SO_2 plasticisation was possibly observed at 80°C in the previous permeation experiment (Figure 4.10), this effect was not sufficient at 22°C to alter the membrane ageing process. As the membranes used here are significantly thicker than the ones used before, this result is not unexpected. Conversely, ageing in the presence of 0.74 kPa NO_x led to significantly faster decrease of performances despite the relatively low critical temperature of NO. This could be caused by the presence of small quantities of NO_2 in the gas, both due to impurities in the original $NO-N_2$ gas mixture (1% NO_2 in total NO_x) and possibly due to oxidation of residual NO with ambient oxygen at the end of the ageing process. The presence of NO possibly affects plasticisation effect which affect negatively membrane performances.



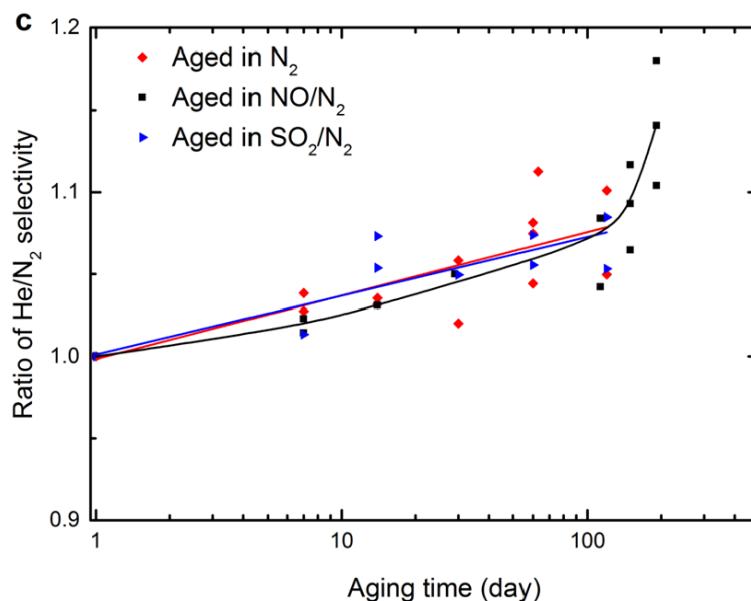


Figure 4.11 Change in permeability of (a) He; (b) N₂ and (c) He/N₂ selectivity as time progresses for CTA membranes at 35°C, 7.5 bar after aging separately in pure N₂, 979 ppm NO in balance N₂ and 1000 ppm SO₂ in balance N₂ at 7.5 bar and 22 ± 2°C. Source [Marius Sandrua, 2013].

In conclusion, this work has shown that cellulose triacetate membranes are relatively stable when exposed to liquid water at pH 3 or pH 7, with a 30% increase in permeability respect of starting condition and no loss of selectivity after immersion for 6 days, after which the performance stabilised. Conversely, caustic solutions (pH 13) hydrolysed and dissolved the membrane significantly over time. The CTA membranes also showed stable performance upon exposure to 0,75 kPa SO₂ for up to 100 days, with the membranes ageing at the same rate as when exposed to inert nitrogen. Conversely, exposure of 0,74 kPa of NO_x resulted in a significantly greater loss of permeability. SO₂ permeated through a CTA membrane more readily than CO₂ and N₂ with a permeability at 35°C of 20 Barrer vs about 0,2-0,6 Barrer for N₂ and 6-10 Barreer for CO₂.

There was some evidence of plasticisation in the N₂ permeability data for both SO₂ and CO₂ mixtures at 80°C in short term permeability testing, but no membrane plasticisation was observed after a 120 days ageing period at 22°C and 0,75 kPa SO₂. The permeability of NO was below detection limits indicating a permeability below 4 Barrer. It should be noted that the ageing studies were conducted with relatively thick membranes. In industrial practice, a membrane with a much thinner dense layer (<1 µm) would be used. The effects observed here would likely occur more rapidly in this thinner structure, as it is well known that both plasticisation and loss of free volume occur more rapidly in thinner glassy systems.

Finally, the results suggest that CTA membranes could be applied in post-combustion capture operations if a sufficiently thin film composite membrane could be prepared. Both water and SO₂ could be tolerated in the flue gas stream under most common operating conditions. However, the control and removal of NO_x down to very low levels are essential to maintain the membrane performance in the long term. This is because, as shown experimentally, there is a sharp drop in membrane performance as the NO_x concentration increases (Figure 4.11). However, primary measures can contribute to make sure that the resulting CO₂ permeate from the gas separation process, even if containing SO₂, can be depleted in NO. Nevertheless, the increased SO₂ concentration may cause concern with downstream corrosion of piping and this may also need careful consideration.

Chapter 5: Case study

5.1 Cogeneration

Cogeneration comes from the attempt to recover all or part of the heat in a useful way which must necessarily be discharged into the environment by a thermal engine system. Such heat, in certain cases, can be usefully used in industry, for example in the form of steam, or it can be used for civil purposes, such as heating buildings. If the plant has such characteristics we speak of combined production of electricity and heat (or simply combined production). The combined production facilities, therefore, convert primary energy, from any source (usually the primary energy is that of a fuel), in electricity and in heat.

Most of the cogeneration plants are located in industrial environments, where the cogenerated heat feeds steam distribution networks within the production sites (refineries and chemical companies, paper mills, textile industries, etc..), there are also cogeneration plants serving district heating (DH) networks where climatic conditions make convenient this type of application. The application of district heating networks for producing cold by means of absorption machines is, on the other hand, limited to a small number of cases.

With reference to the figure below, the cogeneration plant (CHP) provides at the same time electrical and thermal power. This configuration is compared with that in which the same heat output is provided by the heat production plant alone.

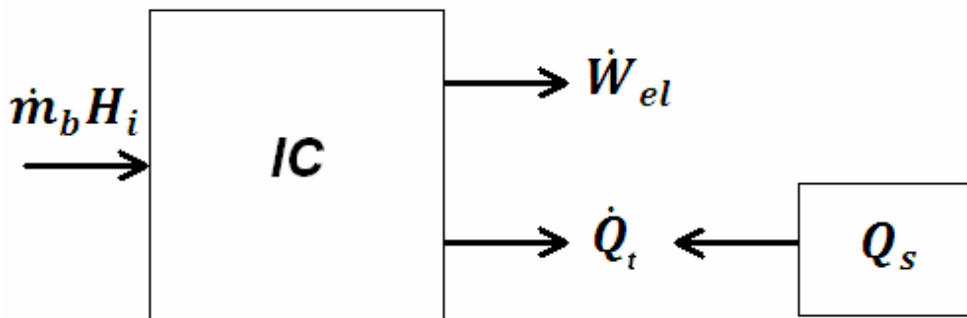


Figure 5.1 Cogeneration plant and only heat plant.

The use of some indexes can help to describe better the cogeneration plant, some of the most important are reported below and have been calculated for our case:

Cogeneration ratio

$$\lambda = \frac{\dot{Q}_t}{P_{el}} = \frac{7}{2.4} = 2.92$$

The cogeneration ratio is the ratio between thermal power and electrical one. This ratio characterizes the plant itself (the topology of the plant determines a particular range of value of this index).

Electrical index

$$I_{el} = \frac{P_{el}}{\dot{Q}_t} = \frac{2.4}{7} = 0.34$$

It is the inverse of the cogeneration ratio.

5.2 Case study

The case of study regards the combined heat and power (CHP) plant of Liegi University. The plant is supplying energy to a district heating network on the University Campus. This network has a total length of 10 km and distributes pressurized hot water at 125°C to approximately 70 buildings representing a total heated area of about 470 000 m². Buildings are different under many aspects, they comprehend classrooms, administrative offices, research centres, laboratories, and a hospital. The hospital represents about 25% of the total heated area and requires steam for the kitchens and air control system, hence the high temperature of the network. The peak power of the network is 56 MW for a total of 60,000 MWh per year. All the buildings are heated between 4:00 and 20:00, while the hospital needs heating and steam 24 h per day, 365 days per year. The Figure 6.2 points out that the two peaks of the day are at 7:00 to heat the buildings in the morning and at 16:00.

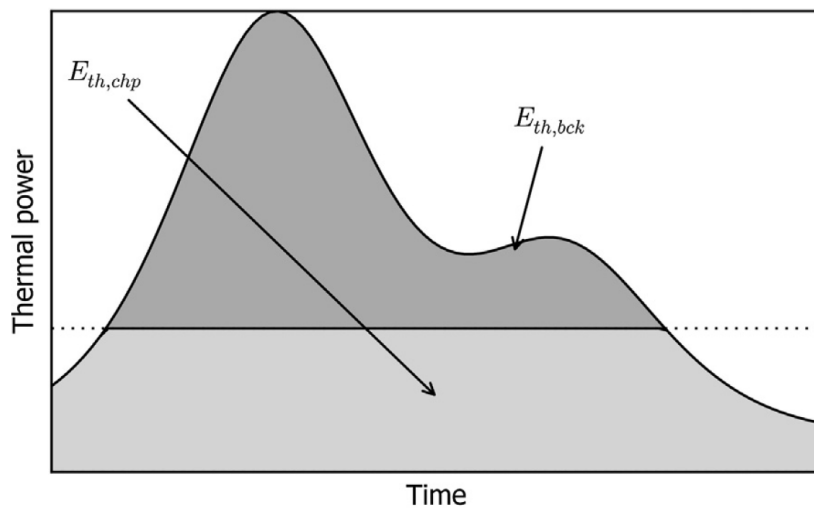


Figure 5.2 Variation of load during the day for a typical heating application. Source [K. Sartor, 2014].

The network is operating since the 60s where the heat was generated by natural gas boilers. In order to cope with the quotas of CO₂ emission level, the University installed in 2012a biomass CHP plant whose purpose is to feed the base heat demand of the campus. It is constituted by a moving grid biomass boiler with nominal primary power of 12 MW providing the steam to a back-pressure turbine and an extraction condensing turbine with nominal electrical power of 2.4 MW. Then the extracted steam is condensed in a heat exchanger which feeds the DH network with a nominal duty of 7 MW. The remaining part of thermal power needed by the network is provided by two natural gas boilers. The fuel is made of wood pellets whose mass composition is 46.38% of C, 5.64% of H, 40.01% of O, 0.08% of N, 0.28% of ashes, 7.6% of water and less than 0.01% of S. With fuel wood pellets, the flame temperature is very high so that exhaust fumes must be recirculated and introduced after the secondary air injection. To maintain the grid temperature in acceptable range, a high excess air is also necessary. The flue gas passes successively through an evaporator (plates), screen tubes, two superheaters, one evaporator and four economizers. Then exhaust gases are filtered and directed to the stack. The steam cycle is representative of a traditional cycle with extractions turbines.

To deduce future consumption, data from 2009, 2010 and 2011 have been analysed and corrected based on the ambient temperature of the last 12 years (degree-days method was used). It resulted that the thermal consumption is 60,834 MWh per year. Thanks to a model developed by [K. Sartor, 2014], it is possible to predict the production of the CHP, using as input the consumption profile. The thermal production results to be 36,394 MWh while 8945 MWh of electricity are delivered. This represents approximately 60% of the thermal needs of the University campus. On average, the thermal and electrical efficiencies are respectively 38.1% and 9.4% giving a total efficiency of 47.5%. Although the CHP plant has a nominal efficiency of about 75% this one decreases when the mass flow rate of steam extracted from the turbine decreases (i.e. heat

production decreases). In the limit, when no heat is produced, the global efficiency reaches the maximal electrical efficiency (around 20%). Based on the thermal energy and installed power, the equivalent utilization time can be assessed which gives $t=5200$ h/y.

The CHP allows a significant saving in terms of CO₂ emissions. Indeed, this case was compared to the separated production of electricity and thermal power where electricity is supposed to be generated by natural gas combined cycle power plant with average efficiency of 55%. In this case, the plant would emit 456 kg of CO₂ per MWh_{el} and the thermal energy produced by a natural gas boiler with 90% efficiency would emit 257 kg of CO₂ per MWh_{th}.

Summarizing the cogeneration plant can generate steam at 4,2 MPa and 420°C. First the steam is expanded in a back-pressure turbine (Figure 5.3). The exhaust steam is split in one flow that is condensed to generate pressurized hot water at 1,2 MPa and 120°C, the remaining one is expanded in a steam turbine.

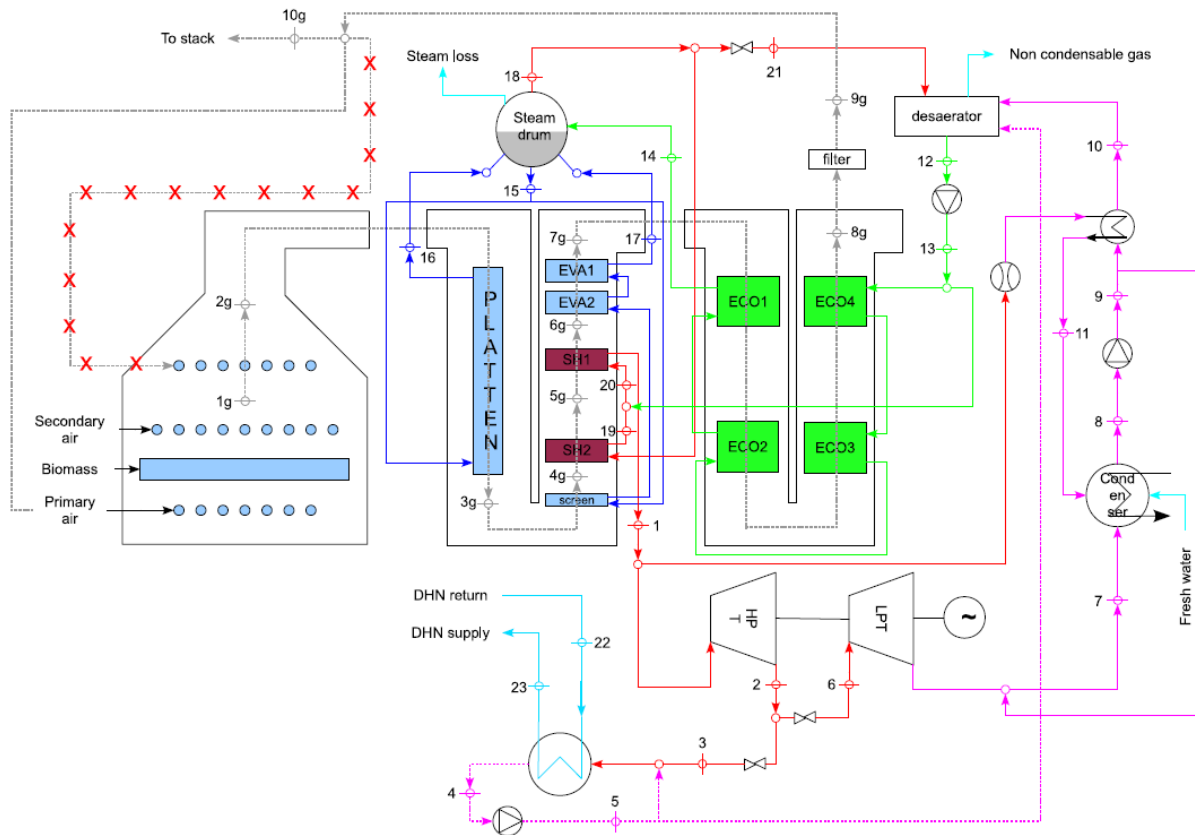


Figure 5.3 Plant configuration of cogenerator. Source [K. Sartor, 2014].

The flue-gas stream (793 kmol/h) is at atmospheric pressure and 170°C, in the table below reports all the percentages of components in flue gas and other technical data, the experimental data will be used in this work for the computational part:

Table 8 Volume gas fraction and data for 12 MW biomass boiler of cogeneration plant calculated by model and experimentally.
Source [K. Sartor, 2014].

	Exp.	Model
Volume gas fraction		
CO ₂ [%]	7.7 (±0.13)	8.0 (±0.15)
O ₂ [%]	12.8 (±0.08)	12.7 (±0.16)
H ₂ O [%]	8.18 (NC)	8.1 (±0.3)
CO [%]	56 · 10 ⁻⁶ (NC)	0 · 10 ⁻⁶ (±0)
Others gas concentration		
NO ₂ [mg m ⁻³]	406 (±4)	399 (±5)
SO ₂ [mg m ⁻³]	34 (±4)	27 (±3)
Flame temp. [°C]	1050 (±10)	1020 (±15)

Chapter 6: Membrane model development.

6.1 Simulation parameters and assumptions

For the model developed in this work some choices and assumptions have been made. In particular, some parameters for the membrane unit must be defined, like inner and outer diameters of hollow fibre, fibre length, permeate side pressure, component permeance, and the membrane area. These parameters depend on the gas composition and physical condition in inlet. In the table below, the most important characteristics of the feed are reported:

Table 9 Flue gas characteristic.

Flue characteristics	Value
CO ₂ mole fraction [%]	7,7
O ₂ mole fraction [%]	12,8
N ₂ mole fraction [%]	71,3
H ₂ O mole fraction [%]	8,18
CO mole fraction [%]	5,60E-05
NO ₂ [mg m ⁻³]	406
SO ₂ [mg m ⁻³]	34
Temperature [°C]	170
Pressure [bar]	1
Flow rate [kmol/h]	793,16

It is possible to think that the temperature of flue gas can be decreased from 170 °C to 40°C permitting to use this additional heat using a heat exchanger, and allowing the membrane to work at nominal condition except for the impurities. However, in the practice, this high temperature is necessary to avoid condensation of vapours containing sulfuric acid, that could damage the exhaust gas equipment. This important issue caused by the presence of impurities is however not the focus of the present work, and in the present model, as SO_x and NO_x are neglected, the flue gas temperature is not an issue. However, this point is critical and further work are necessary to consider these limitations.

For the membrane selection, a polymeric one has been chosen, because they are the most commercialized and widespread ones and the historical data are more reliable, so this permits a better evaluation of the durability of life and performance of the membrane. [Lin, 2007] The characteristics of **Polaris** membrane are reported in the table below:

Table 10 Data sheet of Polaris membrane. Source [Lin, 2007].

Membrane Module Parameters	
Module Type	Shell-and-Tube
Membrane type	Asymmetric Hollow fibre
Flow configuration	Counter-current, shell side
Fibre inner diameter (μm)	300
Fibre outer diameter (μm)	500
Fibre active length (m)	0.5
Permeance, ($10^{-10} \text{ mol/s.m}^2.\text{Pa}$) (Lin et al., 2007)	CO ₂ : 3350 N ₂ : 67 O ₂ : 168 Ar : 168

6.2 Design specifications

The process design choices noticeably affect the economic viability of gas membrane systems. It is necessary to meet the project scope and specifications and the design can differ significantly due to application specificity, and module configurations. The module is in fact the most important part of a membrane process. When some modules are connected in series or parallel, they are called stage. A combination of stages is called a cascade. So, one of most important steps is the choice of the right module configuration, membrane material, and to determine the required membrane, as well as the compression/vacuum work needed to operate the system. Besides module configurations and flow patterns of the feed and the permeate streams, other factors that determine the performance of a membrane gas separation system are membrane selectivity, pressure ratio, and stage cut. As we already said the selectivity is the ratio of the permeabilities of two gases in the mixture while the pressure ratio is the ratio of feed pressure to the permeate side pressure across the membrane. The stage cut is the fraction of the feed gas that permeates the membrane. Selectivity directly impacts the recovery of the process and indirectly impacts membrane area and feed gas flow requirements. Membrane selectivity and pressure ratio are strictly bound because of the practical limit of the pressure ratio achievable in gas separation systems. Large pressure ratio requires large amounts of energy and expensive compressors [Baker, 2000]. The degree of separation required is the other factor that also affects the membrane system design. The target of every gas separation system is to produce a residue stream essentially stripped of the permeable component and a concentrated permeate stream. Unfortunately, the stage-cut, membrane selectivity and pressure ratio in commercial systems are limited, so multi-step or multi-stage or recycle membrane system must be used depending on the system requirements like high purity or high product recovery.

In this work the main objective of the research is to obtain at least 99% of permeate purity and 90% of recovery and check which technology is the most profitable for this purpose, with a special focus on comparing membranes with amine-based capture.

As the number of possible system designs is large, systematic design methods or guidelines are indispensable tools for deriving a close-to-optimal design.

- Preparation of Flow Diagrams.
Firstly, it is advised to build a schematic diagram where parameters like temperatures, pressures and flows are reported. Purity and quantity of permeate gas must be defined and fixed by mass constraints.
- Acquisition of Basic Data.
Being not so mature, membrane technology presents a scarcity of design data. However, it is possible to use tabulated data or ask them to membrane manufactures.

- Detailed Design Calculations.

In general, it has been concluded that counter current flow is the most efficient flow pattern, requiring the lowest membrane area and producing the highest degree of separation, at the same operating conditions. The order of separation efficiency for the four flow patterns is counter current flow > cross flow > concurrent flow > perfect mixing (Figure 6.1).

- Modification of Preliminary Flow Diagrams.

Usually multi-stage and recycle strategies are necessary to achieve higher recoveries and product compositions. Considerable literature exists and exposes the potentiality and energy requirements associated with these approaches. These techniques are typically applied in cases where high recoveries are desired.

- Economic Evaluation of Chosen Design.

This is very important for judging if the proposed process design is economically viable or not. This part of the project is the same as for any other separation operation. After all flows, compositions, and equipment ratings are known; capital, energy, and other operating costs can be assessed by some formulas, usually based on empirical methods.

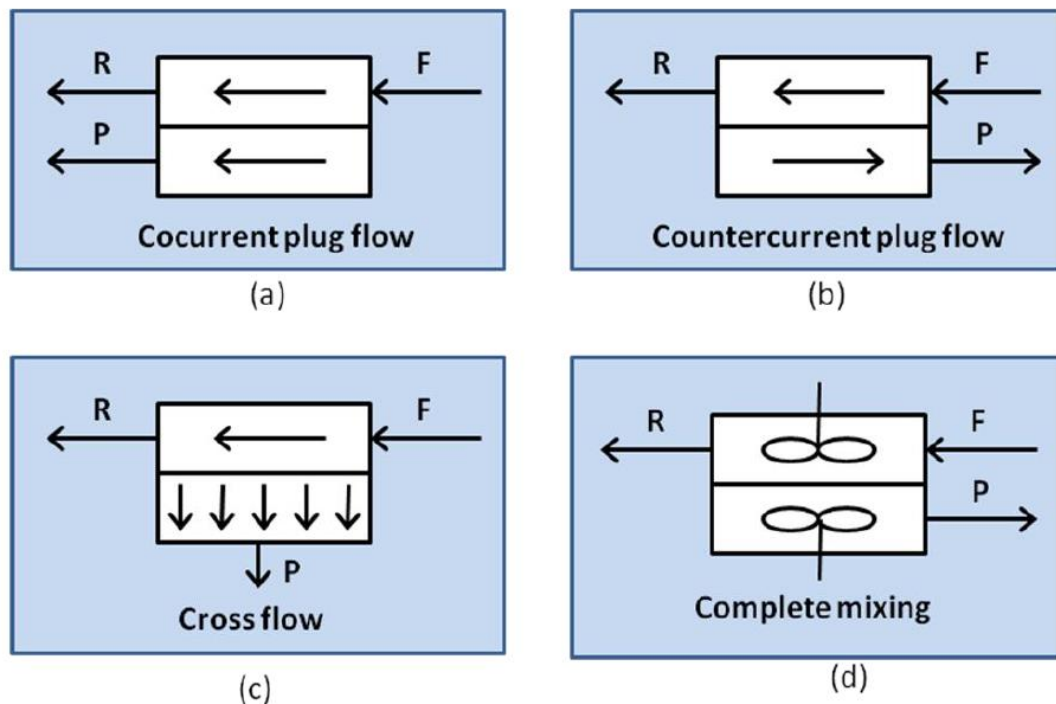


Figure 6.1 Idealized flow patterns in membrane gas separator. Source [V. Bondar, 2000].

6.3 Aspen Custom Modeler

A wide range of simulators for the chemical industry are present on the market such as Aspen Plus. However, membrane operations are not present in any of this software's libraries, so it is necessary to build a custom unit operation. For this reason, the model library of Aspen Plus allows user models that can be linked with Microsoft Excel, Fortran or both to build a customized model. All these options use FORTRAN as programme language. Furthermore, Aspen supplies templates showing how to exchange the necessary data between Aspen and Excel. When the model on Excel and FORTRAN are made, it is possible to insert them in Aspen Plus User Model Library. In addition, there is also the possibility to develop the model in Aspen Custom Modeler which is another software linked with Aspen Plus library.

For the present work Aspen Custom Modeler was used. It is apart from the other modelling tool because it uses an object-oriented modelling language, editors for icons and tasks, and Microsoft Visual Basic for scripts. It permits to build a single component from zero, this will follow the equations and specifications inserted inside it. As we said, this procedure is helpful in the case there are no similar component in literature, as in our case. The interface is on in Figure 6.2:

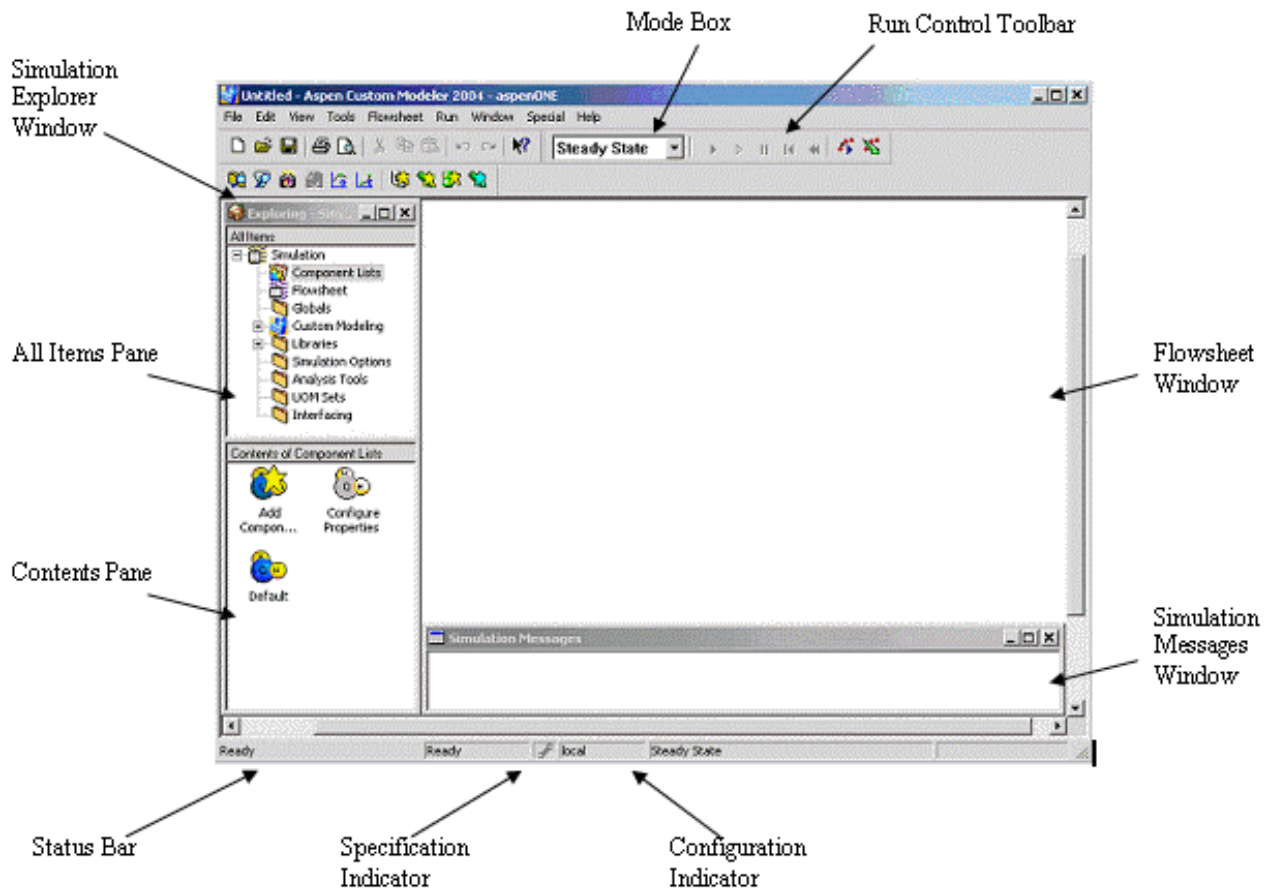


Figure 6.2 Simulation window description in ACM.

With ACM whenever the model equations are modified, one needs only to install it again in Aspen Plus. To implement the model in the software some hypothesis have been made, allowing for a very simple modelling in first approach. In particular:

- Cross-flow with the unobstructed permeate is removed from each cell and mixed to form the permeate module. The retentate goes from cell to cell.
(The permeate that passes through the membrane is contained in the casing that neutralizes leaks. This allows the formation of a single permeate flow due to the contributions of the permeate passing along the membrane surface.)
- Isothermal conditions.
(The temperature change along the membrane is so low that can be considered in isothermal conditions).
- Ideal gas behaviour.
(This assumption incorporates the conditions of operability of the laws presented in the Chapter 3).
- Constant permeabilities.

(In the reality the permeabilities will probably change and decrease membrane efficiency during the time, but this event was already implemented in the last assumption. Then is possible to maintain them constant to simplify the model construction).

- The total pressures in the retentate, permeate and feed are constant.
(The decrease of pressure due to the membrane resistance is low and the real value are not so different).
- The transport mechanism is the Solution-Diffusion mechanism.
(Look Chapter 3).
- Permeability and permeance are independent of pressure.
(As explained in Chapter 5 is possible to see the connection between them, but despite this, since the pressure variation ranges are small, it is possible to consider it constant and with it also the properties that depend on it.)
- The partial pressure of the component in the feed is the partial pressure before the membrane.
(It is possible to assume that there are no losses or changes in composition just before the membrane).
- There is no pressure drop from feed to retentate.
(The pressure drop would be attributed to the permeate which pass through the membrane, but it is so small that can be neglected).
- Volume is constant.
(Are not present big changes of temperature or pressure in each stream).
- Life of the membrane is reduced at 80% of its nominal value due to the presence of impurities.
(Considering the results reported in Chapter 5 for similar membranes subjected to such working conditions, it is right to consider a decrease in separation, efficiency and permeability that are incorporated in the decrease of the useful life of the membrane).

As it was described in Chapter 4, SO_x , NO_x , and H_2O have a greater permeability through polymeric membranes than CO_2 and therefore will enrich the permeate stream. In first approximation for this study it was decided to reduce the life of the membrane to 80% of its nominal value to take account of these phenomena.

6.3.1 Writing code of ACM model.

The equations, variables and parameters of the model have been written in the ACM reference language. Three distinct parts mainly compose the code. First, the variables and parameters are declared stating the name, the type and a brief description, which is optional but quite useful to keep track of the units. When using differential equations, it is also necessary to define the domain and dimension of the variables. In addition, since ACM runs in an equation-oriented environment, degrees of freedom (DOF) need to be taken into account. In particular, to have a solution in the system of equations, the number of variables must be equal to the system's DOF and the system must be represented by a non-singular matrix.

1. NCells = the number of cell which constitute the whole membrane.
2. A [m^2] = the total area of the membrane which is done by the sum of all the cells.
3. L [$\text{m}^3(\text{STP})/(\text{m}^2.\text{h}.\text{bar})$] = the permeability of the gas. The permeability is the rate at which the gas permeates through the membrane after the gas has come to equilibrium in the polymer. The time lag is the time it takes the gas to permeate from the feed side of the membrane to the permeate side; this time can be used to calculate the diffusivity.
4. Lmol [$\text{kmol}/(\text{m}^2.\text{h}.\text{bar})$] = is still the permeability expressed in kmol to evaluate the molar flow rate, it is derived from L.
5. PPerm [bar] = permeate pressure.
6. ACell [m^2] = the area of the single cell.
7. FRet [kmol/h] = molar flow of retentate discretized for each cell.
8. FPerm [kmol/h] = molar flow of permeate discretized for each cell.

9. ZRet = retentate molar composition for each cell and for each component in the component list.
10. ZPerm = permeate molar composition for each cell and for each component in the component list.
11. RhoRet [kmol/m³] = molar density of retentate.
12. RhoPerm [kmol/m³] = molar density of permeate.

```
// Parameters and variables
NCells      as IntegerParameter (Description:"Number of cross flow cells", 100);
A           as Area              (Description:"Total membrane area", Fixed); // (m2)
L(ComponentList) as Notype       (Description:"Permeability in m3(STP)/(m2 h bar)", Fixed);
Lmol(ComponentList) as Notype    (Description:"Molar permeability (kmol/(m2 h bar))");
PPerm       as Pressure          (Description:"Permeate pressure", Fixed); // (bar)
ACell       as Area              (Description:"Area per cross flow cell (m2)");
FRet([0:NCells]) as Flow_Mol     (Description:"Retentate mole flow from cell"); // (kmol/h)
FPerm([1:NCells]) as Flow_Mol     (Description:"Permeate mole flow from cell"); // (kmol/h)
ZRet(ComponentList,[0:NCells]) as MoleFraction (Description:"Retentate mole fraction in cell");
ZPerm(ComponentList,[1:NCells]) as MoleFraction (Description:"Permeate mole fraction in cell");
RhoRet      as hidden Dens_Mol; // Retentate molar density (kmol/m3)
RhoPerm     as hidden Dens_Mol; // Permeate molar density (kmol/m3)
```

Figure 6.3 Variables definition in ACM.

Then ports are specified, ports in Aspen Custom Modeler are necessary to allow the model to be connected to streams, in our case we refer to standard ports already present in the software “MoleFractionPort”. So, we define them for each stream; inlet, permeate, retentate. After this, the retentate inlet conditions are settled by placing the retentate flow at the first cell equal to the inlet. A “for-do” loop is used to set the molar composition at the membrane entrance equal to the feed composition:

```
// Ports
Inlet      as Input  MoleFractionPort;
Retentate  as Output MoleFractionPort;
Permeate   as Output MoleFractionPort;

// Convert permeability to molar basis
Lmol = L*1.01325 / (273.15*0.0831433);

// Retentate inlet conditions
FRet(0) = Inlet.F;
For comp in ComponentList Do
  ZRet(comp,0) = Inlet.z(comp);
EndFor
```

Figure 6.4 Ports definition and retentate inlet specification.

Now all that is needed for the model is present and it is possible to calculate the permeate flow rate. As reported below, the area for each cell is found and then two “for-do” loops are done, one inside the other. The first one defines the mass balance on the retentate, telling that the retentate flow rate in cell “k-1” is equal to the sum of the retentate and permeate flow rates in cell “k”. It is easy to understand that in each discretization point of the membrane, a fraction of the retentate stream goes through the membrane to the “permeate” stream, while the rest which remains “retentate” will be lower, so it is necessary to upload it in each cycle. Then the second “for-do” loop is made to evaluate this fraction of flow that permeates through the membrane at each discretization point, following the principles of the previous chapter. The following formula is derived from (3.9) where permeability P_i is expressed in $\left[\frac{\text{mol} \cdot \text{m}}{\text{m}^2 \cdot \text{s} \cdot \text{Pa}}\right]$. The formula is applied for each component in the mixture gas and it is:

$$F_{perm} \cdot x_{i_{perm}} = A_{cell} \cdot L_{mol_i} \cdot (P_{ret} \cdot x_{i_{ret}} - P_{perm} \cdot x_{i_{perm}})$$

Where:

$$F_{perm.} = \left[\frac{kmol}{h} \right]$$

$$x_i = [molar\ fraction]$$

$$A_{cell} = [m^2]$$

$$Lmol_i = \left[\frac{kmol}{m^2 * h * bar} \right]$$

$$P = [bar]$$

After it the retentate flow rate “k-1” is calculated to be used in the first “for-do” loop. The code is reported below :

```
// Balance equations for each cell
ACell = A/NCells;
For k in [1:NCells] Do
  FRet(k-1) = FRet(k) + FPerm(k);
  For comp in ComponentList Do
    FPerm(k) * ZPerm(comp,k) = ACell * Lmol(comp) * (Retentate.P*ZRet(comp,k) - Permeate.P*ZPerm(comp,k));
    FRet(k-1)*ZRet(comp,k-1) = FRet(k)*ZRet(comp,k) + FPerm(k)*ZPerm(comp,k);
  EndFor
  sigma (foreach (comp in componentlist) ZPerm(comp,k)) = 1;
EndFor
```

Figure 6.5 Balance equations for each cell.

Then with two additional “for-do” loops, the total retentate and permeate flow rates with respective compositions are calculated. Furthermore, temperature and pressure data of streams are saved like specific volume, enthalpy and densities:

```
// Retentate total flow and composition
Retentate.F = FRet(NCells);
For comp in ComponentList Do
  Retentate.z(comp) = ZRet(comp,NCells);
EndFor

// Permeate total flow and composition
Permeate.F = Sigma(FPerm);
For comp in ComponentList Do
  Permeate.F * Permeate.z(comp) = Sigma(Foreach (cell in [1:NCells]) FPerm(cell)*ZPerm(comp,cell));
EndFor

// Other outlet stream conditions
Retentate.T = Inlet.T;
Retentate.P = Inlet.P;
Permeate.T = Inlet.T;
Permeate.P = PPerm;

Call(Retentate.h) = pEnth_Mol_Vap(Retentate.T, Retentate.P, Retentate.z);
Call(Permeate.h) = pEnth_Mol_Vap(Permeate.T, Permeate.P, Permeate.z);

Call(RhoRet) = pDens_Mol_Vap(Retentate.T, Retentate.P, Retentate.z);
Call(RhoPerm) = pDens_Mol_Vap(Permeate.T, Permeate.P, Permeate.z);
Retentate.v = 1/RhoRet;
Permeate.v = 1/RhoPerm;

End
```

Figure 6.6 Retentate and permeate composition plus other outlet streams conditions in ACM.

Is also possible to build the icon of the model, this one will be exported to Aspen Plus too:

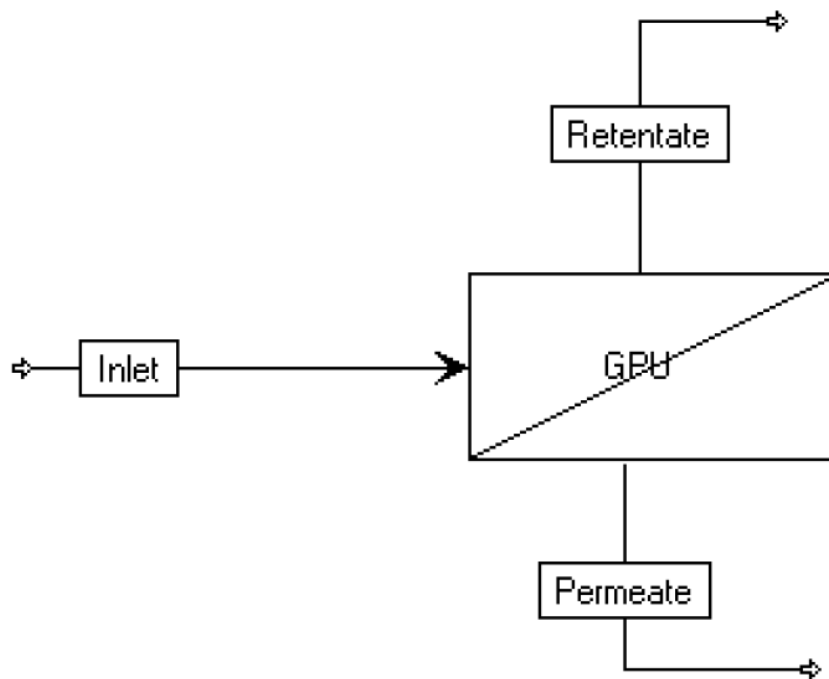


Figure 6.7 Schematic drawing of the base module (Gas Permeation Unit) in ACM.

6.4 Aspen plus

6.4.1 Exporting model from ACM to Aspen Plus

When the model on ACM has been completed is possible to transfer it in the library of Aspen Plus. To do that is necessary to install ‘ Microsoft Visual C++ , Visual Studio and Parallel Studio xe ‘. The right versions to be installed are reported in the “Set Compiler” tool of Aspen Plus. Having used Aspen Plus V11 the versions that can be adopted are reported in the Figure 6.8 below:

```

Set Compiler for V11

11 compiler sections in C:\Program Files\AspenTech\APrSystem V11.0\Engine\xeq\Compilers64.cfg

## Section      State Description
-----
1 IVF14_VS12    ERROR Intel Fortran 2013SP1 and Microsoft Visual Studio 12/2013
2 IVF15_VS12    ERROR Intel Fortran 15/2015 and Microsoft Visual Studio 12/2013
3 IVF16_VS12    ERROR Intel Fortran 16/2016 and Microsoft Visual Studio 12/2013
4 IVF16_VS14    ERROR Intel Fortran 16/2016 and VS 2015 WITH C++ (and express)
5 IVF17_VS14    ERROR Intel Fortran 17/2017 and VS 2015 WITH C++ (and express)
6 IVF17_VS15    ERROR Intel Fortran 17/2017 and VS 2017 WITH C++ (and community)
7 IVF18_VS14    ERROR Intel Fortran 18/2018 and VS 2015 WITH C++ (and express)
8 IVF18_VS15    OK      Intel Fortran 18/2018 and VS 2017 WITH C++ (and community)
9 IVF19_VSB     ERROR Intel Fortran 19/2019 and Bundled VS 2015 shell and Win10 SDK
10 IVF19_VS14   ERROR Intel Fortran 19/2019 and VS 2015 WITH C++ (and express)
11 IVF19_VS15   ERROR Intel Fortran 19/2019 and VS 2017 WITH C++ (and community)

The current compiler option settings in order of searching
  IVF18_VS15 for current user in HKEY_CURRENT_USER registry
  Not set for current machine in HKEY_LOCAL_MACHINE registry
  IVF17_VS15 in file C:\Program Files\AspenTech\APrSystem V11.0\Engine\xeq\Compilers64.cfg

Enter option (1:11) for current USER, 0 to skip, -1 to delete:

```

Figure 6.8 Capture of the set compiler of Aspen Plus V11.

When the software is installed correctly the line (8 in our casse) displays “OK”. Now it is th possible for the two programs (ACM and Aspen Plus) to communicate with each others with the same language.

Furthermore, ACM give an example to show the transfer from one software tool to the other, the file for this example will be in the folder ‘ C:\Program Files (x86)\AspenTech\AspenCustom deler V11.0\Examples\ModelExport ’

Below are reported the steps necessary for model transfer:

- In ACM, in the Simulation Explorer, under **Custom Modeling, Models**, right-click the model name (**GasPermeationUnit** in the present case) and select the **Exported Model Properties** wizard.
- Explore the various options available through the wizard for configuring the install package and accept the default options as saved in **GasPermeationUnit.acmf**.
- In the Simulation Explorer, under **Custom Modeling, Models**, right-click **GasPermeationUnit** and select the **Package Model for Aspen Plus/HYSIS** command.
- Select a convenient folder where **GasPermeationUnit.atmlz** is to be saved and click **OK**. In addition, the model is installed in the %LOCALAPPDATA%\AspenTech\AES\AM Models\V11\ folder, making it immediately available to Aspen HYSYS and Aspen Plus.

So, it will be possible to find in the “ACM model” library of Aspen Plus all the models built in ACM. The exported model described above simulates a single stage arrangement with feed compression or permeate vacuum, and without any recycle stream. This is the simplest configuration possible and this individual stage may consist in the reality of several permeators arranged in parallel so to achieve the right flowrate for the feed flow.

6.4.2 Module construction in Aspen Plus

The goal is to produce a permeate flow comparable to the ones from other technologies as said in Paragraph 1.6. As said before the terms of comparison are the purity so the mole fraction of CO₂ present, and the quantity

of CO₂ captured. So with the following patterns the researched purity will be 99% and at least 90% of CO₂ capture rate (CO₂ separated over CO₂ inlet). To achieve these percentages, it will be necessary to apply multi-stages patterns, recycle system, feed compression, permeate vacuuming or permeate sweeping.

Such configurations are represented below respectively in compression and vacuum condition. [Mohammad Hassan Murad Chowdhury, 2011]

- Configuration 1: figures a single-stage membrane process where the FEED is compressed before the membrane unit. Then the membrane unit separates the flue gas in a CO₂ rich permeate stream (PERMEATE) and a CO₂ lean retentate stream (RETENTAT). As the retentate stream is still at high pressure, an EXPANSOR recovers the mechanical energy contained in the retentate.
- Configuration 2: the single stage membrane uses a blower for slight feed compression and vacuum pump for permeate vacuuming at 0.25 bar to maximise the transmembrane pressure difference.

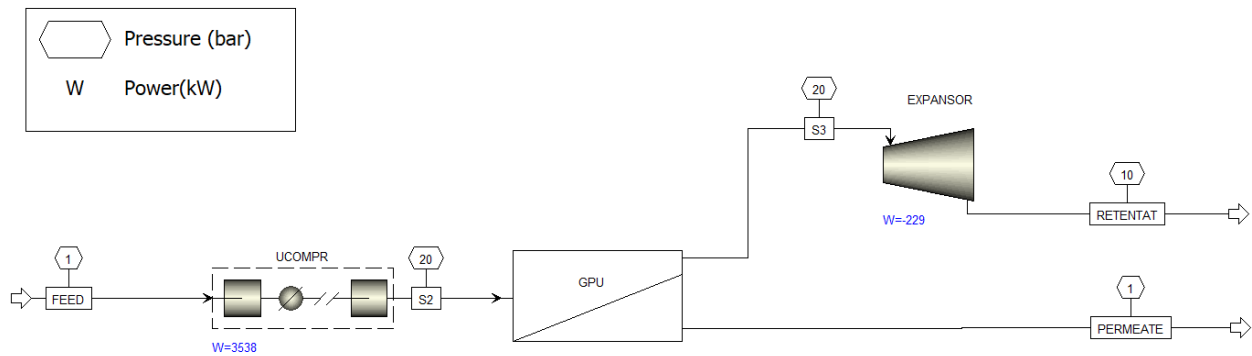


Figure 6.9 Configuration 1.

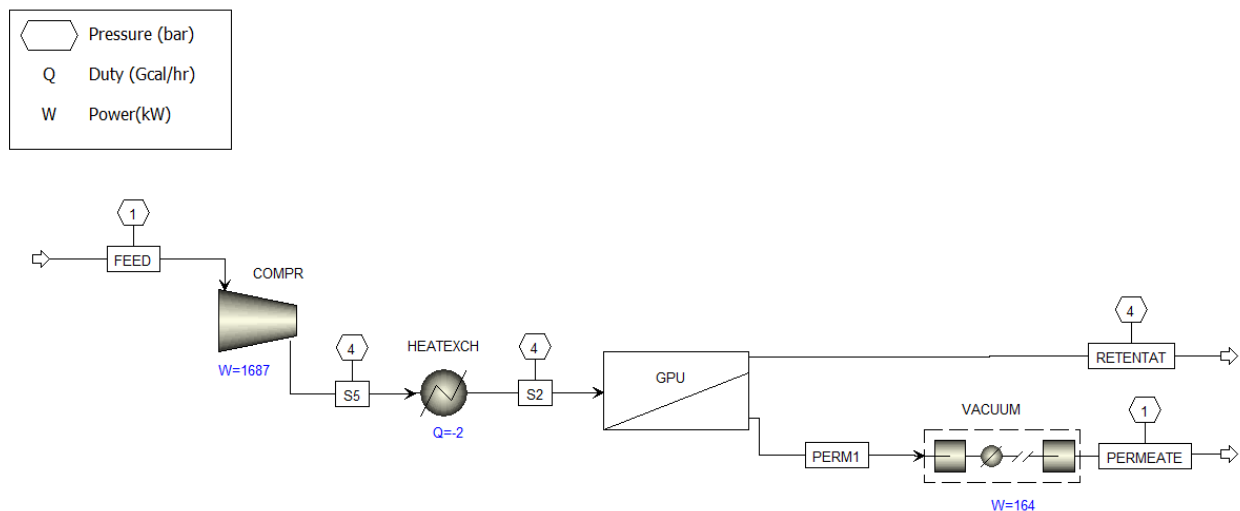


Figure 6.10 Configuration 2.

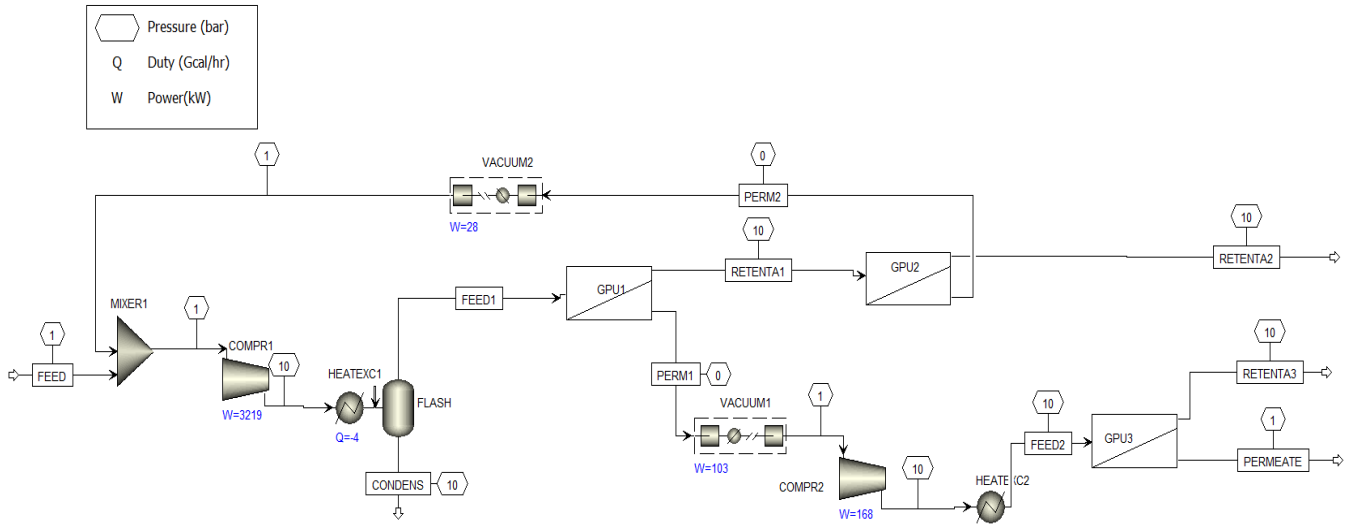


Figure 6.11 Configuration 3.

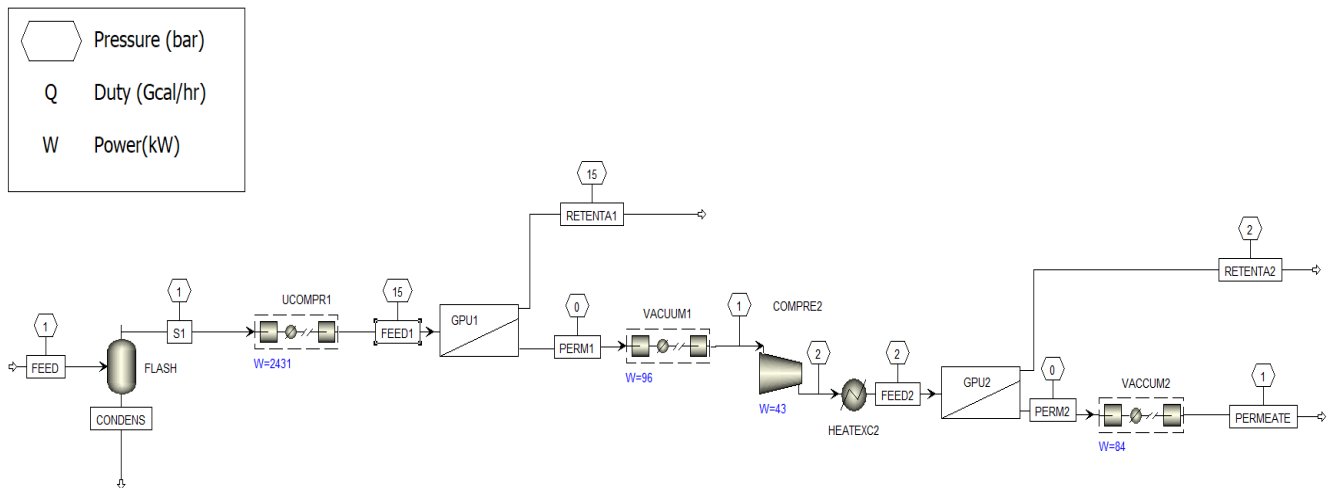


Figure 6.12 Configuration 4.

- Configuration 3: was developed by [Lin, 2007] with feed compression and permeate vacuum. The FEED after being compressed is fed to the 1st membrane unit which is attached to a permeate vacuum pump. The retentate stream, works with another membrane stage also in vacuum condition. Then the CO₂ rich stream is recycled recompressed and mixed in MIXER1 with the flue gas stream. The permeate stream from the 1st stage is compressed and fed to the third membrane stage to get the desired purity in the final permeate stream. The permeate stream will be then compressed to a specified pressure for transportation or injection in a site, but this aspect has not been considered in this work. In particular, Lin configuration was tested with three different vacuum conditions (0.33 bar, 0.25 bar, 0.1 bar), and it resulted that the highest purity compared with energy consumption is reached with 0.25 bar vacuum condition. Thus, the permeate which works in vacuum condition works at 0.25 bar.
- Configuration 4: considers feed compression with permeate vacuum approach for both the first and second separation stages. With respect to configuration 3, it needs only two membrane modules in series without any sweep recycling.

These two last configurations are capable to achieve 98-99% of purity in CO₂ of the permeate flow. The main characteristics of the four configurations presented are reported below:

Table 11 Data characteristic of Configuration 1 and 2.

Process configuration			Configuration 1	Configuration 2
Stream name		Flue-in	Permeate	Permeate
Mole fraction	CO ₂	0.0796	0.61	0.73
	N ₂	0.704	0.34	0.23
	O ₂	0.135	0.05	0.04
	H ₂ O	0.0815	0	0
Total flow	kmol/h	793.16	80.4	101.6
Temperature	K	313	313	313
Pressure	[bar]	1	1	1
Permeate vacuum condition	[bar]		-	0.25
Permeate compressor pressure	[bar]		20	-
CO₂ capture rate (stage-cut)	[%]		85%	85%
Stage-cut in each membrane stage	[%]		85%	85%
Total membrane area	[m ²]		500	5000
Feed compressor power	[MWe]		5.1	1.69
Permeate vacuum pump power	[MWe]		-	0.164
Net (Capture) power consumption	[MWe]		5.1	1.85

Table 12 Data characteristic of Configuration 3 and 4.

Process configuration			Configuration 3	Configuration 4
Stream name		Flue-in	Permeate	Permeate
Mole fraction	CO ₂	0.0796	0.999	0.987
	N ₂	0.704	0.004	0.0056
	O ₂	0.135	0.0039	0.0058
	H ₂ O	0.0815	7.31e-7	3.36e-6
Total flow	[kmol/h]	793.16	57.14	61.1
Temperature	K	313	313	313
Pressure	[bar]	1	1	1
Permeate vacuum condition	[bar]		0.25	0.25
Permeate compressor pressure	[bar]		10	15
CO ₂ capture rate (stage-cut)	[%]		88.3%	88%
Stage-cut in each membrane stage	[%]		80%-54%-98%	87%-98%
Membrane area in each stage	[m ²]		250-300-10	200-200
Total membrane area	[m ²]		560	400
Feed compressors power	[MWe]		3.39	2.474
Permeate vacuum pumps power	[MWe]		0.131	0.18
Net (Capture) power consumption	[MWe]		3.52	2.654
Energy per ton of CO ₂ separated	[MWhe/ton]		1.31	0.99

In conclusion, Configuration 3 results produce a permeate with higher purity but need more membrane area and energy to maintain the vacuum and compression condition. The Configuration 4 instead permits to also have a high purity (almost 99%) with the same stage-cut but with a 30% lower area and less energy consumption compared to Configuration 3. For this reason, Configuration 4 has been chosen as final pattern.

6.5 Other configurations

The object of this work is to achieve a 99% purity of CO₂ with a good stage-cut (80%-90%) but during the studies for the best pattern many configurations have been developed. However, many of them could not achieve these goals. It is also useful to talk about them because there are some utilities of CO₂ where a high purity is not necessary. For example, it can be reused inside greenhouses to favour chlorophyll photosynthesis. The different configuration is reported below:

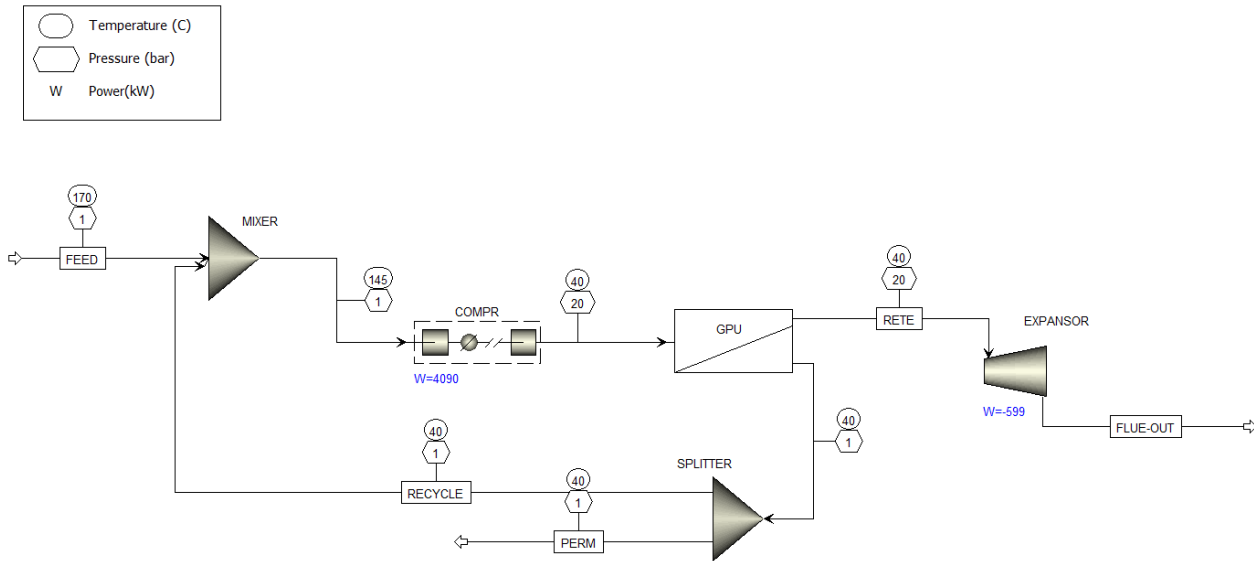


Figure 6.13 Configuration 5.

- Configuration 5: represents one stage membrane in compression with 60% of recycle of part of the permeate and an expander to recover the energy of compression in the retentate stream.

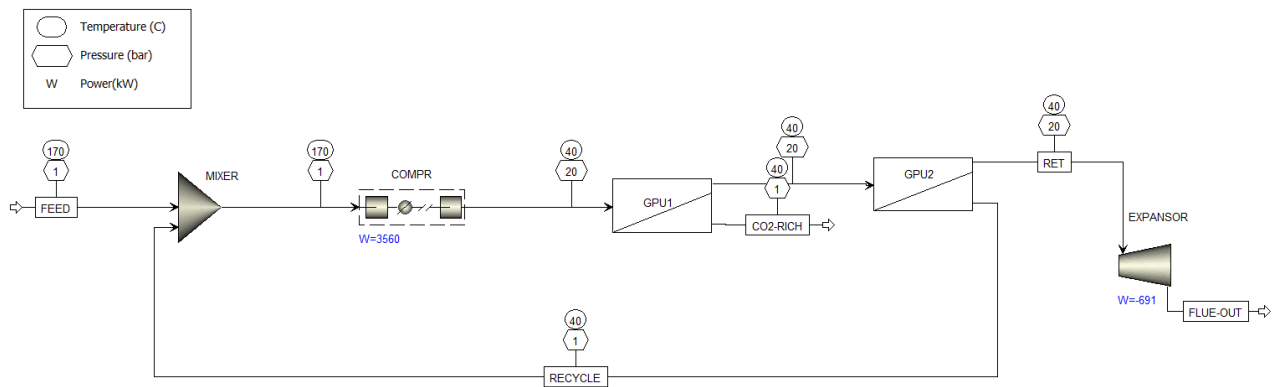


Figure 6.14 Configuration 6.

- Configuration 6: represents a two-stage cascade membrane in compression conditions with a recycle of the permeate of the second membrane and an expander in the retentate stream.

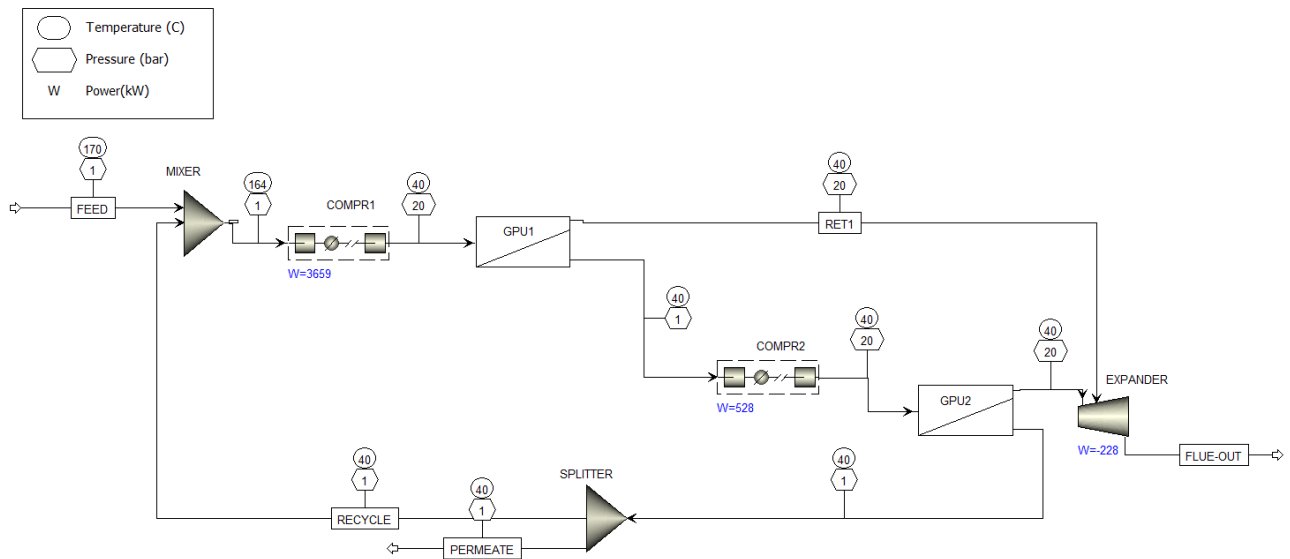


Figure 6.15 Configuration 7.

- Configuration 7: like Configuration 6, this configuration applies the second membrane on the permeate stream of the first one with a compression system and recovers expansion energy from both the retentate streams in outlet.

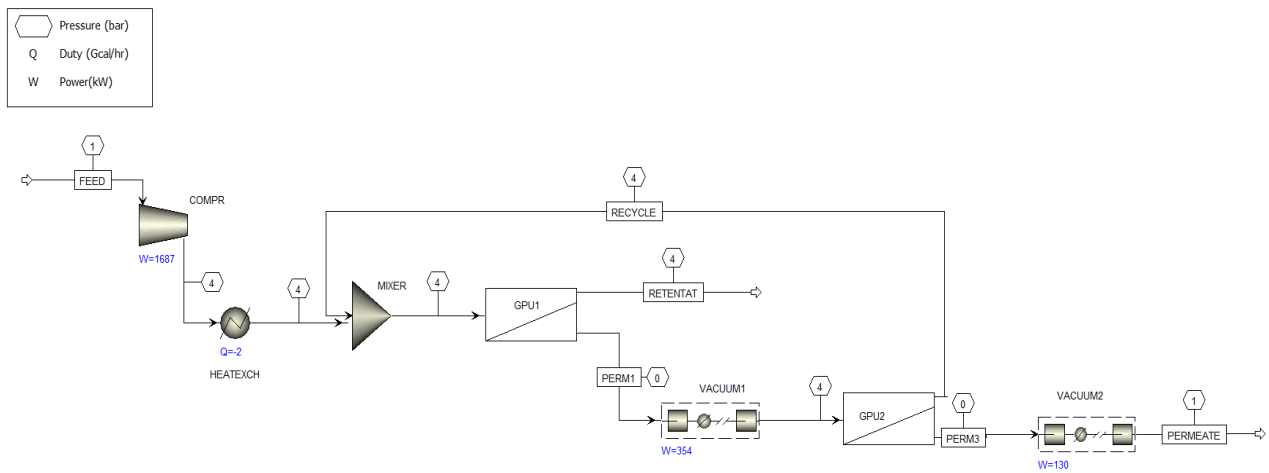


Figure 6.16 Configuration 8.

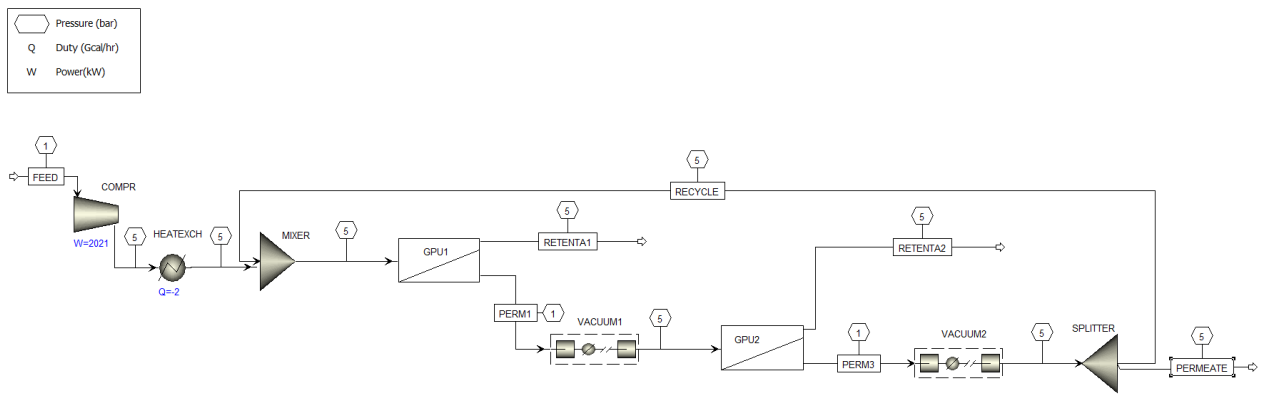


Figure 6.17 Configuration 9.

- Configurations 8 and 9: are both characterized by two-stage cascade membrane configurations with vacuum permeate condition and feed compression. These configurations 8 and 9 use respectively retentate and permeate (fraction) recycling from the 2nd stage.

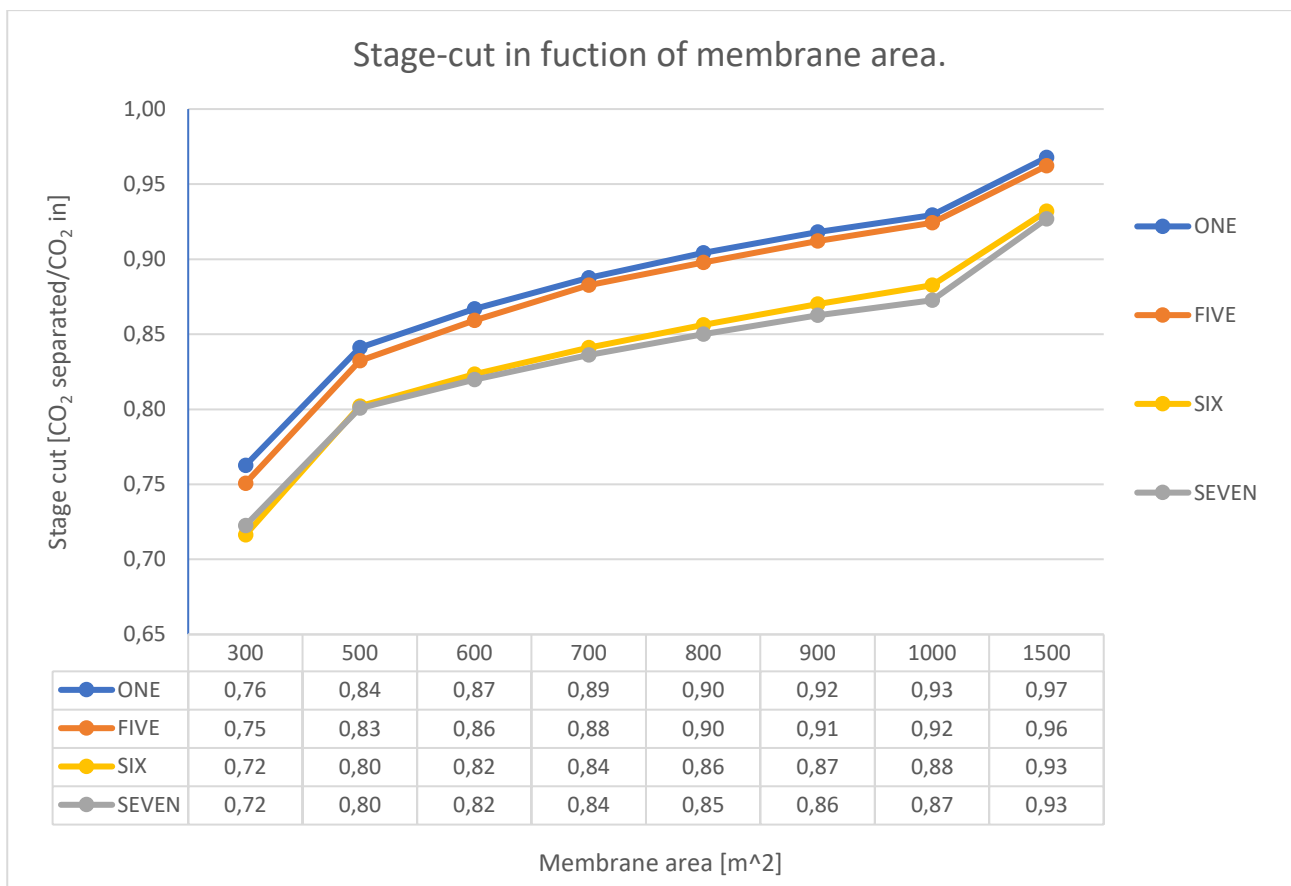


Figure 6.18 Stage-cut in function of membrane area.

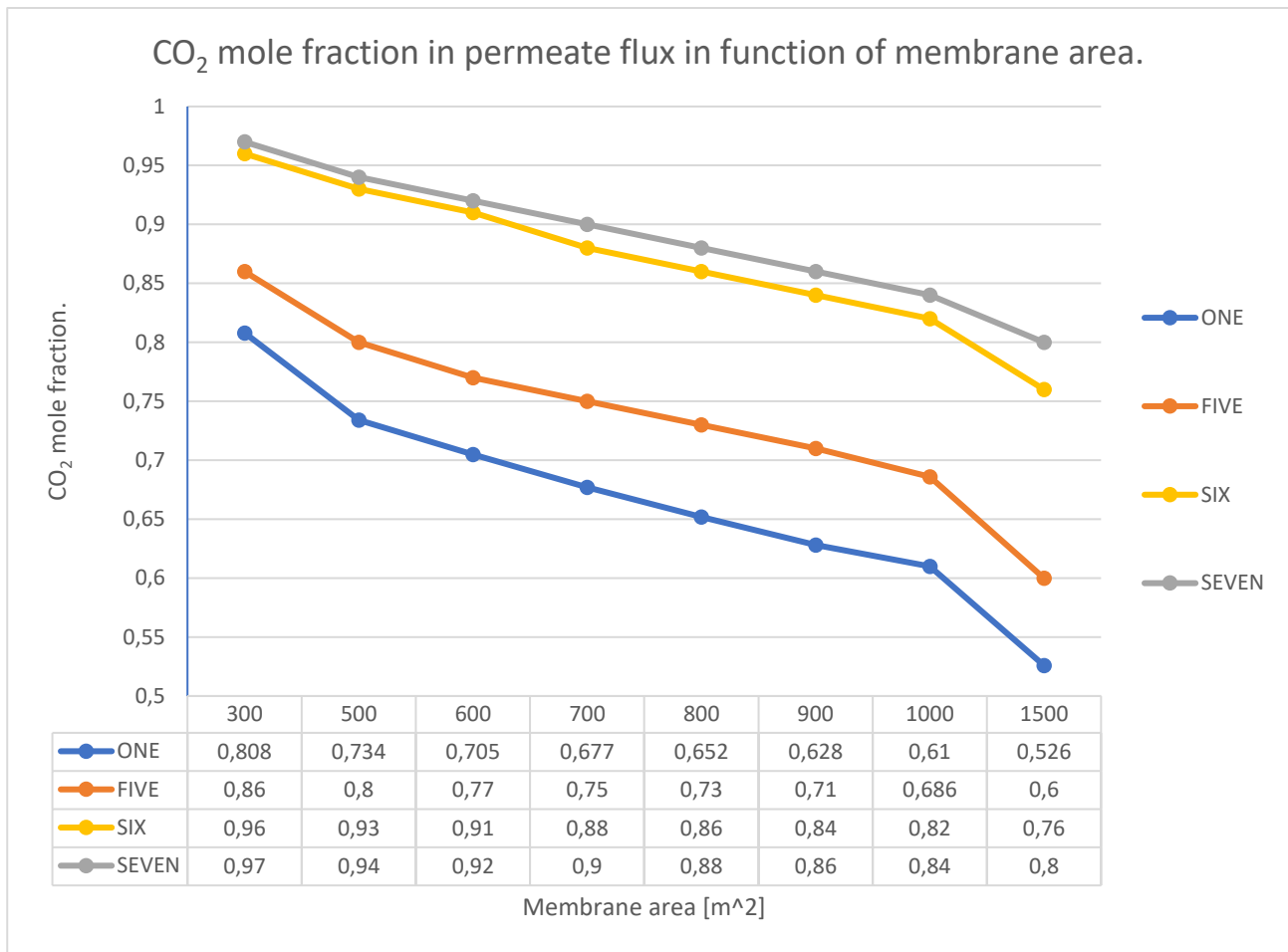


Figure 6.19 CO₂ mole fraction in permeate flux in function of membrane area.

In Figure 6.18 and Figure 6.19 the stage-cut and the mole fraction of CO₂ in the permeate stream are represented in function of the area of the membrane. The comparison regards the patterns with compression system. For the sake of simplicity, this sensitivity study has considered an approximated flue gas composition of 10vol-% CO₂ and the rest of it being nitrogen. Looking at Figure 6.18, it is possible to understand how the increase of the area enhances the CO₂ separation rate, a major area in fact raises the probability of the gas to permeate the membrane. However, a larger quantity of separated CO₂ also enhances the N₂ in the permeate and this affects the purity. Figure 6.19 reports how the purity decreases when increasing the membrane area. A smaller area brings to a higher concentration of CO₂ in the permeate but at the same time to lower quantity of separation. It shows also how the type of recycle loop considerably impacts the purity of the permeate stream. In fact, looking at Figure 6.19 we can see that the six and seven configurations compared to the other two reach a higher purity of the permeate output, in terms of CO₂. This is because the recycling is carried out on the permeate flow and not on the retentate flow as in eight and nine and the “quality” of the stream is higher. The situation is reversed when looking at the amount of CO₂ removed, Figure 6.18. In this case the recycling on the retentate and not on the permeate allows the eight and nine configurations to reach higher values of separate CO₂. However, the highest purity percentage achieved with these patterns is 97% which is not enough for our goal.

Chapter 7: Amine absorption

Absorption technology is the most used in the separation processes of CO₂. There is a difference between physical absorption and chemical absorption (also called reactive absorption) and also between adsorption and absorption.

In absorption the (absorbed) component is captured by an (absorbent) material, usually a gas, a liquid or a solid is retained in a liquid. As said, it can be chemical or physical, depending on the nature of the interactions. Chemical absorption implies the establishment of chemical reactions in the bulk liquid while physical absorption is essentially mechanical, as it is due to entrapment of solids in vacancies and interstices.

Adsorption instead is a superficial phenomenon only. It is the accumulation of species occurring only from one part of the interface, while we speak of absorption if the accumulation of species occurs on both sides of the interface and in the bulk solution.

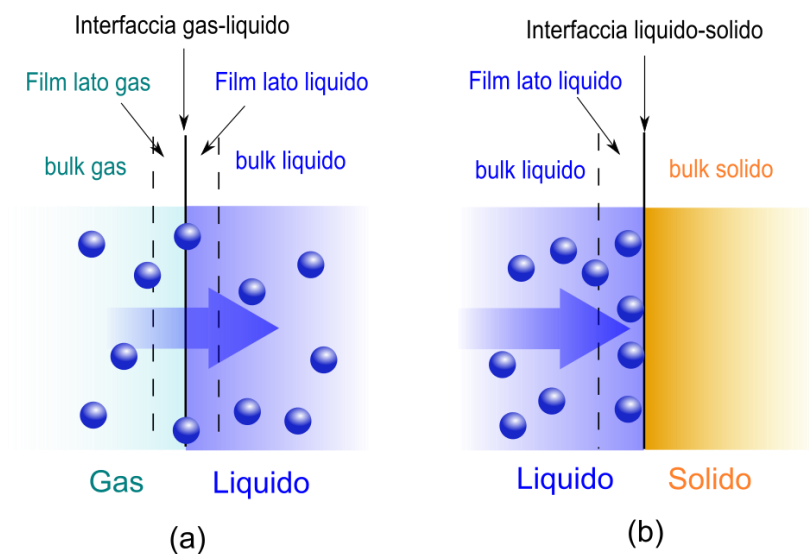


Figure 7.1 Mechanism of gas-liquid absorption (left) and liquid-solid adsorption (right). The blue dots represent the solute molecules. Source [Daniele Pugliesi, 2009].

So in chemical absorption the CO₂ chemically binds to the solvent and for this reason the relation between the CO₂ partial pressure and CO₂ loading in the solvent solution is not linear, the behaviour is represented in Figure 7.2 below:

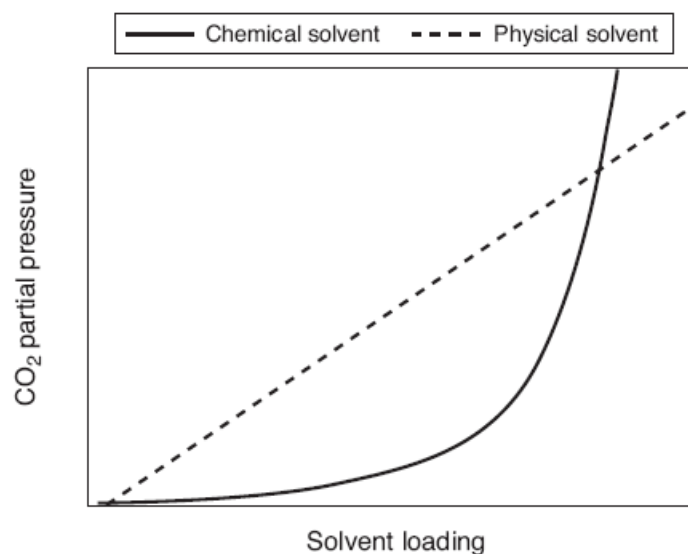


Figure 7.2 Comparison between chemical and physical absorption. Source [Grégoire Leonard, 2008-2009]

In function of the partial pressure of the CO₂, it is more convenient to use one kind of absorption or the other. From Figure 7.2 it is possible to see how it is more profitable to use chemical solvents at low CO₂ -partial pressures as their loading is much higher. So, in our case where the concentration of CO₂ is around 8%, the chemical absorption is the best choice.

This technology as said is based on the reactive absorption of the CO₂ into an amine solvent³. Amines are organic compounds containing nitrogen, they can be considered as compounds derived from ammonia by substitution of one, two or three hydrogen atoms with alkyl or aryl groups. In organic chemistry alkyl (or alkyl group) is the generic name of the functional group corresponding to an alkane⁴ deprived of a hydrogen atom [IUPAC, Gold book "Alkanes"], and also aryl (or aryl group) which is a monovalent radical⁵ derived from an aromatic hydrocarbon (organic compounds which contains one or more aromatic rings) from which a hydrogen atom directly bound to the ring has been removed [IUPAC, Gold book "Aryl groups"].

On base of the number of alkyl or aryl groups linked to nitrogen, the amines are classified in primary, secondary and tertiary amines, respectively if the nitrogen is linked with one, two or three groups (Figure 7.3).

³ Alternatives to amine exist and are being thoroughly studied, but they are out of the scope of the present work.

⁴ **Alkanes** are organic compounds consisting only of carbon and hydrogen (for this reason they belong to the largest class of hydrocarbons), having brute formula C_nH_(2n+2). Alkanes are "saturated", i.e. they contain only single C-C bonds (therefore, with the same number of carbon atoms, they have the maximum number of hydrogens possible compared to other hydrocarbons), unlike alkenes (which contain double bonds C=C) which are called "unsaturated" and alkynes (which contain triple bonds C≡C). Alkanes are also "acyclic", that is they do not contain closed loop chains (unlike cycloalkanes).

⁵ **Radical** (or free radical) is a very reactive molecular entity having a very short average life, constituted by an atom or a molecule formed by more atoms, that presents an odd electron: such electron makes the radical extremely reactive, able to bind itself to other radicals or to subtract an electron to other near molecules.

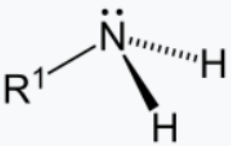
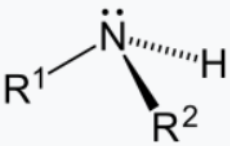
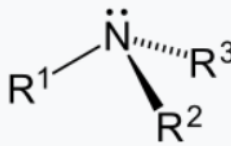
Primary (1°) amine	Secondary (2°) amine	tertiary(3°) amine
		

Figure 7.3 Classification of amine in primary, secondary and tertiary.

In this work the amine solvent used will be the monoethanolamine refigured in Figure 7.4 below:

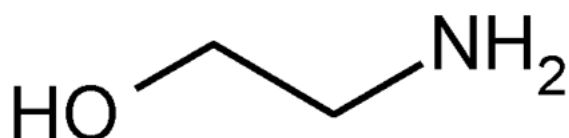


Figure 7.4 MEA amine structure.

7.1 Plant design

Generally the flue gas from the plant enters a bit in over-pressure in the absorber. The absorber can contain stainless steel rings of a few centimetres randomly arranged or stacked corrugated and perforated stainless sheets that form a honeycomb structure. The first lay-out is called random packing and it is cheaper with high liquid rate. The second type, structured packing column, favours instead low pressure drop, the capability of handling various fluid characteristics such as acid and many other corrosive materials and permits also a greater stable operating range [Bennet and Kovak, 2000].

In the absorber the CO₂ will be then in contact with the chemical absorbent which will be introduced by the top of the column and flows under gravity over the solid surface of the packing. On the contrary, the flue gas is blown from the bottom through the interstices in the packing (Figure 7.3). Due to the packing is possible to have a larger area of contact between the gas and the liquid. Pall rings, Intalox saddles, Raschig rings, and Berl saddles, as shown in Figure 7.4, are the most common random packings used in industrial operations. They are usually made of inert materials that are cheap and light, such as porcelain, chemical stoneware, or carbon, plastic, steel, and metal alloys.

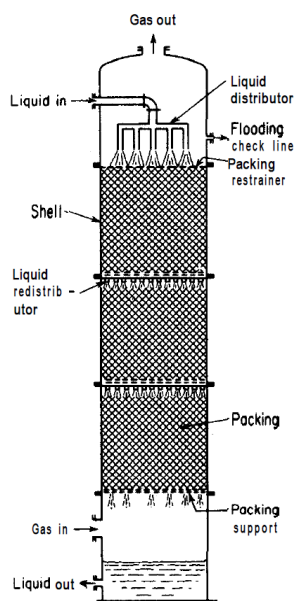


Figure 7.5 Cross-sectional view of packed tower in operation. Source [Max S.Peters,1991].

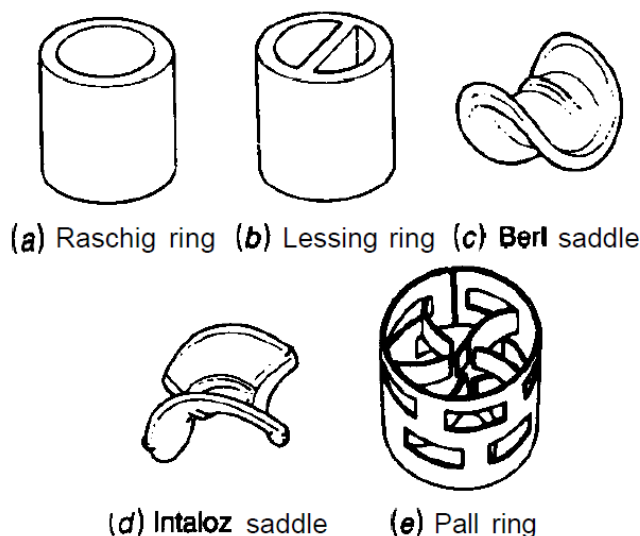
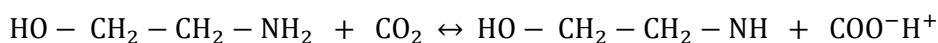


Figure 7.6 Single pieces of typical random packings. Source [Max S.Peters,1991].

Amine absorbs in a range of temperature between 40-60°C, the temperature depends on the type of absorbents [Bailey ,2005]. Furthermore, the chemical absorption is an exothermic reaction, so it is favoured at low temperature. The absorption mechanism in the solvent can be summarized in two main steps: formation of a zwitterion⁶ and instantaneous removal of a proton by a base B to form a carbonate. In aqueous solutions, the base B can be either water, an amine molecule or an OH⁻ ion. The first reaction is rate-determining [Danckwerts, 1979; Versteeg and Van Swaaij, 1988.]

⁶ **Zwitterion** is an electrically neutral molecule as a whole, but it has both positive and negative localized charges.



The flue gas then passes in the water-washing column and a demister where the water is separated from the gas. It is finally released to the atmosphere, as most of its CO_2 has been captured by the solvent. The rich solvent is then pumped to a regeneration column, the stripper, where it is heated to desorb the CO_2 . The temperature are in a range of 100/140°C. Furthermore, is present an lean-rich heat exchanger: which recovers part of the heat from the hot lean solvent to pre-heat the cold-rich solvent before its entrance into the stripper. The regenerated solvent “lean solvent” will be sent back to feed the absorber. A cooler brings this solvent to the right entrance temperature (Figure 7.7). After the desorption column, the CO_2 product gas still contains some water, so a condenser is necessary. The final product will easily achieve a CO_2 -purity of 99% by volume.

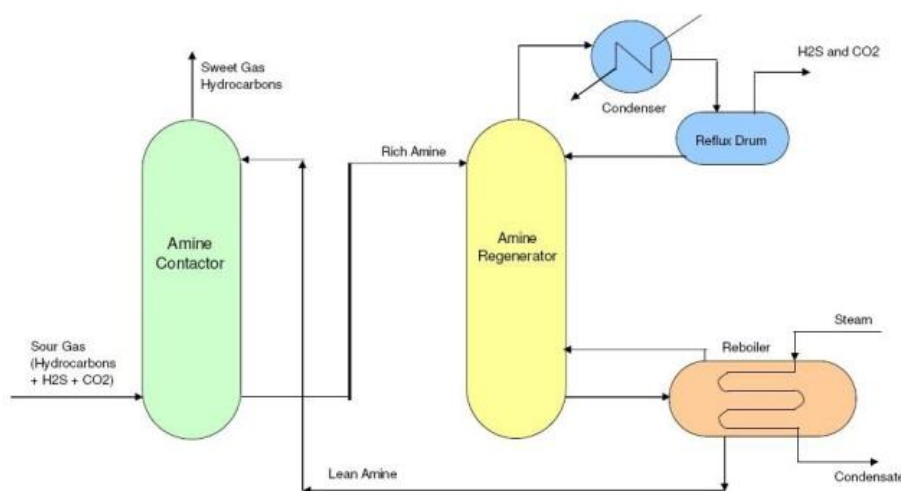


Figure 7.7 Simplified plant of amine absorption. Source [Dr. Mark Jordi,2016].

7.2 Possible solvents

The absorption technology is one of the most mature CO_2 capture technologies under the research point of view, and many amine and non-amine (e.g. carbonate) solvent have been studied in order to capture CO_2 in post-combustion processes. Secondary and primary amines can be used alone or as rate promoters with tertiary amines, hindered amines or potassium carbonate thanks to their faster absorption kinetics [Rochelle ,2016].

Class	Typical reaction	$-\Delta H_{\text{abs}}$ (kJ/mol)	Kinetics
Carbonate	$\text{CO}_3^{2-} + \text{CO}_2 + \text{H}_2\text{O} \leftrightarrow 2\text{HCO}_3^-$	40	Very slow
Tertiary amine	$\text{R}_3\text{N} + \text{CO}_2 \leftrightarrow \text{R}_3\text{NH}^+ + \text{HCO}_3^-$	60	Slow
Hindered amine	$\begin{array}{c} \text{H}_3\text{C} \quad \text{CH}_3 \\ \diagdown \quad \diagup \\ \text{C} \\ \diagup \quad \diagdown \\ \text{HO} \quad \text{NH}_2 \end{array} + \text{CO}_2 \leftrightarrow \text{AMPH}^+ +$	60–70	Moderate
Secondary or primary amines	$\begin{array}{c} \text{HCO}_3^- \\ 2\text{R}_2\text{NH} + \text{CO}_2 \leftrightarrow \text{R}_2\text{NHCOO}^- \\ + \text{R}_2\text{NH}_2^+ \end{array}$	70–80	Fast

Figure 7.8 Aqueous amine and carbonate chemistry. Source [Rochelle, 2016].

In the Figure 7.8, it is showed that secondary and primary amines have a faster kinetics, but the energy released by CO₂ absorption is higher than in the case of tertiary or hindered amine. This means higher temperature to regenerate the solvent and due to this also a faster degradation rate.

In particular, in Carbon Capture processes solvent degradation may be a critical drawback. Thermal and oxidative degradation are the principal's mechanisms observed. The oxidative degradation occurs especially at the absorber condition due to the O₂ content in the flue gas while thermal one is a problem at the stripper condition where the amine must be regenerated by increasing temperature.

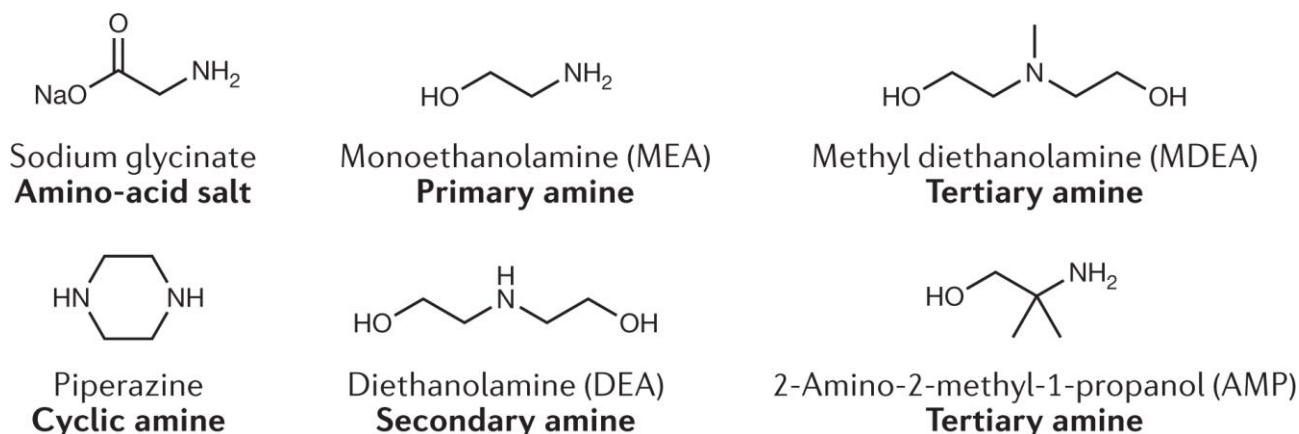


Figure 7.9 List of some amines. Source [Noel Vicente].

In Figure 7.9 are listed some of the traditional amines used in water solution to capture CO₂. Monoethanolamine (MEA) 30% wt. in water solutions are the most studied solvent. The CO₂ desorption process is characterized by high consumption of thermal energy (necessary to reverse the absorption reaction and to release CO₂). For this reason, one of the main aims of improvement is to minimize this energy consumption. The CO₂ removal in percentage and the energy consumption in the CO₂ plant are function of the amine circulation rate, absorption column height, absorption temperature and recovery temperature. A literature value of heat consumption at 85% of CO₂ removed is 4 MJ/kg CO₂.

In this study, the model developed by [Grégoire Leonard, 2008-2009] has been taken as reference. This model represents a pilot plant for CO₂ capture absorption. In particular, it was scaled-up for our case study. Many assumptions have been made to assist the convergence of process loop calculations; initial value have been given for three process streams (tear streams). It is also important to be sure that the mass balance of water in the process is closed. Water accumulation or water loss in the steady-state process would make the calculations diverge.

Regarding the model approach for the columns, Equilibrium model has been chosen. In this model columns are simulated through the succession of equilibrium stages in which no mass or heat transfer limitations occurs. Due to this aspect the packing characteristics or column dimensions are not necessary. [Austgen, 1989] ,[Jou, 1982]. This simplified assumption gives results quite close to the reality and is acceptable in first approach (Léonard et al., 2011).

7.3 Model construction

7.3.1 Pilot model

An existing model representing a pilot plant (presented in Figure 7.8) was developed in Aspen Plus at the University of Liège several years ago, and as said the present work consisted in scaling it up to the conditions of the cogeneration plant. The inlet flue gas of the pilot plant model was considered free from all contaminants, and this assumption has been kept. The design objective is set for 90 % CO₂ capture with 96% of purity (mole fraction).

Table 13 Flue gas composition of pilot plant.

Mole flow [kmol/h]	111.54
Mole fraction [%]	
CO ₂	15.62
H ₂ O	13.4
N ₂	75.85
O ₂	6.69

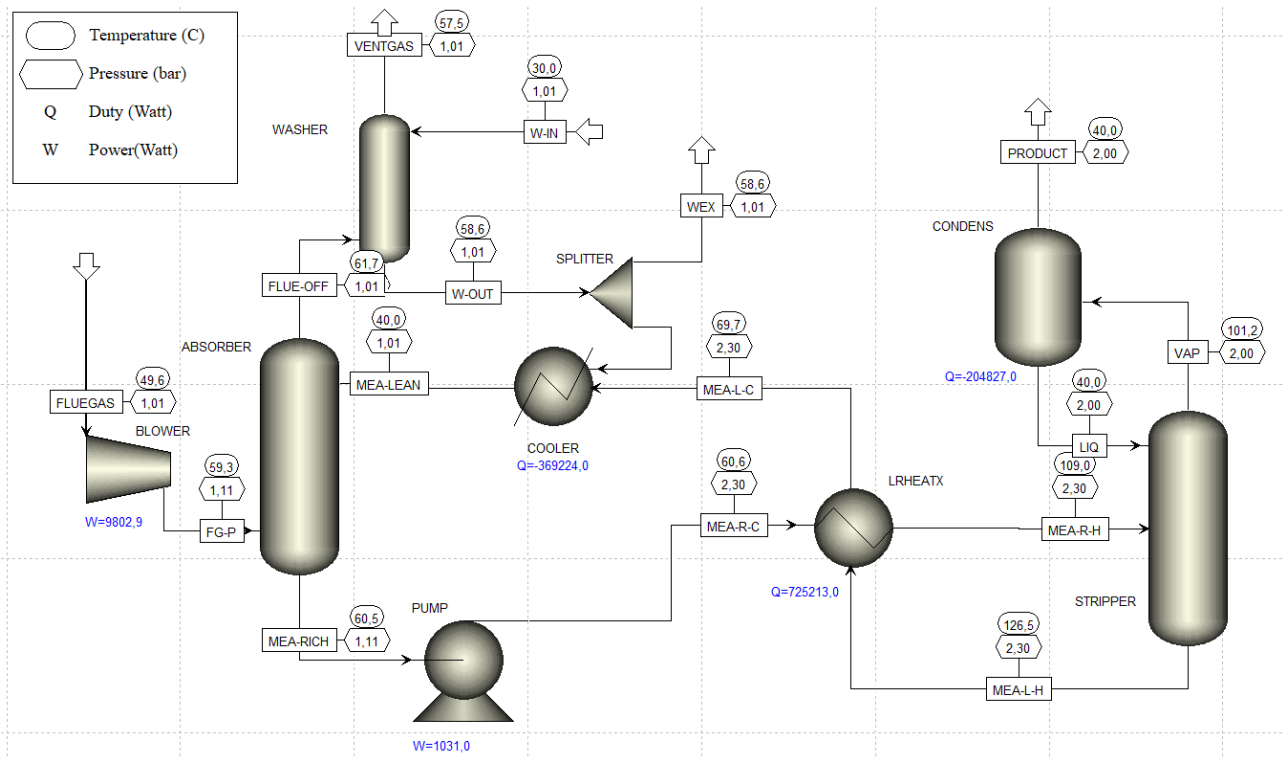


Figure 7.8 Plant of amine capture pilot plant on Aspen Plus.

Some general assumptions have been made for the construction of the absorption model by amine:

- Corrosion and degradation due at the O₂ in the inlet flue gas is negligible.
- Liquid phase reaction only.
- Negligible heat loss.

- Negligible solvent degradation.

To calculate fluid thermodynamic and transport properties, it is necessary to specify the property method and solution chemistry of MEA-CO₂-water system which is an aqueous electrolyte solution of ionic and molecular species. Electrolyte solutions are extremely nonideal because of the presence of charged species. The Electrolyte NRTL model was used for modelling this kind of solutions. The convergence of the model can depend on different things such as the recycle structure of the flowsheet, the nonlinear models of absorber and stripper, and initial estimates to initialize the columns. For the initial estimate to initialize absorber and stripper a proposal can be to decompose the process flowsheet into a stand-alone absorber and a stand-alone stripper [Alie, 2005]. This procedure is needed because due to losses from evaporation in the absorber and stripper the amount of make-up MEA and water changes. The recycled loop in the flowsheet should be closed during the simulation run. It is possible then to vary properly the water make-up to keep a constant percentage of MEA solution (30% is a common value). This will avoid build-up of high concentration of MEA which can favour corrosion. Also, the pressure profile in the columns needs to be updated after each iteration because dependent upon process operating conditions, column type, and column internal configurations. It is the same for hydrodynamic performance criteria such as down comer flooding for tray column. This indicator should be checked explicitly during process design for stable and feasible operation [Alie, 2004]. Especially in the stripper model, care should be taken so that the reboiler temperature does not exceed the MEA solvent degradation limit, around 120°C.

The flowsheet mainly consists of the following Aspen Plus unit operation blocks:

Blower: in Aspen Plus this unit operation is specified to model Blower to increase the flue gas pressure to overcome the pressure drop in the absorber unit. COMPR represents a single stage compressor. A polytrophic efficiency of 85% and a mechanical efficiency of 95% is assumed. The outlet pressure of the Blower is set to 1.11 bar as an input variable by the operator.

Pump (rich): All pumps are modelled with the Aspen Plus Pump unit operation model. Outlet pressure or pressure rise need to be specified to calculate pump's power requirement. For the rich solvent pump, pressure rise to 2.3 bar is necessary to reach the operating pressure required in the Stripper.

Lean/Rich Heat Exchanger: In the LRHEATEX, the rich amine is preheated prior to regeneration by hot lean amine coming from the bottom of the regenerator. It is modelled in Aspen Plus using two-stream heat-exchanger unit operation model, HeatX. The exchanger is modelled using a short-cut approach in simulation mode, with a heat exchange area of 80 m² and 5°C as minimum approach temperature.

Cooler: After passing through the lean-rich heat exchanger, the lean amine must be further cooled in a Cooler before it is pumped back into the absorber column. The cooler lowers the lean amine temperature to the desired Absorber inlet temperature such as 40°C. The Cooler is modelled with Aspen Plus Heater unit operation model which is mainly used as thermal and state phase changer.

Splitter : is used to split a single stream to multiple streams. FSplit is used to implement a splitter operation.

Absorber and Stripper : are modelled with the Aspen Plus- RadFrac unit operation model. RadFrac directly includes mass and heat transfer in the system of equations representing the operation of separation process units. Absorbers does not have any condenser or reboiler. The inlets and outlets are connected to the top and bottom of the column for Absorber. The pressure at the top of the Absorber is fixed at 101.3 kPa. For the Stripper, a condenser at the top is modelled by an extra unit, while a reboiler included at the bottom of the column is considered. This reboiler is modelled as an equilibrium stage. Increasing the Stripper pressure also raises the temperature which in turn helps to lower energy requirements for solvent regeneration with MEA solvent. But is necessary to avoid excessive degradation of MEA (30 %wt) solution due to temperature rise in the reboiler beyond 126.6°C.

7.3.2 Case study

After introducing the composition and flow rate of flue gas of the University of Liège cogeneration unit into the available amine model, it was necessary to perform some changes to reach convergence. In first attempt

the only change of flow rate and composition leads the system in error because the lower percentage of CO₂ in the flue gas leads to a lower flow rate of the CO₂ product at the stripper outlet. As a consequence, less water exits the solvent loop with this CO₂ product stream and this induces sur-plus of water in the loop, and leading the system to divergence. It was then necessary to reduce the water accumulation in the solvent loop. The solution was to rise the temperature of the CONDENSER from 40°C to 80°C. Doing that, a lower quantity of water will condense so the LIQ stream will decrease and the PRODUCT stream will instead increase, letting grow also the molar fraction of water leaving the process. However, due to this the PRODUCT stream will have a lower CO₂ purity (76% and the rest being water). To bring the purity at 99% is then necessary to add another flash (that will work at 20°C, removing excess water out of the process) which will produce “PRODUCT1” with 98.7% of CO₂ purity and will separate most of the water in it. The CO₂ capture rate is almost 99%, this value is too high because means that the process is oversize. Usually capture rate are around 90%-95%, otherwise would be excessively expensive a cause of reboiler increase duty. Then a possible future work could be to optimize the size of the plant. Another change has been done to bring the flue-gas in inlet to the optimal condition of the absorber. A cooler has been introduced to bring the flue-gas from 170°C to 40°C in order to reach an acceptable inlet temperature in the absorber column. This is also combined with a flash that separates the condensed water. However, as already mentioned, this flue gas pre-treatment requires more investigation as impurities in the flue gas are currently making this condensation unsafe for the equipment (sulfuric acid condensation).

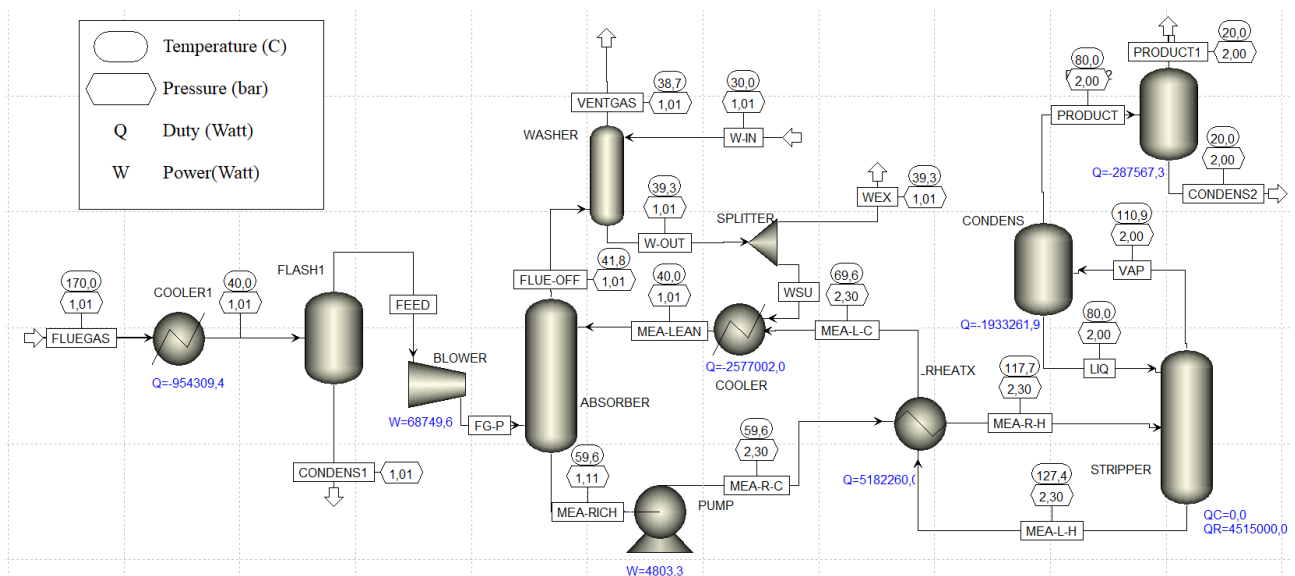


Figure 7.9 Amine plant for CHP Liegi University.

Below, the fundamental inputs of the absorber and stripper columns are:

Table 14 Data inputs of absorber and stripper columns.

ABSORBER		
Internal tray type		Packed
Material		Metal
Height	[m]	12
Diameter	[m]	1.86
Total pressure drop	[mbar]	27.4
STRIPPER		
Reboiler duty	[kW]	4515

Reboiler pressure	[bar]	2.3
Reboiler temperature	[°C]	127.4
.Feed temperature	[°C]	117.7
Height	[m]	10
Diameter	[m]	1.6

The dimensions (height and diameter) of the columns as said before are probably oversize. However, they are comparable in height to those found in large scale capture plants. In fact, the height is a fundamental factor for the purification of CO₂ present in exhausted fumes. As the fumes must travel a greater distance in close contact with the amine and water solution and this enhance the probability to get captured.

The amine technology is then a good option to reach our goal because high purity is an easy target. However, the thermal energy needed in the stripper represents a strong constraint for the operational cost. Finally, the plant presented is only a simplified version of a real plant. Some arrangements should be done to make it more performant. For example, it could be possible to close the loop of the water in the washing section at the absorber outlet, in order to decrease the required water make-up.

Chapter 8: Economic analysis

Economics is an essential parameter to be investigated during the development of any new technology or process or modification of an existing process configuration besides the technical evaluation. The economic assessment of a process depends on the method of analysis used and, on the value, assigned to economic parameters. For this reason, economic assessments made by different evaluators may differ considerably from each other. The economic study provides estimates for capital (CAPEX) and operational (OPEX) cost. The capital one is based on equipment sizes and capacities and their associated costs, while opex regards the operational cost of the plant and so all expenses like energy or manufacturing that are strictly linked to the operation of the plant. The information on both equipment and operating cost was obtained from bare module cost method [Turton, 2013] and www.matche.com. Thanks to these two sources it was possible to evaluate the components in function of the size and typology. Both have been compared and they lead to similar result for similar component, the necessity to use both is due to the fact that some component, as vacuum pumps for instance are present only in www.matche.com and some others are available only following Turton method. For more details please refer to Appendix B.

CO₂ dehydration system and CO₂ pipeline for transportation and sequestration are not included in the cost analysis, and it can be assumed that they would be similar costs whatever the chosen CO₂ capture technology.

Flue gas pre-treatment system is also not considered, although it may significantly affect the project conclusions. Indeed, this is mostly related to the tolerance of technologies to impurities (discussed in Chapter 4), which was considered to be outside the scope of the present work, but that needs to be imperatively studied in future works.

In addition, it has been assumed that the heat and electricity supplies from the separation plants come from outside. This makes it possible to make a comparison of the consumption, released from the cogeneration plant supplies. Furthermore the model assumes that the biomass is not managed in sustainable way.

8.1 Membrane cost evaluation

The information about membrane cost was found in the work of [Merkel ,2010]. The assumptions and specifications used in this economic evaluation for membrane gas separation-based capture process are presented in the Table below:

Table 15 Assumption and specifications for membrane separation plant.

	Source	Value
Project life	[K. Sartor, 2014, 132]	20 years
Plant operation	[K. Sartor, 2014, 132]	5200 h/year
Membrane cost	[Merkel,2010]	50 €/m ²
Membrane life	Assumption	3 years
Membrane replacement cost	[Mohammad Hassan Murad Chowdhury, 2011]	25% total membrane cost (per year operation cost)
Membrane CO ₂ permeance, 10 ⁻¹⁰ mol/s.m ² .Pa	[Lin, 2007]	3350
Membrane CO ₂ /N ₂ selectivity	[Lin, 2007]	50
Labour cost		45€/h/operator

The life of the membrane was reduced from 4 to 3 years to take in consideration all negative effects due to impurities like NO_x or SO_x or also harsh operational conditions. This assumption is not precise but the lack of more information regarding this technology are big, and these aspects are the most studied.

The capital and operational cost have been produced for Configuration 4. Indeed, this one was chosen as final configuration because it permits similar purity of permeate compared with Configuration 3 and a minor energy consumption and membrane area, respectively smaller by 25% and 29%.

Table 16 Summarizing table about power consumption, CO₂ capture and economic evaluation about membrane.

SUMMARIZING TABLE FOR MEMBRANE		
	Unit	Value
Power needed (electrical)	MWe _{el}	2,65
Power needed (thermal)	MW _{th}	0
CO ₂ emitted without capture	ton/h	3,08
	ton/MWh	1,28
	ton/year	16.016,00
CO ₂ emitted with capture	ton/h	0,40
	ton/MWh	0,17
	ton/year	2.082,08
CO ₂ captured per year	ton/year	13.933,92
Cost of CO ₂ avoided	€/ton CO ₂	71
CAPEX	€	2.163.192
OTHER OPEX	€/year	727.726
ENERGY CONSUMPTION	€/year	690040
TOTAL OPEX (year 1)	€/year	1417766
	€/ton CO ₂	101,7
TOTAL COST CO ₂ capture (20 years)	TOTAL COST €/20years	19.831.701

To calculate the total cost of CO₂ capture during the lifetime of the plant, has been made a cashflow balance over 20 years, so that OPEX are discounted, as the price of money decreases. An interest rate of 5% has been considered.

The power needed to run the plant is essentially electrical and higher than the one generated by the cogeneration plant (2.4 MWh).

Table 17 Power consumption of membrane separation plant.

POWER	POWER	Units	
	Process Configuration		Conf. 4
	Vacuum Pump 1	kWe	96
	Vacuum Pump 2	kWe	84
	Feed compressor	kWe	2431
	Compressor	kWe	43
	TOTAL	kWe	2654
		MWe	2,65

Under an energetic point of view, the membrane plant does not need heat from outside, but instead, a big thermal duty needs to be extracted from the capture process. Looking at the table below and considering one

hour of functioning, it is possible to see that 4.34 MWh need to be removed. This can be a good opportunity to recover some heat, and for this reason in Table 18 are reported temperature value of flue gas to evaluate the quality of the heat.

Table 18 Energy cooling duty about membrane separation plant.

ENERGY DUTIES	COOLING DUTY	T [°C]	MW
	Feed compressor	390	2,99
	Vacuum Pump 1	240	0,10
	Vacuum Pump 2	240	0,08
	Heat echanger	100	0,04
	Flash	170	1,13
	TOTAL		4,34

8.2 Amine plant cost evaluation

The same sources have been used for amine plant as for membranes. In addition, some specifications have been made only for the amine plant in order to have a more complete general picture. Furthermore, it must be precised that the bare cost module method for absorber and stripper or columns in general, could be underestimated following previous experience of using this method (discussion with G. Léonard). Further assumptions have been made regarding materials, for more details please refer to Appendix B.

In addition, the higher stage-cut percentage respect standards values, can be caused by an oversizing of some components in the plant which leads consequently to higher investment and operational costs. A good improvement of this work could be to fix the model so to have 90%-95% of stage-cut and not the actual 98,7%.

Table 19 Assumption and specifications for membrane separation plant.

	Source	
Project life	[K. Sartor, 2014, 132]	20 years
Plant operation	[K. Sartor, 2014, 132]	5200 h/year
MEA price	[Karl Stéphane,2013]	1.6 €/kg
MEA degradation rate	[Rao and Rubin, 2002]	1,5 kg/ton CO ₂ captured
Biomass price	[K. Sartor, 2014, 132]	33 €/MWh
Electricity price	[K. Sartor, 2014, 132]	50 €/MWh
Labour cost		45€/h/operator

The cost of biomass has been reported as essential in the calculation of the operational cost of the system. This is because the burner delegated to the heat production that will then be supplied to the stripper was assumed to be a biomass burner. Regarding the total operating cost, it can be divided into two main categories: manufacturing cost and general expenses. Manufacturing cost as we have seen for membrane includes all expanses connected with the manufacturing operation or the physical equipment of a process plant. These can be subdivided in direct production cost and fixed cost. General expanses instead include administrative and R&D cost (Appendix B for more details). However below are presented as well as the membrane the most representative values:

Table 20 Summarizing table about power consumption, CO₂ capture and economic evaluation about membrane.

SUMMARIZING TABLE FOR AMINE		
	Unit	Value
Power needed (electrical)	MWel	0,07
Power needed (thermal)	MWth	4,52
Cost of CAPEX per CO ₂ in captured life plant	€CAPEX/ton CO ₂	9,26
CO ₂ emitted without capture	ton/h	3,08
	ton/MWh	1,28
	ton/year	16.016,00
CO ₂ emitted with capture	ton/h	0,04
	ton/MWh	0,02
	ton/year	208,21
CO ₂ captured per year	ton/year	15.807,79
Cost of CO ₂ avoided	€/ton CO ₂	89,6
CAPEX	€	2.928.553,2
OTHER OPEX	€/year	940.867
ENERGY CONSUMPTION	€/year	827922,4
TOTAL OPEX (year 1)	€/year	1.768.789
	€/ton CO ₂	111,89
TOTAL COST CO ₂ capture (20years)	€/20years	24.971.575

Differently from the membrane plant, the amine one, needs and releases heat. Most of the heat as already said regards the stripper component. In this case the outlet of the stripper “lean solvent” exchange in LRHEATX part of its thermal duty to the inlet in the stripper “rich solvent”. This permit a significant saving of energy. In the table below, the energy demand and consumption are reported for an hour of work. Unfortunately not all the surplus heat available can be used because the exergy of it is low and in the plant only the stripper needs energy but it is characterized by a higher temperature level.

Table 21 Energy cooling duty about membrane separation plant.

ENERGY DUTIES	COOLING DUTY	T [°C]	[MW]
	COOLER1	170	0,95
	COOLER	70	2,58
	CONDENS	111	1,90
	FLASH2	80	0,30
	TOTAL COOLING DUTY		5,73
	HEATING DUTY	T [°C]	[MW]
	STRIPPER	127,4	4,50

8.3 Summarizing results

For both technologies are reported the principals' value in the table below were is possible to make an economic comparison.

Table 22 Summarizing table of principals characteristics of CO₂ capture processes.

SUMMARIZING TABLE			
	Unit	Membrane	Amine
CAPEX	€	2.163.192	2.928.553
Power needed (electrical)	MWel	2,65	0,1
Power needed (thermal)	MWth	0	4,5
Cost of CO ₂ avoided balanced in life plant	€/ton CO ₂	71,2	89,6
Cost of CAPEX per CO ₂ in captured life plant	€CAPEX/ton CO ₂	7,76	9,26
OTHER OPEX	€/year	727.726	940.866
ENERGY CONSUMPTION	€/year	690040	827922
TOTAL OPEX (year 1)	€/year	1.417.766	1.768.789
TOTAL COST Capture (20years)	€/20years	19.831.701	24.971.574

The results show that membranes are more profitable in terms of both investment and operating costs. This price gap leads to a difference of just over €5 million at the end of the plant's life. Then, with regard to these results, membrane separation is economically preferable.

Chapter 9: Conclusion and perspectives

Conclusion

Environmental concerns have received increased attention by the scientific community which is warning about the effects of anthropogenic greenhouse gas emissions on the environment. In this context, CO₂ capture and storage technologies are proposed as one of the solutions to a decarbonated energy mix. Their object is to capture CO₂ which comes from fossil fuel combustion and to re-use or store it in the ground.

The objective of the present study is to evaluate different CO₂ capture technologies that could be applied to small-scale CO₂ emitting units, based on a case study done for the biomass-fired cogeneration plant available at the University of Liège. The latter provides both thermal and electrical energy to the campus and is interconnected with the district heating network for the heating of neighbouring buildings. The study wants to highlight the characteristics of membranes (not yet mature but very promising due to its compactness and flexibility of use) and amines (technology consolidated in the capture of CO₂ in large scale plants but still unknown its potential in small scale plants).

The first part of the work regards membrane technology, a promising option in the CO₂ capture scenario. A particular focus has been done on the material. In particular, the three main materials are proposed to constitute the membrane layer:

- *Polymeric membranes*: are the most used because also the first more widespread in this sector. Permeability and selectivity are high but they suffer particularly from pollutants and harsh condition as high temperature or high pressure. In the last decade, some improvement have been taking place, leading to the development of TR polymers where TR means “Thermally re-arranged”. This is characterized by higher resistance at higher pressure and temperature but also to higher values of permeability and selectivity. The drawback is the incapability to produce them at large scale.
- *Zeolites and carbonate membranes*: are also promising, they achieve a higher value of permeability and selectivity also in harsh condition compared to polymeric ones. They are differentiated in dense and porous membranes but the research is still on-going to find a better way to produce them without constructive problems encountered in the production.
- *Hybrid membrane*: are a mix between the first two. Two main patterns are described in the literature, namely Matrix Mixed Membranes(MMMs) and composite membranes. Polymer/zeolite composite membranes could be an ideal material for post-combustion CO₂ capture because the correct combination of different mechanisms and configurations will gain benefits which will enforce the strength and durability of the membranes without decreasing their performances. However, research is still on-going to confirm these hopes.

Furthermore, in this work, a basic membrane model and several possible configurations have been developed to produce a permeate with high purity and high stage-cut. The software used is Aspen Custom Modeler for the base module of the membrane and then Aspen Plus for the search of the best process configuration. Vacuum and compression conditions have been used separately and then together to reach the goal. Only two configurations achieved 99% of purity with stage-cut higher than 80% and one of them was selected to do then the comparison with amine technology.

The second part of this work regards the post-combustion CO₂ capture with amine solvents. It is the most mature CO₂ capture technology for a large-scale application like coal or natural gas-fired power plants. Similar to membranes, it is possible to retrofit existing plants by treating the flue gases after the combustion (both technologies are thus called post-combustion technologies). Two main drawbacks of this technology impact its widespread :

- The high energy requirement of the process for regenerating the amine solvent that has absorbed CO₂.

- The environmental impact related to the emission of amine solvents and degradation products into the atmosphere.

The starting point of amine absorption was the study of an existing pilot model plant developed in Aspen Plus in previous work at University of Liège. The available process model was up-scaled to consider a bigger flue gas flow rate so to match with the flow rate of the cogeneration plant of Liege University. The solvent used in the simulation is an aqueous solution of monoethanolamine (MEA). In first attempt, changing only the flue gas flow rate without changing the composition, the model reacted without any error. However, the composition of the flue gas of the cogeneration plant is characterized by a higher percentage of oxygen and a lower level of CO₂. This led the system in error because a surplus of water was registered in the solvent loop. It was thus necessary to remove an additional part of the water in the CO₂ product condenser. In order to finally achieve 99% purity of CO₂, a second flash tank was added at the outlet of the product stream.

Finally, an economic analysis was performed for both technologies based on simulation results. It pointed out that membrane plant is a more advantageous investment. The amine one is characterised by higher CAPEX cost and a higher total OPEX. The amine as said needs a lot of thermal energy to regenerate the solvent which impacts significantly the OPEX. In conclusion, amine technology appears as the most mature and robust technology which make it more reliable. Membranes are also promising, both from economical and working point of view but some aspects bonded to the young development of the technology must be assessed.

Perspective

The further steps for the improvements are quite numerous. The CCS technology in general would be more profitable from a reduction of the energy consumption in the capture process and from an increase of capture efficiencies. A continuous improvement would permit to recover high energy amounts and this would contribute to a significant reduction of CO₂-emissions.

A possible in-depth study that could be done on both technologies is to consider the presence of impurities in the incoming fumes of the plants. In fact, in the present work a strong assumption has been made regarding the treatment of impurities and the reaction of the plant to them. Since the study focuses on small plants, the possible presence of NO_x, SO_x, humidity or other substances can be a crucial factor in the competitiveness of these technologies.

Another study that may cover both technologies is the analysis of the plants' response to the variation of input fumes. In particular, it can be thought to vary the molar composition of the flue gases also the temperature and pressure and thus establish which plants and in which conditions and ranges have a greater efficiency.

Talking about membrane first an important step could be the use of more improved membrane. As said in Chapter 3, there is a lot of room for improvement in this technology and in many materials already very good results have been found. It remains to be seen how to find a sustainable and cost-effective method for the large-scale production of these materials.

In addition, is also possible to think to a different lay-out of the plant of separation which would need less energy consumption, for instance the compression energy could be reduced with better membrane materials and pattern.

About amines, the model developed is very simplified and leaves many aspects behind. One of these is the possibility to close the water loop so that there is no need to use a new one at each cycle. Moreover, the conditions of oxidation and deterioration of the solvent are not taken into account and could be fundamental aspects in small scale use.

Another important aspect is that the stage-cut found is relatively high respect standards values of amine absorption and this is probably caused by a wrong oversizing of components which leads to a higher estimation of total price of the technology.

In conclusion, another fundamental and not negligible aspect is to extend the study also on PSA technology, the latter presented in the Introduction Chapter is, together with the other two, one of the most promising and used technologies in the field of CO₂ capture and therefore cannot be excluded.

Appendix A

The following section presents the steps of the economic analysis. Consisting of the calculation of the capital cost (CAPEX) and operational cost (OPEX) of the plant. As already mentioned in Chapter 8, reference has been made to the Turton R method for the calculation. , 2013 and a component calculation software available at www.matche.com. All value found by these two sources are in dollar, but here are reported in euro knowing that 0.89€ are equivalent to 1\$ (2020).

Regarding CAPEX, it includes so-called fixed costs, which generally account for 30%-40% of total expenditure. The cost of machinery and plant components is a long-term investment that must be made only once during the life of the plant (except for breakdowns or components with a shorter life than the plant), they also do not depend on the level of production.

There are several methods for the calculation of the capital cost, in this study the Bare Module Costs method was adopted. It estimates the capital cost of major components according to the conditions of the base case. Pressure stresses or materials that are too expensive are not considered and the following formula is applied:

$$\log_{10}C^0 = K_1 + K_2\log_{10}A + K_3(\log_{10}A)^2$$

C^0 is the cost at ambient pressure.

A is a capacity or size parameter.

K_i are empirical constants.

The results of this first step are reported in the Table 23. After this was calculated the bare module cost in real conditions. For heat exchangers, pumps vessels and towwers this is calculated following the formula below:

$$C_{BM} = C^0(B_1 + B_2F_mF_p)$$

B_1 and B_2 are constants

F_m and F_p are the material and pressure factor.

After C_{BM} calculation the effect of time was considered, in fact with the increase of time there is also a cost increases (inflation). To consider that an inflation index was introduced Chemical Engineering Plant Cost Index (CEPCI), equal to (609.5/397) where 609.5 refers to 2019 and 397 to year 2001.

The following step was to find the total module cost of the plant which take in account unexpected contingency due to costs and fees and valid for plant expansion C_{TM} . This last one was considered as Fixed Cost of Investment (FCI) for the further steps.

Below are reported the tables for membrane plant:

Table 23 Calculation procedure for CAPEX of membrane separation plant part 1.

CAPEX	Description	Type	Material Construction	Costing source	Size factor	Factor value	K1	K2	K3	C0 [€]
	Membrane	Hollow fibre module, Polarys	Polymers	Merkel, 2010	Area, m ²	400				17800
	Flue gas cooler	SS shell & tubes	SS tubes & CS shell	Turton R. et al., 2013	Area, m ²	800	4,8306	0,8508	0,3187	99088
	Heat exchanger	U-tube	CS-shell/Cs-tube	Turton R. et al., 2013	Area, m ²	100	4,1884	0,2503	0,1974	24015
	Vacuum pump1	Blower type (two stage) incl. Electric motor	SS	www.matche.com	Flow rate (Cubic feet/min)	4746				26200
	Vacuum pump2	Blower type (two stage) incl. Electric motor	SS	www.matche.com	Flow rate (Cubic feet/min)	3742				24300
	Feed Compressor	Centrifugal compressor inclufing drive, gear mounting, base plate and cooler	SS	www.matche.com	Power, (kW)	2431	2,2897	1,3604	0,1027	54000
	Compressor	Centrifugal compressor	SS	Turton R. et al., 2013	Power, (kW)	43	2,2897	1,3604	0,1027	13834
	Total									259237

Table 24 Calculation procedure for CAPEX of membrane separation plant part 2.

CAPEX	Description	Type	C1	C2	C3	Work. Press. [barg]	Fm	Fp	B1	B2	CBM2001	CBM2019
	Membrane	Hollow fibre module, Polarys									17800	27328
	Flue gas cooler	SS shell & tubes	0,0388	- 0,1127	0,08183	1	1,8	1,01	1,63	1,66	460934	707656
	Heat exchanger	Blower type (two stage) incl. Electric motor	0,0388	- 0,1127	0,08183	1	2,7	0,98	1,63	1,66	144377	221657
	Vacuum pump1	U-tube	0	0	0	1	2,3	1	1,89	1,35	130869	200919
	Vacuum pump2	Blower type (two stage) incl. Electric motor	0	0	0	1	2,3	1	1,89	1,35	121379	186348
	Feed Compressor	Centrifugal compressor including drive, gear mounting, base plate and cooler	0	0	0	14	2,3	1	1,89	1,35	269730	414107
	Compressor	Centrifugal compressor	-0,394	0,3957	- 0,00226	1	2,3	0,53164	1,89	1,35	48981	75199
	Total										1,194,070	1,833,214
	Ctm (FCI)											
	2,163,192											

Operating cost are of different types :

- Direct costs: vary with production rate but not necessarily directly proportional
- Fixed costs: do not vary with production rate but relate “directly” to production function
- General expenses: functions to which operation must contribute- overhead burden

Table 25 Calculation procedure for OTHER OPEX costs of membrane separation plant.

OTHER OPEX		Unit or basis	Value
	Process Configuration		4
	DIRECT PRODUCTION COST		
	Membrane replacement	25% of membrane cost	0,415
	Maintenance and repair (M)	5% of FCI	108159,6
	Operating labor (OL)	One job per shift 36€/h	187200,0
	Supervision and supports (S)	30% of OL	56160,0
	Operating supplies	15% of M	16223,9
	Laboratory charges	10% of OL	5616,0
	FIXED COST		
	Local taxes and insurance	3,2% of FCI	69222,2
	Plant overhead cost	70,8% (OL) + 3,6% (FCI)	210412,5
	GENERAL EXPENSES		
	Administrative	17,7%(OL) + 0,9%(FCI)	52603,1
	R & D	5% of total manufacturing cost (COM)	22129,1
	Total		727,726.9

Table 26 Calculation procedure for DIRECT PRODUCTION costs of membrane separation plant.

DIRECT PRODUCTION COST ANALYSIS		Unit	Value
	Process configurations		4
	Net generating capacity without CO2 capture	MWe	2,4
	Hour of work of the CHP per year	h/year	5200
	Base plant cost of electricity	€/MWh	50
	Stage-cut	CO2captured/CO2inlet	0,87
	CO2 emitted without capture	ton/h	3,08
		ton/MWh	1,28
		ton/year	16016
	CO2 emitted with capture	ton/h	0,4004
		ton/MWh	0,17
		ton/year	2082
	CO2 captured per year	ton/year	13933,92
	Cost of CO2 avoided	€/tonCO2	43,1
	CO2 cost per CAPEX in 20 years	€CAPEX/tonCO2separated in20years	16,6
	Annual energy consumption CO2 capture cost	€/year	690040
Total OPEX per year			
1.417.766,9			

From this point are reported the calculations for Amine Plant, the procedure is the same of the membrane one. Since fumes and amines are possible corrosive substances, it has been assumed that most of the material used is Stainless Steel (SS).

Table 27 Calculation procedure for CAPEX of amine separation plant part 1.

CAPEX	Description	Type	Material construction	Costing source	Size factor	Factor value	K1	K2	K3	C0 [€]
	COOLER1	Cooling pond	Al tube	www.matche.com	Power, kW	954				24000
	COOLER2	Cooling pond	Al tube	www.matche.com	Power, kW	2577				64000
	LRHEATX	U-tube	CS-shell/Cs-tube	Turton R. et al., 2013	Area, m ²	600	4,1884	-0,2503	0,1974	92465
	AMINE SOLVENT	MEA	MEA	Karl Stéphane, 2013	Mass, kg	7144				11431
	BLOWER	Axial, small	SS	www.matche.com	Flow rate (Cubic feet/min)	12352,48171				24920
	FLASH1	Process vessel, vertical	SS	Turton R. et al., 2013	Volume, m ³	4,71	3,4974	0,4485	0,1074	6272
	CONDENS	Process vessel, vertical	SS	Turton R. et al., 2013	Volume, m ³	3,14	3,4974	0,4485	0,1074	4969
	FLASH3	Process vessel, vertical	SS	Turton R. et al., 2013	Volume, m ³	3,14	3,4974	0,4485	0,1074	4969
	WASHER	Process vessel, vertical	SS	Turton R. et al., 2013	Volume, m ³	18,85	3,4974	0,4485	0,1074	15611
	PUMP	Variable speed	SS	Turton R. et al., 2013	Power, kW	4,50	3,3892	0,0536	0,1538	2749
	STRIPPER	Process vessel, vertical	SS	Turton R. et al., 2013	Volume, m ³	31,42	3,4974	0,4485	0,1074	22856
	ABSORBER	Tower, tray or packed	SS	Turton R. et al., 2013	Volume, m ³	37,70	3,4974	0,4485	0,1074	26342
	STRIPPER PACKING	Packing	SS	Turton R. et al., 2013	Volume, m ⁴	31,42	2,4493	0,9744	0,0055	7410
	ABSORBER PACKING	Packing	SS	Turton R. et al., 2013	Volume, m ⁵	37,70	2,4493	0,9744	0,0055	8878
	WASHER PACKING	Packing	SS	Turton R. et al., 2013	Volume, m ⁶	18,85	2,4493	0,9744	0,0055	4470
	TOTAL									321,343

Table 28 Calculation procedure for CAPEX of amine separation plant part 2.

CAPEX	Description	C1	C2	C3	Diameter vessel [m]	Working pressure [barg]	Fm	Fp	B1	B2	C0	CBM2001	CBM2019
	COOLER1	0,03881	-0,11272	0,08183		0,1	1,8	1,71	1,63	1,66	24000	161850	248483
	COOLER2	0,03881	-0,11272	0,08183		1	1,8	1,09	1,63	1,66	64000	313428	481195
	LRHEATX	0,03881	-0,11272	0,08183		1,3	2,7	1,06	1,63	1,66	92465	591757	908503
	AMINE								0	1	11431	11431	17549
	BLOWER	0	0	0		0,12	2,8	1,00	1,89	1,35	24920	141296	216927
	FLASH1				1,5	0	3,1	0,64	2,25	1,82	6272	36766	56445
	CONDENS				1,5	1	3,1	0,78	2,25	1,82	4969	33065	50763
	FLASH3				1,5	1	3,1	0,78	2,25	1,82	4969	33065	50763
	WASHER				1,8	0,1	3,1	0,69	2,25	1,82	15611	95461	146557
	PUMP	-0,3935	0,3957	-0,00226		1,3	2,3	0,45	1,89	1,35	2749	9023	13853
	STRIPPER				1,9	1,3	3,1	0,91	2,25	1,82	22856	168603	258850
	ABSORBER				2,6	0,12	3,1	0,77	2,25	1,82	26342	174020	267167
	WASHER PACKING	0	0	0		1,3	7	1,00	0	1	4470	51873	79638
	ABSORBER PACKING	0	0	0		1,3	7	1,00	0	1	8878	62149	95415
	STRIPPER PACKING	0	0	0		0,12	7	1,00	0	1	7410	31289	48036
	TOTAL										321343	1,915,074	2,481,825
Ctm													
		2,928,553											

Table 29 Calculation procedure for OTHER OPEX costs of amine plant.

OTHER OPEX		Unit or basis	
	DIRECT PRODUCTION COST		
	Amine refilling cost per year	1,6 €/year	38438,4
	Maintenance and repair (M)	5% of FCI	146427,66
	Operating labor (OL)	One job per shift \$45/h	234000,00
	Supervision and supports (S)	30% of OL	70200,00
	Operating supplies	15% of M	21964,15
	Laboratory charges	10% of OL	7020,00
	FIXED COST		
	Local taxes and insurance	3,2% of FCI	93713,70
	Plant overhead cost	70,8% (OL) + 3,6% (FCI)	271099,91
	GENERAL EXPENSES		
	Administrative	17,7%(OL) + 0,9%(FCI)	67774,98
	R & D	5% of (COM)	28666,28
	Total purchase cost [€]		940,866.7

Table 30 Calculation procedure for DIRECT PRODUCTION costs of amine plant.

DIRECT PRODUCTION ANALYSIS		Unit	Value
	Mass of Amine	kg, [Karl Stéphane,2013]	7144
	Cost of Amine per kg	€/kg	1,6
	Net generating capacity without CO2 capture	MWe	2,4
	Hour of work of the CHP per year	h/year	5200
	Base plant cost of electricity	€/MWh [K. Sartor, 2014, pag 141]	50
	Base plant cost of biomass	€/MWh [K. Sartor, 2014, pag 141]	33
	Stage-cut	CO2captured/CO2inlet	0,987
	CO2 emitted without capture	ton/h	3,08
		ton/MWh	1,28
		ton/year	16016,00
	CO2 emitted with capture	ton/h	0,04
		ton/MWh	0,02
		ton/year	208,21
	Makeup MEA (degrad+evap) per year	1,5kg/ton CO2 captured	23711,69
	Makeup MEA cost	€/year	33765,44
	CO2 captured per year	ton/year	15807,79
	Cost of CO2 avoided	€/tonCO2	52,37
	CO2 cost per CAPEX in 20 years	€CAPEX/tonCO2separated in20years	9,26
	Annual energy consumption CO2 capture cost	€/year	827,922.4
Total OPEX per year			
1,768,789.1			

List of figures

Figure 1.1 CO ₂ concentration 1000-2100. Source [Hiroshi Otha, 2006]	7
Figure 1.2 Annual global total greenhouse gas emissions. Source [IPCC Side Event ,2018]	8
Figure 1.3 Global greenhouse gas emission levels for majors emitters. Source[IPCC Side Event ,2018]	8
Figure 1.4 Potential emission reduction in 2030. Source [IPCC Side Event ,2018]	9
Figure 1.5 Energy transport mix in Europe. [FuelsEurope, 2020]	10
Figure 1.6 Global primary energy consumption. Source [Vaclav Smil, 2017]	11
Figure 1.7Temperature variation from 1880 to 2010. Source[NOAA's 2015]	12
Figure 1.8 Global temperature respect time and CO ₂ concentration. Source [NASA 2010]	13
Figure 1.9 Emission spectrum for the Sun and for the Planet Earth	14
Figure 1.10 Wavelength characteristic of sun (left) and earth (right). Source [Yang Chen ,2006]	14
Figure 1.11 Absorption spectra of CO ₂ and H ₂ O vapor. Source [Robert Rohde ,2014]	15
Figure 1.12 Carbon dioxide concentration with time. Source [NASA, 2008]	15
Figure 1.13 Carbon emission per year in Gigatons. Source [Global Carbon project ,2019]	16
Figure 1.14 Graphical benchmark of temperature difference between 1890(left) and 2019(right). Source [NASA, 2010]	16
Figure 1.15 Sea level increase during years. Source [NASA, 2019]	17
Figure 1.16 Comparison Artic region 1984(left) 2016(right)	18
Figure 1.17 Projections of temperature difference. Source[IPCC Side Event ,2018]	18
Figure 1.18 Projections of sea level increase difference. Source[IPCC Side Event ,2018]	19
Figure 1.19 1.21 TRIAS energetica. Source [Freiburg,1996]	19
Figure 2.1 Flow sheet representation of CO ₂ capture process. Source [EASAC, 2013]	23
Figure 2.2 Pre-Combustion Capture scheme process. Source [José D. Figueroa, 2008]	24
Figure 2.3 Pre-Combustion Capture scheme process. Source [José D. Figueroa, 2008]	25
Figure 2.4 Monoethanolamine structure	25
Figure2.5 Oxy-combustion CO ₂ capture process. Source [José D. Figueroa, 2008]	26
Figure 3.1 Separation mechanism through size on the left and indirect selectivity on the right. Source [D. Havas and H. Lin, 2017]	30
Figure 3.2 Separation process through non-dispersive contact. Source[P. Luis and T. Gerven, 2012]	31
Figure 3.3 Separation process through liquid support. Source[P. Luis and T. Gerven, 2012]	32
Figure 3.4 Separation process through permeation. Source[P. Luis and T. Gerven, 2012]	33
Figure 3.5 The correlations of polymer specific volume versus temperature. Source [Yoshimizu ,2012]	36
Figure 3.6 Molecular structure of PIM-1. Source[P. Luis and T. Gerven, 2012]	37
Figure 3.7 Robeson plot for polymeric membranes for the gas mixture CO ₂ /CH ₄ . TR, thermally rearranged. Source [P. Luis and T. Gerven, 2012]	37

Figure 3.8 Integration of zeolite and polymeric membrane using (a) Composite membrane (b) Mixed Matrix Membrane. Source [Y. Chen , 2015].	40
Figure 3.9 (a) SEM image of the cross-section of a hollow fiber membrane (left) and diagram of a hollow fiber membrane module (right). (b) Functional diagram of a flat spiral wound membrane (left) and picture of a spiral wound membrane module ready for in. Source [M. G. De Angelis, 2015].	42
Figure 3.10 Schematic drawing of (a) Hollow fibre module for shell-side feed, (b) Hollow fibre module for bore-side feed, (c) Tubular module, (d) Plate-and-frame module, and (e) Spiral-wound module (Source: Baker, 2000; Mulder, 1996). Source [Baker, 2000]	43
Figure 4.1 Influence of air excess and humidity on maximal flame temperature. Source[Sunil Kumar, 2002]	46
Figure 4.2 Simulation results of NO _x emissions versus temperature. Source[Sunil Kumar, 2002]	47
Figure 4.3 CO ₂ permeability (a) and CH ₄ (b) at different relative humidity in mPI and mTR-PBO polymer. Source [M. G. De Angelis, 2015]	49
Figure 4.4 (a) Ideal selectivity at 35°C, at different relative humidity, in mPI and mTR-PBO membranes. (b) Relative variation of ideal selectivity respect dry value, at different relative humidity, , in mPI and mTR-PBO membranes. Source [M. G. De Angelis, 2015]	50
Figure 4.5 Pilot membrane module. Source [Marius Sandrua, 2013]	51
Figure 4.6 Raw data for permeate flow rate and CO ₂ content measured from 17 August to 6 October 2011. Source [Marius Sandrua, 2013]	52
Figure 4.7 The change of permeate flux at different relative humidity of water in CO ₂ /N ₂ separation by cellulose acetate membrane. Source [Marius Sandrua, 2013]	53
Figure 4.8 Gas separation performance of CTA membranes at 10 bar, 35°C after immersion in pH (3, 7 and 13) solutions (a) permeability of CO ₂ ; (b) permeability of N ₂ ; (c)selectivity of CO ₂ /N ₂ . Source [Marius Sandrua, 2013]	54
Figure 4.9 Gas permeability in CTA thin film composite membranes. (a) permeability of CO ₂ in 10 v/v% CO ₂ in N ₂ ; (b) permeability of N ₂ in 10 v/v% CO ₂ in N ₂ ; (c) permeability of SO ₂ 1000 ppm SO ₂ in N ₂ . Source [Marius Sandrua, 2013]	53
Figure 4.10 N ₂ permeability in CTA thin film composite membranes with 10 v/v% CO ₂ in N ₂ gas feeding and 1000 ppm SO ₂ in N ₂ gas feeding. Source [Marius Sandrua, 2013]	57
Figure 4.11 Change in permeability of (a) He; (b) N ₂ and (c) He/N ₂ selectivity as time progresses for CTA membranes at 35°C, 7.5 bar after aging separately in pure N ₂ , 979 ppm NO in balance N ₂ and 1000 ppm SO ₂ in balance N ₂ at 7.5 bar and 22 ± 2°C. Source [Marius Sandrua, 2013]	59
Figure 5.1 Cogeneration plant and only heat plant.	60
Figure 5,2 Variation of load during the day for a typical heating application. Source [K. Sartor,2014]	61
Figure 5.3 Plant configuration of cogenerator. Source [K. Sartor,2014]	62
Figure 6.1 Idealized flow patterns in membrane gas separator. Source [V. Bondar, 2000]	66
Figure 6.2 Simulation window description in ACM.,	67
Figure 6.3 Variables definition in ACM.	69
Figure 6.4 Ports definition and retentate inlet specification	69
Figure 6.5 Balance equations for each cell	70
Figure 6.6 Retentate and permeate composition plus other outlet streams conditions in ACM.	70
Figure 6.7 Schematic drawing of the base module (Gas Permeation Unit) in ACM.	71
Figure 6.8 Capture of the set compiler of Aspen Plus V11	72
Figure 6.9 Configuration 1.	73
Figure 6.10 Configuration 2.	73

Figure 6.11 Configuration 3.	74
Figure 6.12 Configuration 4.	74
Figure 6.13 Configuration 5.	77
Figure 6.14 Configuration 6.	77
Figure 6.15 Configuration 7.	78
Figure 6.16 Configuration 8.	78
Figure 6.17 Configuration 9.	79
Figure 6.18 Stage-cut in function of membrane area.	79
Figure 6.19 CO ₂ mole fraction in permeate flux in function of membrane area	80
Figure 7.1 Mechanism of gas-liquid absorption (left) and liquid-solid adsorption (right). The blue dots represent the solute molecules. Source [Daniele Pugliesi, 2009].	81
Figure 7.2 Comparison between chemical and physical absorption. Source [Grégoire Leonard,2008-2009].	82
Figure 7.3 Classification of amine in primary, secondary and tertiary	83
Figure 7.4 MEA amine structure	83
Figure 7.5 Cross-sectional view of packed tower in operation. Source [Max S.Peters,1991].	84
Figure 7.6 Single pieces of typical random packings. Source [Max S.Peters,1991]	84
Figure 7.7 Simplified plant of amine absorption. Source [Dr. Mark Jordi,2016]	85
Figure 7.8 Aqueous amine and carbonate chemistry. Source [Rochelle, 2016]	85
Figure 7.9 List of some amines. Source [Noel Vicente]	86
Figure 7.8 Plant of amine capture pilot plant on Aspen Plus.	87
Figure 7.9 Amine plant for CHP Liegi University.	89

List of table

TABLE 1 ADVANTAGES AND DISADVANTAGES OF DIFFERENT CO ₂ CAPTURE APPROACHES. SOURCE [JOSÉ D. FIGUEROA, 2008, 112]	26
TABLE 2 OVERVIEW OF DEVELOPMENT OF POST-COMBUSTION CAPTURE AND HIGH-TEMPERATURE SOLIDS-LOOPING PROCESSES. SOURCE [2019 IEAGHG REPORT, 112].	27
TABLE 3 THE KINETIC DIAMETER AND CRITICAL TEMPERATURE OF SOME COMMON GASES IN GAS SEPARATION PROCESS.	30
TABLE 4 CO ₂ /N ₂ SEPARATION PERFORMANCE USING ZEOLITE-BASED MEMBRANE. SOURCE [Y. CHEN , 2015, 61]	39
TABLE 5 PARAMETERS FOR MEMBRANE MODULE DESIGN. SOURCE [BAKER, 2000, 69].	42
TABLE 6 PRINCIPAL GAS SEPARATION MARKETS, PRODUCERS, AND MEMBRANE SYSTEMS. SOURCE [BAKER, 2000, 69]	42
TABLE 7 TEST PARAMETERS AND FLUE GAS COMPOSITION (MCR IS MAXIMUM CONTINUUM RATING, SCR SELECTIVE CATALYTIC REDUCTION) . SOURCE [MARIUS SANDRUA, 2013, 75].	49
TABLE 8 VOLUME GAS FRACTION AND DATA FOR 12 MW BIOMASS BOILER OF COGENERATION PLANT CALCULATED BY MODEL AND EXPERIMENTALLY. SOURCE [K. SARTOR,2014, 132]	61
TABLE 9 FLUE GAS CHARACTERISTIC.	62
TABLE 10 DATA SHEET OF POLARIS MEMBRANE. SOURCE [LIN, 2007, 91]	63
TABLE 11 DATA CHARACTERISTIC OF CONFIGURATION 1 AND 2.	73
TABLE 12 DATA CHARACTERISTIC OF CONFIGURATION 3 AND 4.	74
TABLE 13 FLUE GAS COMPOSITION OF PILOT PLANT.	85
TABLE 14 DATA INPUTS OF ABSORBER AND STRIPPER COLUMNS.	87

TABLE 15 ASSUMPTION AND SPECIFICATIONS FOR MEMBRANE SEPARATION PLANT.....	89
TABLE 16 SUMMARIZING TABLE ABOUT POWER CONSUMPTION , CO ₂ CAPTURE AND ECONOMIC EVALUATION ABOUT MEMBRANE.....	90
TABLE 17 POWER CONSUMPTION OF MEMBRANE SEPARATION PLANT.....	90
TABLE 18 ENERGY COOLING DUTY ABOUT MEMBRANE SEPARATION PLANT.....	91
TABLE 19 ASSUMPTION AND SPECIFICATIONS FOR MEMBRANE SEPARATION PLANT.....	91
TABLE 20 SUMMARIZING TABLE ABOUT POWER CONSUMPTION , CO ₂ CAPTURE AND ECONOMIC EVALUATION ABOUT MEMBRANE.....	92
TABLE 21 ENERGY COOLING DUTY ABOUT MEMBRANE SEPARATION PLANT.....	92
TABLE 22 SUMMARIZING TABLE OF PRINCIPALS CHARACTERISTICS OF CO ₂ CAPTURE PROCESSES.....	93
TABLE 23 CALCULATION PROCEDURE FOR CAPEX OF MEMBRANE SEPARATION PLANT PART 1.....	98
TABLE 24 CALCULATION PROCEDURE FOR CAPEX OF MEMBRANE SEPARATION PLANT PART 2.....	99
TABLE 25 CALCULATION PROCEDURE FOR OTHER OPEX COSTS OF MEMBRANE SEPARATION PLANT.....	100
TABLE 26 CALCULATION PROCEDURE FOR DIRECT PRODUCTION.....	100
TABLE 27 CALCULATION PROCEDURE FOR CAPEX OF AMINE SEPARATION PLANT PART 1.....	101
TABLE 28 CALCULATION PROCEDURE FOR CAPEX OF AMINE SEPARATION PLANT PART 2.....	102
TABLE 29 CALCULATION PROCEDURE FOR OTHER OPEX COSTS OF AMINE PLANT.....	103
TABLE 30 CALCULATION PROCEDURE FOR DIRECT PRODUCTION COSTS OF AMINE PLANT.....	103

Nomenclature

c_i	Concentration of component I, mol/m ³
D_{if}	Gas diffusivity coefficient of component i, m ² /s
D_i	Inside diameter of hollow fibre, m
D_o	Outside diameter of hollow fibre, m
J_i	Permeance of component i, mol/m ² .s.Pa
J_i	Flux of component i, mol/m ² .s
K_i	Sorption coefficient of component i, mol/m ³ .Pa
L	Effective fibre length, m
l	Membrane thickness, m
M_i	Molecular weight of component i
N	Number of fibres in the module
P_i	Permeability coefficient of component i, mol.m/m ² .s.Pa
P	Feed side pressure, Pa
p	Permeate side pressure, Pa
R	Ideal gas constant, Pa.m ³ /mol.K
T	Temperature, K
x_i	concentration of component i, mol fraction

Bibliography

- Aaron, D. and Tsouris C., Separation of CO₂ from flue gas: a review. Separation. Science and Technology, 2005. 40: p. 321-348.
- Abu-Zahra, M. R. M., et al. CO₂ capture from power plants: Part II. A parametric study of the economical performance based on mono-ethanolamine. International Journal of Greenhouse Gas Control 2007; 1: 135-42.
- Achoundong, C., Bhuwania, N., Burgess, S., Karvan, O., Johnson, J., Koros, W.J., 2013. Silane modification of cellulose acetate dense films as materials for acid gas removal. Macromolecules 46, 5584_5594.
- Aerosol indirect effects on clouds and global climate, Yang Chen,2006

- Ahn S, You Y-W, Lee D-G, Kim K-H, Oh M, Lee C-H. Layered, two- and four-bed PSA processes for H₂ recovery from coal gas. *Chem Eng Sci* 2012.
- Alie, C. F., CO₂ capture with MEA: integrating the absorption process and steam cycle of an existing coal-fired power plant, MSc Thesis, University of Waterloo. 2004.
- Alie, C., L. Backham, E. Croiset, P.L. Douglas, Simulation of CO₂ capture using MEA scrubbing: a flowsheet decomposition method, *Energy Conversion & Management*, 46 (2005) 475.
- B. Wang, W. W. Ho, J. D. Figueroa and P. K. Dutta, *Langmuir* 31 (24), 6894-6901 (2015).
- Bailey, P. Feron, Post-combustion Decarbonisation Processes, *Oil & Gas Science and Technology – Rev. IFP*, Vol. 60 (2005), No. 3, pp. 461-474, 2005.
- Baker, R. W., Future directions of membrane gas separation technology, *Ind. Eng. Chem. Res.*, 41 (2002) 1393.
- Baker, R. W., *Membrane Technology and Applications*, McGraw-Hill, NY, (2000).
- Bartok W, Sarofim AF. Fossil fuel combustion: a source book. Wiley Interscience publication. New York: Wiley; 1991.
- Bennett, D.L. and K.W. Kovak, Optimize distillation columns, *Chem. Eng. Prog.*, May 2000, p. 19.
- C Lau, P. Li, et al., “Reverse-selective polymeric membranes for gas separations”, *Progress in polymer science*, 38:5, 740-766, 2013.
- C. H. Lau, P. Li et al., “Reverse-selective polymeric membranes for gas separation”, *Progress in Polymer science*, 38(740-766), Elsevier, 2013.
- C. P. Pappis,” Climate change, supply chain management and enterprise adaptation : implications of Global Warming on the Economy”, LinkHershey : Information Science Reference, 2011.
- Carbon capture and storage in Europe, EASAC policy report ,20 May 2013 .
- Chen, D.-W. Park and W.-S. Ahn, *Appl. Surf. Sci.* **292**, 63-67 (2014).
- Chen, X.Y., Vinh-Thang, H., Ramirez, A.A., Rodrigue, D., Kaliaguine, S., 2015. Membrane gas separation technologies for biogas upgrading. *RSC Adv.* 5, 24399_24448. Available from: <https://doi.org/10.1039/C5RA00666J>.
- Cho, Y.J., Park, H.B., 2011. High performance polyimide with high internal free volume elements. *Macromol. Rapid Commun.* 32, 579_586. Available from: <https://doi.org/10.1002/marc.201000690>.
- D. Havas, H. Lin, “Optimal membranes for biogas upgrade by removing CO₂: High permeance or high selectivity?”, *Separation Science and Technology*, 52:2, 186-196, 2017.
- Danckwerts, 1979. The reaction of CO₂ with ethanolamines. *Chem. Eng. Sci.* 34(4), 443-446
- Daniele Pugliesi, [https://it.wikipedia.org/wiki/Assorbimento_\(chimica\)#/media/File:Assorbimento_e_adsorbimento.svg](https://it.wikipedia.org/wiki/Assorbimento_(chimica)#/media/File:Assorbimento_e_adsorbimento.svg), 2005.
- Dr. Mark Jordi, Measuring Amine Strength in Absorption and Regeneration Solutions Using Handheld Raman, 2016.
- E. Powell and G. G. Qiao, *J. Membr. Sci.* **279** (1), 1-49 (2006).
- Freeman, B., Basis of permeability/selectivity trade-off relations in polymeric gas-separation membranes, *Macromolecules*, 32 (1999) 375.
- Grégoire Léonard , FRITCO₂T, [www.chemeng.uliege.be/FRITCO₂T](http://www.chemeng.uliege.be/FRITCO2T), 2018
- Grégoire Leonard, Modeling of a pilot plant for the CO₂-reactive absorption in amine solvent for power plant flue gases, 2008-2009.
- Hennis, J.M.S., and M.K. Tripodi, Multicomponent membranes for gas separations, U.S. Patent 4,230,463, 1980.
- Hiroshi Otha, <http://www.esd-asiapacific.com/fasid/cc/cc.html>, 2006
- Horn, N., Paul, D., 2011. Carbon dioxide plasticization and conditioning effects in thick vs thin glassy polymer films. *Polymer (Guildf)* 52, 1619_1627. Available from: <https://doi.org/10.1016/J.POLYMER.2011.0>
- Hosseini, S.S., Peng, N., Chung, T.S., 2010. Gas separation membranes developed through Integration of polymer blending and dual-layer hollow fiber spinning process for hydrogen and natural gas enrichments. *J. Membr. Sci.* 349, 156_166. Available from: <https://doi.org/10.1016/j.memsci.2009.11.043>.
- Hsieh, H.P., 1996. *Inorganic Membranes for Separation and Reaction* (Google eBook). Elsevier.
- IEAGHG report, 2019.

- IPCC Side Event - COP 24 - 5 December 2018, Emission Gas report
- IPCC, 2014: Climate Change 2014: Synthesis Report. Contribution of Working Groups I, II and III to the Fifth Assessment Report of the Intergovernmental Panel on Climate Change [Core Writing Team, R.K. Pachauri and L.A. Meyer (eds.)]. IPCC, Geneva, Switzerland, 151 pp
- IPCC, <https://www.ipcc.ch/sr15/chapter/chapter-2/>, Mitigation Pathways Compatible with 1.5°C in the Context of Sustainable Development.
- IPCC. Climate change 2014: synthesis report. Geneva, Switzerland: IPCC; 2014. p. 151.
- IPCC's report, "Climate Change 2014, Synthesis Report Summary for Policymakers", 2014.
- IUPAC, Gold book "Alkanes", <http://goldbook.iupac.org/A00222.html>
- IUPAC, Gold book "Aryl groups", <http://goldbook.iupac.org/A00464.html>
- IUPAC, Gold book, "heteroaryl group" <http://goldbook.iupac.org/H02792.html>
- J. Li, J. Shao, Q. Ge, G. Wang, Z. Wang and Y. Yan, Microporous Mesoporous Mater. **160**, 10-17 (2012).
- James Rodger Fleming, Historical Perspectives on Climate Change, 2005.
- Juliann M. Cossia "Global Warming in the 21st Century", Nova Science Publishers, 2011.
- K. Adewole, L. Ahmada, et al., "Current challenges in membrane separation of CO₂ from natural gas: A review", International Journal of Greenhouse Gas Control, 17, 46-65, 2013.
- K. Sartor, S. Quoilin, P. Dewallef, 2014, Simulation and optimization of a CHP biomass plant and district heating network
- K. Sartor*, Y. Restivo, P. Ngendakumana, P. Dewallef, Prediction of SO_x and NO_x emissions from a medium size biomass boiler., 2014.
- K.-i. Okamoto, H. Kita and K. Horii, Ind. Eng. Chem. Res. 40 (1), 163-175 (2001).
- Khakpay, P. Scovazzo, "Reverse-selective behavior of room temperature ionic liquid based membranes for natural gas processing", Journal of Membrane Science 545, 204-212, (2018).
- Kookos, I.K., A targeting approach to the synthesis of membrane networks for gas separations, J. Memb. Sci., 208 (2002) 193.
- Koros, W.J., and R. T. Chern, Separation of gaseous mixtures using polymer membranes, in Handbook of Separation Process Technology, in R. W. Rousseau (Ed.), John Wiley and Sons, Inc. (1987).
- Kuehene, THE UNIVERSITY OF MELBOURNE SCHOOL OF CHEMICAL AND BIOMEDICAL ENGINEERING DEPARTMENT OF CHEMICAL ENGINEERING, The impact of impurities on the performance of cellulose triacetate membranes for CO₂ separation, HIEP THUAN LU, jenuary 2018.
- L. M. Robeson, "Polymer membranes for gas separation", Current Opinion in Solid State and Materials Science 4 (549-552), PERGAMON, 1999.
- L. M. Robeson, J. Membr. Sci. **62** (2), 165-185 (1991).
- L. Robeson, B. Freeman, D. Paul and B. Rowe, J. Membr. Sci. 341 (1), 178-185 (2009).
- L. Shan, J. Shao, Z. Wang and Y. Yan, J. Membr. Sci. **378** (1), 319-329 (2011).
- L. Zhao, Y. Chen, B. Wang, C. Sun, S. Chakraborty, K. Ramasubramanian, P. K. Dutta and W. W. Ho, J. Membr. Sci. 498, 1-13 (2016).
- Li, N., Fane, A., Winston, W.S., Matsuura, T., 2011. Advanced Membrane Technology and Applications. Wiley-VCH Verlag GmbH.
- Lin, H, T. Merkel and R. Baker, The Membrane Solution to Global Warming, 6th Annual Conference on Carbon Capture & Sequestration, Pittsburgh, Pennsylvania, May 2007,
- Lin, H, T. Merkel and R. Baker, The Membrane Solution to Global Warming, 6th Annual Conference on Carbon Capture & Sequestration, Pittsburgh, Pennsylvania, May 2007, http://www.netl.doe.gov/publications/proceedings/07/carbon-seq/data/papers/tue_189.pdf
- Lin, H, T. Merkel and R. Baker, The Membrane Solution to Global Warming, 6th Annual Conference on Carbon Capture & Sequestration, +Pittsburgh, Pennsylvania, May 2007, http://www.netl.doe.gov/publications/proceedings/07/carbon-seq/data/papers/tue_189.pdf
- Lopes FVS, Grande CA, Rodrigues AE. Activated carbon for hydrogen purification by pressure swing adsorption: multicomponent breakthrough curves and PSA performance. Chem Eng Sci 2011;66(3):303e17.
- Lysen E., The Trias Energica, Eurosun Conference, Freiburg, 1996
- M. A. Morrison and P. J. Hay, J. Chem. Phys. **70** (9), 4034-4043 (1979). V. Bondar, B. Freeman and I. Pinnau, J. Polym. Sci., Part B: Polym. Phys. **38** (15), 2051-2062 (2000).

- M. C. Lovallo, A. Gouzinis and M. Tsapatsis, *AIChE J.* **44** (8), 1903-1913 (1998).
- M. G. De Angelis, M. Giacinti Baschetti, M. Minelli, L. Olivieri (Università di Bologna) P. Deiana, C. Bassano (ENEA), SINTESI, CARATTERIZZAZIONE E PROVA DI MEMBRANE PER LA SEPARAZIONE DELLA CO₂ E LA PURIFICAZIONE DEL SYNTHETIC NATURAL GAS (SNG, Settembre 2015
- M. Zimmerman, A. Singh and W. J. Koros, *J. Membr. Sci.* **137** (1), 145-154 (1997).
- Marius Sandrua, Taek-Joong Kima, Wieslaw Capalab, Martin Huijbersc, May- Britt Häggd, Pilot scale testing of polymeric membranes for CO₂ capture from coal fired power plants *, 2013.
- Mark Z. Jacobson “Air pollution and global warming: history, science, and solutions”, Cambridge University Press, 2012.
- Mark, J.E., 1999. *Polymer Data Handbook*. Oxford University Press.
- Marvin Rausand, Qualification of new technology for capture of CO₂ in coal-fired power plants July 2007, Thesis for: MSc in Energy and Environmental Engineering Advisor:
- Massood Ramezan, T. J. S. Carbon Dioxide Capture from Existing Coal-Fired Power Plants U.S. Department of Energy-National Energy Technology Laboratory, : Novemer, 2007.
- Max S.Peters, Klaus D. Timmerhaus, *Plant design and economical for chemical engineers*, 1991.
- Merkel, T.C., H. Lin, X. Wei, and R. Baker, Power plant post-combustion carbon dioxide capture: An opportunity for membranes, *J. Memb. Sci.*, **359** (2010) 126.
- Mohammad Hassan Murad Chowdhury, *Simulation, Design and Optimization of Membrane Gas Separation, Chemical Absorption and Hybrid Processes for CO₂ Capture*, Canada, 2011.
- Miettinen H, Paulsson M, Stromberg D. Laboratory study of N₂O formation from burning char particle, 2013
- Mike Hulme “On the origin of ‘the greenhouse effect’: John Tyndall’s 1859 interrogation of nature”, University of East Anglia, Norwich
- Mulder, M., *Basic Principles of Membrane Technology*, 2nd ed., Kluwer Academic Publishers, Netherlands, (1996).
- N. Bryan, E. Lasseguette, M. van Dalen, N. Permogorov, A. Amieiro, S. Brandani and M.-C. Ferrari, *Energy Procedia* **63**, 160-166 (2014).
- N. P. Patel, C. M. Aberg, “Morphological, mechanical and gas-transport characteristics of crosslinked polypropylene glycol: Homopolymers, nanocomposites and blends”, *Polymer Volume 45*, Issue 17(5941-5950), 2004.
- NASA, https://climate.nasa.gov/climate_resources/24/graphic-the-relentless-rise-of-carbon-dioxide/ , Global climate change, 2004.
- NASA, <https://climate.nasa.gov/vital-signs/sea-level/>, 2019
- NASA, <https://earthobservatory.nasa.gov/features/CarbonCycle> , , earth observatory, By Holli Riebeek Design by Robert Simmon , June 16, 2011
- NOAA/NCEI , <https://www.co2.earth/>, 2020.
- NOAA’s , The recent global surface warming
- Noel Vicente, *Sulfur Recovery: The Big Picture—Part III, The Amine Unit, Amine Unit Introduction and Process Flow*
- Nunes, S., Peinemann, K., 2001. *Membrane Technology*. Wiley-VCH Verlag GmbH, Weinheim, FRG. Available from: <https://doi.org/10.1002/3527600388>.
- Oexmann, J. *Post-Combustion CO₂ Capture: Energetic Evaluation of Chemical Absorption Processes in Coal-Fired Steam Power*, 2012.
- P. Luis, T. Gerven, et al., “Recent developments in membrane-based technologies for CO₂ capture”, *Progress in Energy and Combustion Science: an international review journal*, **38:3**, 419-448 (2012).
- P. Patel, A. Hunt et al., “Tunable CO₂ transport through mixed polyether membranes” Volume 251, Issues 1–2 (51-57), 2005, *Journal of Membrane Science*.
- Paul, D.R. and Yampol'skii Y.P., *Polymeric gas separation membranes*. 1993: CRC Press.
- Paul, D.R., and Yu.P. Yampol'skii, *Polymeric gas separation membranes*, CRC Press, Inc., Florida, USA (1994).
- Pfaff, I., et al. Optimised integration of post-combustion CO₂ capture process in greenfield power plants. *Energy* 2010; **35**: 4030-41.

- R. Khalilpoura, K. Mumford, et al., “Membrane-based carbon capture from flue gas: a review”, *Journal of Cleaner Production*, 103, 286-300, 2015.
- R. Krishna and J. M. van Baten, *J. Membr. Sci.* **360** (1), 323-333 (2010).
- R. Raharjo, H. Lin et al., "Relation between network structure and gas transport in crosslinked poly(propylene glycol diacrylate)", *Journal of Membrane Science*, Volume 283, Issues 1–2(253-265), 2006, *Journal of Membrane Science*.
- R. W. Baker, *Membrane Technology and Applications*. (John Wiley & Sons, Ltd, 2012)
- Robert Falkner, “The handbook of global climate and environment policy”, LinkChichester U.K. : Wiley-Blackwell, 2013.
- Robert Rohde, NASA, CO₂ H₂O absorption atmospheric gases unique pattern energy wavelengths of energy transparent to others, 2014.
- Robertson, Du, N., Park, H.B., , G.P., Dal-Cin, M.M., Visser, T., Scoles, L., et al., 2011. Polymer nanosieve membranes for CO₂-capture applications. *Nat. Mater.* 10, 372_375. Available from: <https://doi.org/10.1038/nmat2989>.
- Robeson, L.M., 2008. The upper bound revisited. *J. Membr. Sci.* 320, 390_400. Available from: <https://doi.org/10.1016/j.memsci.2008.04.030>.
- Robeson, L.M., 2008. The upper bound revisited. *J. Membr. Sci.* 320, 390_400. Available from: <https://doi.org/10.1016/j.memsci.2008.04.030>.
- Robeson, L.M., Liu, Q., Freeman, B., Paul, D., 2015. Comparison of transport properties of rubbery and glassy polymers and the relevance to the upper bound relationship. *J. Membr. Sci.* 476, 421_431. Available from: <https://doi.org/10.1016/J.MEMSCI.2014.11.058>.
- Rochelle, Conventional amine scrubbing for CO₂ capture, 2016.
- Roeder,; Kather, A. Part Load Behaviour of Power Plants with a Retrofitted Post-combustion CO₂ Capture Process. *Energy Procedia* 2014; 51: 207-16.
- S. Choi, J. H. Drese and C. W. Jones, *ChemSusChem* **2** (9), 796-854 (2009).
- S. M. Auerbach, K. A. Carrado and P. K. Dutta, *Handbook of zeolite science and technology*. (CRC press, 2003).
- Spillman, R., 1995. *Economics of Gas Separation Membrane Processes*. Elsevier, Amsterdam.
- Sreedhar, R. Vaidhiswaran, et al., “Process and engineering trends in membrane based carbon capture, Renewable and Sustainable Energy Reviews, vol. 68, 659-684 2017.
- Stern, S.A., Polymers for gas separation: the next decade, *J. Memb. Sci.*, 94 (1994) 1.
- Sunil Kumar, <http://cleanboiler.org/workshop/how-is-nox-formed/>, 2002.
- T. C. Bowen, R. D. Noble and J. L. Falconer, *J. Membr. Sci.* 245 (1–2), 1-33 (2004).
- The chemical mechanism of SO_x formation and elimination in coal combustion process Edyta KRAWCZYK, Monika ZAJEMSKA, Tomasz WYLECIAŁ Faculty of Materials Processing Technology and Applied Physics, Częstochowa University of Technology, Poland, 2013.
- The urgency of the development of CO₂ capture from ambient air Klaus S. Lacknera, Sarah Brennana , Jürg M. Mattera,c, A.-H. Alissa Parka,b, Allen Wrighta , and Bob van der Zwaana, 2012.
- Turton R., Bailie R., Whiting W., Shaeiwitz J., Bhattacharyya D., 2013. *Analysis, Synthesis, and Design of Chemical Processes*, 4th edition, Pearson.
- U.S. Energy Information Administration | International Energy Outlook 2016, <https://www.eia.gov/outlooks/ieo/pdf/transportation.pdf>, Transportation energy consumption, Chapter 8, pag 127.
- Vaclav Smil (2017). *Energy Transitions: Global and National Perspectives*. & BP Statistical Review of World Energy
- Van Loo S, Koppejan J, editors. *The handbook of biomass combustion and co-firing*. London: Earthscan; 2008.
- Vermeulen I, Block C, Vandecasteele C. Estimation of fuelnitrogen oxide emissions from the element composition of the solid or waste fuel. *Fuel* 2012;94(0):75e80.
- Versteeg G., Van Swaaij, 1988, On the kinetics between CO₂ and Alkanolamines both in aqueous and non-aqueous solutions- I primary and secondary amines. *Chem. Eng. Sci.* 43(3), 573-585.
- W. S. Broecker, “Climatic Change: Are We on the Brink of a Pronounced Global Warming?”, *Science*, New Series, Vol. 189, No. 4201 (1975), pp. 460-463, American Association for the Advancement of Science

- W. Yave, A. Car, S. S. Funari, S. P. Nunes and K.-V. Peinemann, *Macromolecules* **43** (1), 326-333 (2009).
- W., B.R., *Membrane Technology and Applications*. 2 ed. 2004, California, U.S.: John Wiley & Sons Ltd.
- Y. Chen, B. Wang, L. Zhao, P. Dutta and W. W. Ho, *J. Membr. Sci.* **495**, 415-423 (2015).
- Y. Chen, L. Zhao, B. Wang, P. Dutta and W. W. Ho, *J. Membr. Sci.* **497**, 21-28 (2016).
- Yampolskii, Y., Pinnau I., and Freeman B.D., *Materials science of membranes for gas and vapor separation*. 2006: Wiley Online Library.
- Yoshimizu, H., Ohta S., Asano T., Suzuki T., and Tsujita Y., Temperature dependence of the mean size of polyphenyleneoxide microvoids, as studied by Xe sorption and ¹²⁹Xe NMR chemical shift analyses. *Polym J*, 2012. **44**(8): p. 821-826.
- Yuan Wanga , Li Zhaoa,* , Alexander Ottoa, Martin Robinius, Detlef Stoltena 13th International Conference on Greenhouse Gas Control Technologies, GHGT-13, 14-18, November 2016, Lausanne, Switzerland , Review of Post-combustion CO₂ Capture Technologies from, Coal-fired Power Plants,
- Z. Yeo, T. Chew, et al., “Conventional processes and membrane technology for carbon dioxide removal from natural gas”, *Journal of Natural Gas Chemistry* **21** 282–298, (2012).
- Zhao, L., et al. Multi-stage gas separation membrane processes used in post-combustion capture: Energetic and economic analyses. *Journal of Membrane Science* **2010**; **359**: 160-72.

